IntechOpen

Advanced Casting Technologies

Edited by T.R. Vijayaram

ADVANCED CASTING TECHNOLOGIES

Edited by **T.R. Vijayaram**

Advanced Casting Technologies
http://dx.doi.org/10.5772/intechopen.68254
Edited by T.R. Vijayaram

Contributors

Gabriel Plascencia, Claudio Méndez, Ricardo Rafael Ambriz, David Jaramillo, Rianti Sulamet-Ariobimo, Williams S. Ebhota, Tien-Chien Jen, Vasudev Shinde, David Weiss, Raj Sahu, Mohit Sahu, Victor Omidiji

Notice

First published in London, United Kingdom, 2018 by IntechOpen
eBook (PDF) Published by IntechOpen, 2019
IntechOpen is the global imprint of INTECHOPEN LIMITED, registered in England and Wales, registration number: 11086078, The Shard, 25th floor, 32 London Bridge Street
London, SE19SG – United Kingdom
Printed in Croatia

British Library Cataloguing-in-Publication Data
A catalogue record for this book is available from the British Library

Additional hard and PDF copies can be obtained from orders@intechopen.com

Advanced Casting Technologies
Edited by T.R. Vijayaram

p. cm.

Print ISBN 978-1-78923-032-1

Online ISBN 978-1-78923-033-8

eBook (PDF) ISBN 978-1-83881-297-3

Meet the editor

Dr. T.R. Vijayaram, a director (research) and professor in Mechanical Engineering, Galgotias University, Greater Noida, UP, India, is an expert in metallurgical, manufacturing, and mechanical engineering. He grew up in the famous Temple City, Madurai, India, and received his BS degree in Mechanical Engineering from Madurai Kamaraj University, followed by his ME degree in Industrial Metallurgy from PSG College of Technology, Bharathiar University, Coimbatore. He earned his PhD research degree in Mechanical Engineering from the Universiti Putra Malaysia (UPM), Selangor, Malaysia. He has worked as a rector researcher in Metallurgy at DCCI, University of Genoa, Italy. His passion in academics, research, and education led him to obtain an MBA degree in Educational Management and an MA degree in Sociology from the University of Madras. He is also a chartered engineer (India) and a member of several professional and scientific bodies in India and abroad like ISTE, IEI, IIF, Kolkata and SAE, USA. Recently, Professor Dr. T.R. Vijayaram has received the Distinguished Scientist Award in Metallurgical and Materials Engineering for his outstanding contribution in metallurgy. He has published more than 210 papers in international and national journals, conferences, broadsheets, and magazines.

Contents

Preface

The field of metal casting technology has advanced substantially in the past few decades. Major casting processing advancements have been made in experimental and simulation areas. Newly developed advanced casting technologies allow foundry researchers to explore detailed phenomena associated with new casting process parameters helping to produce defect-free castings with good quality. Moreover, increased computational power allows foundry technologists to simulate advanced casting processes to reduce casting defects.

In view of rapid expansion of knowledge and capability in the exciting field of casting technology, it is possible to develop new casting techniques. This book is intended to discuss many casting processing technologies. It is devoted to advanced casting processing technologies like ductile casting production and thermal analysis, casting of metal matrix composites by vortex stir casting technique, aluminum DC casting, evaporative casting process, and so on.

This book entitled *Advanced Casting Technologies* has been organized into seven chapters and categorized into four sections. Section 1 discusses the production of ductile iron casting and thermal analysis. Section 2 depicts aluminum casting. Section 3 describes the casting manufacturing aspects of functionally graded materials and evaporative casting process. Section 4 explains about the vortex stir casting technique to process metal matrix composite castings.

All the chapters discussed in detail the processing steps, process parameters involved in the individual casting technique, and also its applications.

The goal of the book is to provide details on the recent casting technologies. I would like to thank InTechOpen publication, Croatia, Europe, who has taken efforts and provided me an opportunity as chief editor.

Dr. T.R. Vijayaram
Galgotias University
Greater Noida, Uttar Pradesh
India

Ductile Iron Casting

Chapter 1

Thin Wall Ductile Iron Castings

Rianti Dewi Sulamet-Ariobimo,
Johny Wahyuadi Soedarsono and
Tresna Priyana Soemardi

Additional information is available at the end of the chapter

http://dx.doi.org/10.5772/intechopen.72117

Abstract

The use of austempered ductile iron (ADI) as an alternative material has increased, and it is predicted that it will reach 300,000 tons by the year of 2020 due to its characteristics especially design flexibility. When the reduction in weight is considered as a parameter for energy saving, ADI is presented as thin wall austempered ductile iron (TWADI). To produce a good quality TWADI, a good quality thin wall ductile iron (TWDI) must be used as a raw material. Good quality TWDI is produced by casting design. This chapter discusses the production of thin wall ductile iron, including its characterisation and defect. The discussion includes the background of thin wall casting (TWC) and TWDI, applying TWC in general casting, the problems in producing TWDI, characterisation of the TWDI and specific defects.

Keywords: thin wall casting, ductile iron, austempered ductile iron, vertical casting, ingate position, premature solidification, single matrix for microstructure

1. Introduction

Thin wall casting (TWC) is developed to produce lighter casting products. The weight reduction in TWC is gained by thinning out the wall thickness of products in whole like plates or partially. Thinning of the cast product will disturb the pouring time and speed up the solidification rate. The pouring time will shorten since the volume of the cast product is decreased due to depletion process. To overcome this, foundrymen tends to increase the pouring temperature. The increase in pouring temperature will expand the temperature differences, which will result in higher solidification rate.

Increasing pouring temperature could not be applied while producing ductile iron (FCD) since the process includes liquid treatment processes, known as inoculation and nodulation. Both processes are limited by temperature and time. The effect of liquid treatment will reduce

if the limit of temperature and time is exceeded. This condition will disturb the formation of spheroidal graphite and cause failure in production.

Thin wall ductile iron (TWDI) is ductile iron casted in TWC. The thicknesses of some products of FCD were reduced in certain parts. Caldera defined TWDI as ductile iron casting with wall thickness below 5 mm [1], while Stefanescu limited its thickness below 3 mm [2]. But the properties of TWDI should fulfil the properties of FCD. TWDI has made it possible for ductile iron to compete with aluminium in terms of weight [3]. The size of the thinnest TWDI plate is 1 mm [4–7].

2. Problems in producing thin wall ductile iron

Problems in producing thin wall ductile iron occur due to its thickness. In general casting, to avoid premature solidification, pouring temperature is raised when the casting product is thin. Premature solidification will lead to defects as presented in **Figure 1**. However, this method cannot be applied in producing TWDI since there is temperature limitation for liquid treatment process. Liquid treatments, i.e. inoculation and nodulation (Mg treatment), are applied to liquid metal to produce nodule graphite. Liquid treatment will fail if the temperature limit is exceeded.

Figure 1. Shrinkage defect formation due to premature solidification [8].

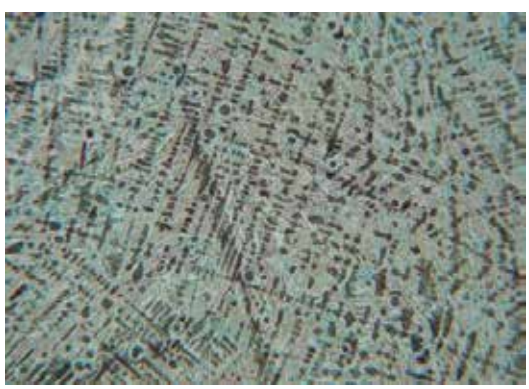

Figure 2. Carbides formation in TWDI [8].

Another issue that should also be considered is the formation of carbides as shown in **Figure 2**. Carbides form as a result of high solidification rate, and solidification rate increases when the thickness of the casting product decreases. Carbides formation in TWDI is to be strongly avoided. To deal with it, solidification rate should be maintained.

3. Designing TWDI products

As mentioned previously, the classification of TWDI is made based on the thickness of casting products which can be applied either in the whole part of product such as plate as shown in **Figure 1** or in just some parts such as in the connecting rod invented by Martinez [9] as shown in **Figure 2**. The thickness of the casting products should not exceed 5 mm.

Soedarsono, Soemardi and Sulamet-Ariobimo have designed two series of plates. In the first series, they designed five plates with the same length and width but different thicknesses. The length is 150 mm while the width is 75 mm. The thicknesses are varied from 5 mm to 1 mm with 1 mm interval. As in the second series, they designed also five plates with the same length, width and thickness. The length and width are still the same as the first series, and the thickness is 1 mm. Since it is just plates, designing the product is not challenging but designing the gating system will be challenging since the design of gating system determines the plates formation. The gating system design made by Soedarsono, Soemardi and Sulamet-Ariobimo is discussed in the following section (**Figure 3**).

Contrary to the plates' design, applying thin wall casting in components are challenging since the part or parts of component being modified should be carefully selected to ensure that the thinning process will not disturb the function and properties of the component. Martinez invented TWDI connecting rod by modifying the I-beam part. I-beam is not a critical part in connecting rod. Martinez modified the solid I-beam to hollow I-beam as presented in **Figure 4**. The wall thickness of the hollow I-beam is 4 mm. The hollow I-beam reduces 100 g of weight of the connecting rod.

Figure 3. TWDI plates [8].

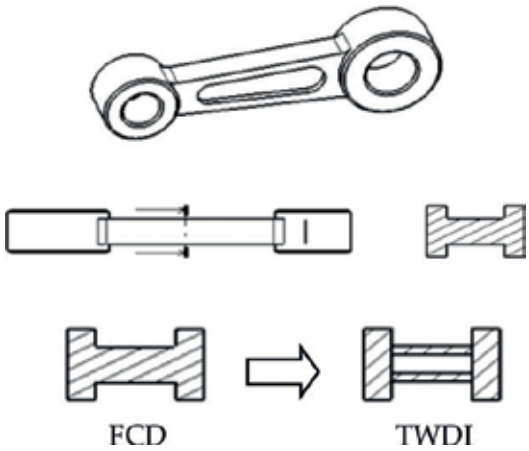

Figure 4. TWDI connecting rod invented by Martinez [9].

4. Casting design for TWDI

There are several ways to maintain cooling rate, but among all of them, casting design is the easiest one. Casting design covers the cast products, gating system and risers. Casting design is important since it determines the quality of the products and their production cost. Regarding TWDI, the casting design should consider fluidity, pouring temperature, pouring time and solidification rate of the molten metal. The casting design should ensure that premature solidification does not occur [10]. The main cause of premature solidification is pouring disruption. To deal with this, pouring stability should always be maintained.

Many researchers used steps design to produce TWDI plates. Javaid [11] designs are presented in **Figure 5**. Javaid used this design to study the effects of chemical composition and process parameters on tensile and impact properties, while Showman [12–14] used groove steps design as shown in **Figure 6** for studying the effects of cooling rate on skin effect formation. Pedersen used both horizontal and vertical steps design, as shown in **Figure 7**, to gain cooling rate from various plate thicknesses. Javaid also modified steps design as presented in **Figure 8** to analyse the effects of position on plates.

Besides the steps design, Stefanescu used horizontal and vertical design as shown in **Figure 9a** and **b**. The vertical design was made after unsatisfactory data gained from its horizontal design [18, 19]. Stefanescu defined his vertical design as gating system, casting products and risers. The casting products were plates of 250 mm in height and 1000 mm in length. The thicknesses of the plates were 6.0, 2.5 and 3.5 mm, which were arranged vertically with cylindrical risers in between. The diameter of the riser is 25 mm, and the number of risers is four [19]. Stefanescu used counter gravity system to maintain the filling rate.

Schrems developed a horizontal design as shown in **Figure 10**, and INTEMA team developed several designs as shown in **Figure 11**. From his design, Schrems found that the condition of the plates together with their thickness affects mechanical properties and reducing cooling rate will make TWDI characteristic equal to general casting. INTEMA used the design shown in **Figure 11a** and **b** to evaluate the graphite characterizations. The results obtained from the

http://dx.doi.org/10.5772/intechopen.72117

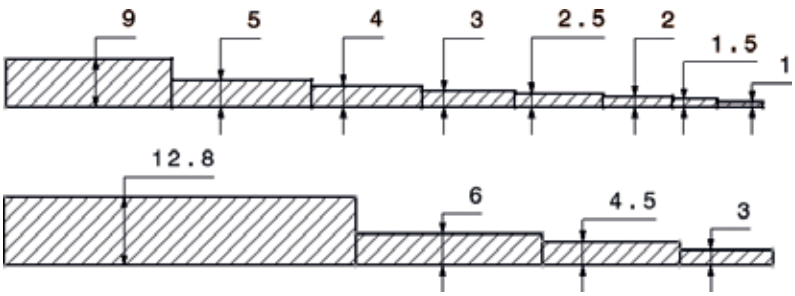

Figure 5. Javaid designs [11].

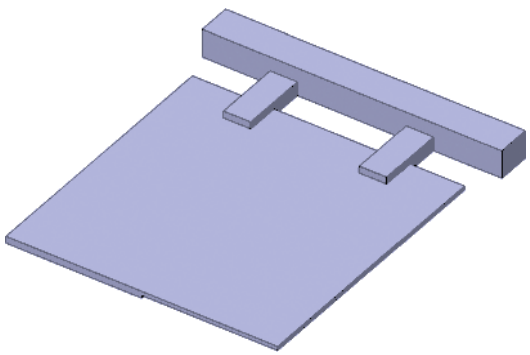

Figure 6. Showman designs [12–14].

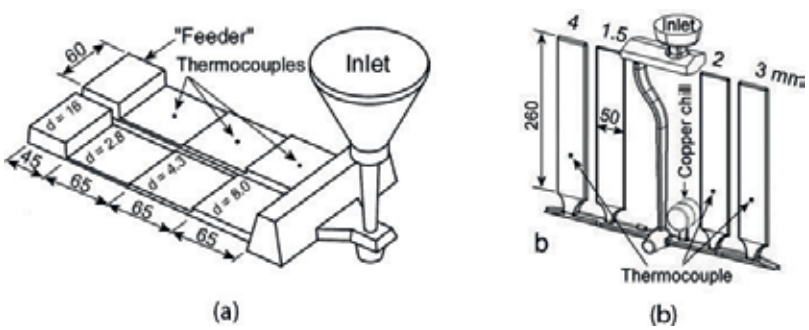

Figure 7. Pedersen designs [15–17]. (a) Horizontal design; (b) vertical design.

first two designs were used to develop the other designs as shown in **Figure 11c** and **d**. The new designs were used for further research.

Labreque used the design shown in **Figure 12** to study the effects of cooling rate on microstructure and mechanical properties of TWDI. The design developed by Labreque resembles industrial condition. Filling process was maintained by using pouring basin, while the adjustment of undercooling temperature and cooling rate was controlled by using material known as low-density alumina silicate. This combination leads to the similarity of TWDI with the specification of ductile iron.

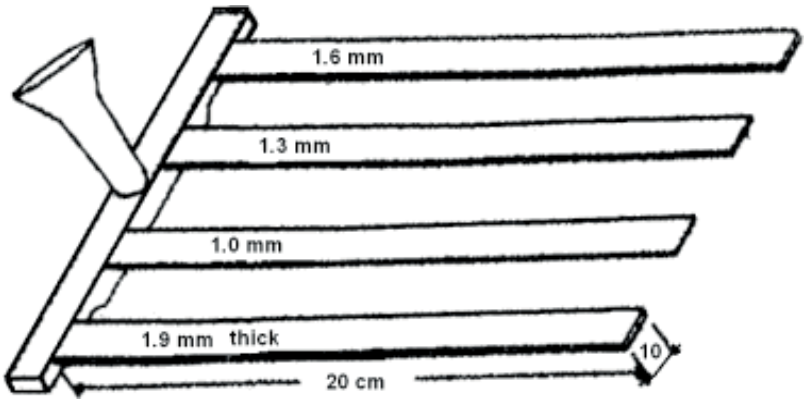

Figure 8. Javaid designs [11].

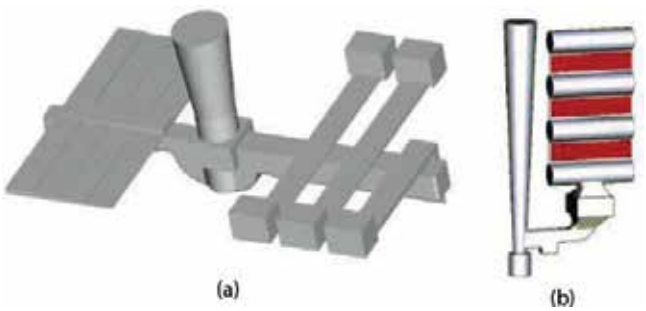

Figure 9. Stefanescu designs [2, 18–20]. (a) Horizontal design; (b) vertical design.

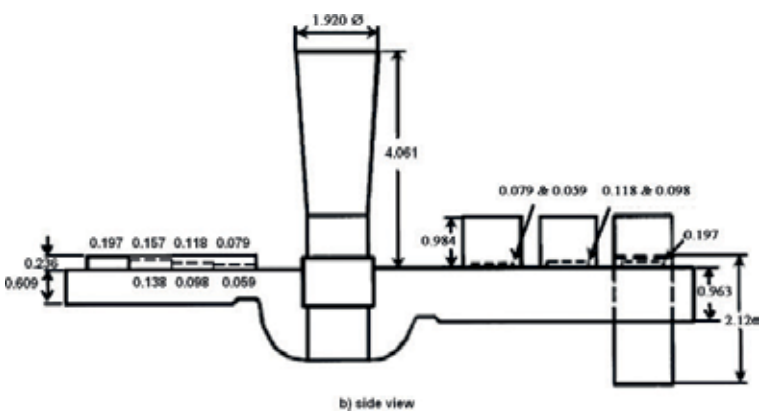

Figure 10. Schrems design [21, 22].

http://dx.doi.org/10.5772/intechopen.72117

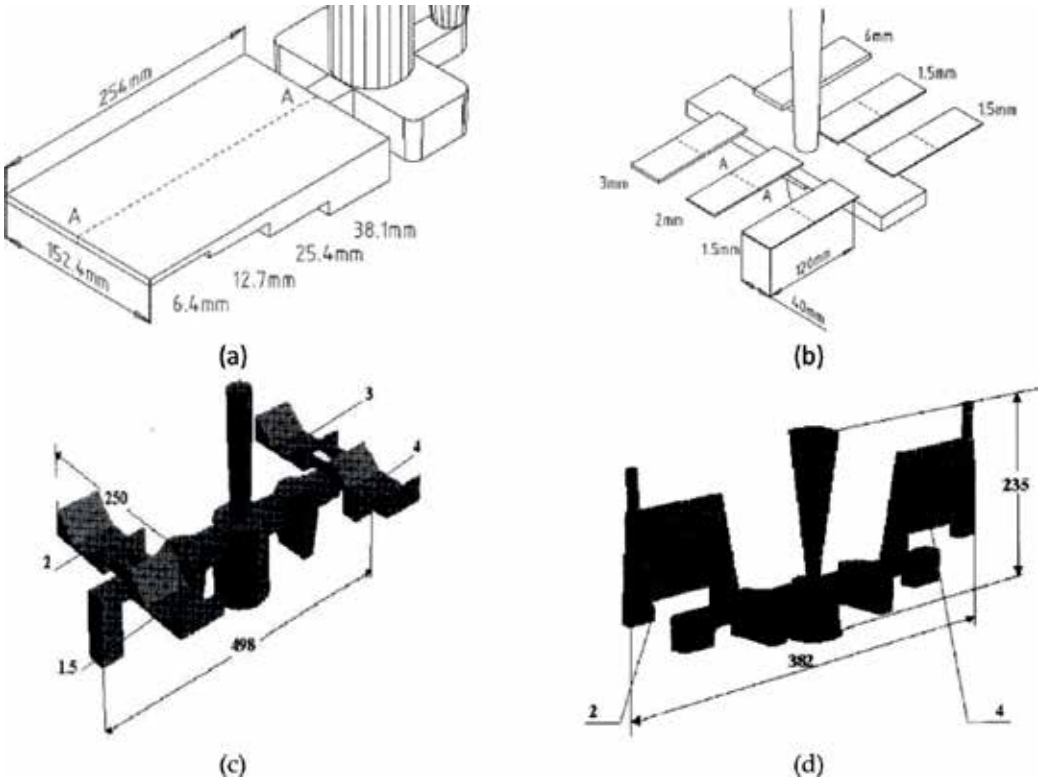

Figure 11. INTEMA designs [23–27].

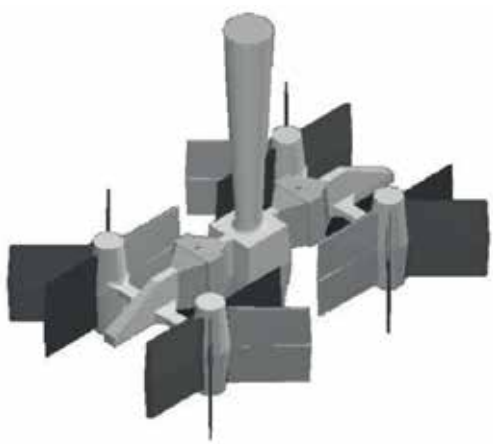

Figure 12. Labreque design [28–30].

This section shows that all researchers are producing their TWDI plates using varied casting designs in horizontal and vertical casting position. This demonstrates how important is an appropriate gating system design to produce TWDI products, whether plates or components.

5. Purposed casting design for TWDI plates

As mention previously, Soedarsono, Soemardi and Sulamet-Ariobimo in their works developed vertical casting designs to produce their plate series. They developed two models of vertical casting design. The first model was based on Stefanescu vertical casting design which used gating system and risers as presented in **Figure 13**.

Soedarsono, Soemardi and Sulamet-Ariobimo modified the Stefanescu design in the number, dimension and thickness of the plates produced. Stefanescu design produced three plates with the dimension of 100 mm × 25 mm and thicknesses of 2.5, 3.5 and 6.0 mm. The design purposed by Soedarsono, Soemardi and Sulamet-Ariobimo produced five plates with the dimension of 150 mm × 75 mm and thicknesses of 1.0, 2.0, 3.0, 4.0 and 5.0 mm. The casting design consists of down sprue, runner, ingate, risers and plates. Every plate is clamped by risers.

Soedarsono, Soemardi and Sulamet-Ariobimo also modified the arrangement of the plates. Since it is a vertical casting design, they placed the thinnest plate near the ingate. This is contrary to the general rule of casting. In the general rule of casting, ingate should not be placed in the thinnest part since it could block the filling process due to first place to solidify. But Soedarsono, Soemardi and Sulamet-Ariobimo assumed that the heat in the running liquid metal will prevent the thinnest part of the casting to solidify or known as premature solidification. Therefore, as long as the liquid metal runs along the system, the thinnest part will not solidify and premature solidification

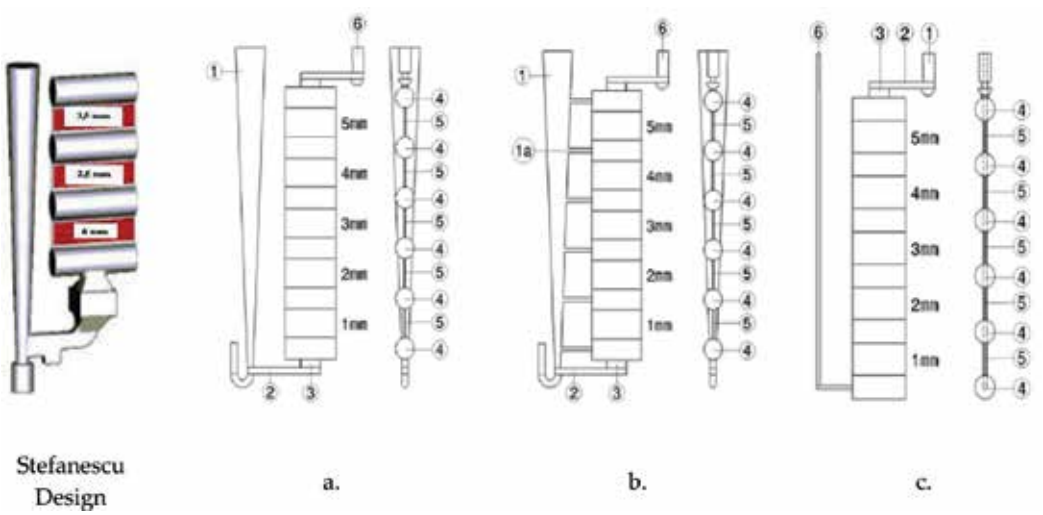

Figure 13. Soedarsono designs [3–8, 31–33]. Vertical casting. 1—Down sprue; 1a—supporting gate; 2—runner; 3—ingate; 4—riser; 5—plate; 6—gas tunnel.

will not happen so the liquid metal can fulfil the mould. This assumption was verified during the casting process. A minor disturbance during the pouring process resulted in defective products.

Soedarsono, Soemardi and Sulamet-Ariobimo proposed three types and all of them produced TWDI plates with ferrite matrix. After evaluating the microstructures and tensile properties of every plates resulting from every types [3, 4, 31–33], they chose the first type which is presented in **Figure 13a** for further developments.

Soedarsono, Soemardi and Sulamet-Ariobimo also developed vertical casting design to produce TWDI without using gating system as the second model shown in **Figure 14**. The dimension and thickness of the plates produced are same as the previous designs. In this model, they proposed two types of design. These designs produced TWDI plates with perlite matrix.

Both models were able to produce TWDI plates. This showed that the casting design proposed were able to produce TWDI plates. Comparing the design of both models revealed that the advantage of the second model is high casting yield, while the first design tends to reduce the casting failure. Both models have their own solidification rate as shown by the microstructures. The first model has ferrite as a matrix, and the second one has perlite. Microstructures represent solidification rate. The conclusion made based on the microstructure formation is that the second model has higher solidification rate than the first one.

Later Soedarsono, Soemardi and Sulamet-Ariobimo modified the chosen design presented in **Figure 13a** for further development. They changed the thickness of the plate from 1 to 5 mm to only 1 mm in all position to discover the ability of the casting design. Experimental studies showed that all plates were formed during the casting process and presented with ferrite matrix.

Based on the latest design, Sulamet-Ariobimo and Gumilang modified the design of vertical casting. They reduced the number of the plates and minimised the dimension of the gating system to gain higher casting yield. The improved design is presented in **Figure 15**. This design produced TWDI in perlite matrix.

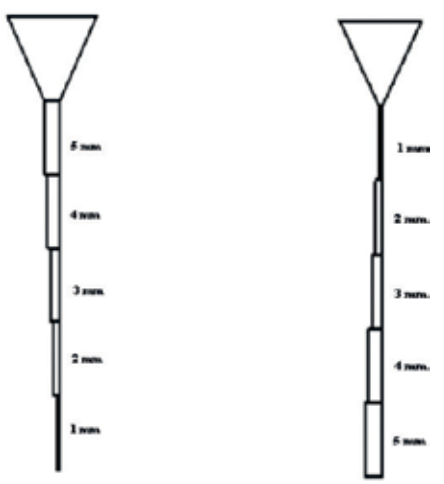

Figure 14. Soedarsono designs [6]. Vertical casting without gating system.

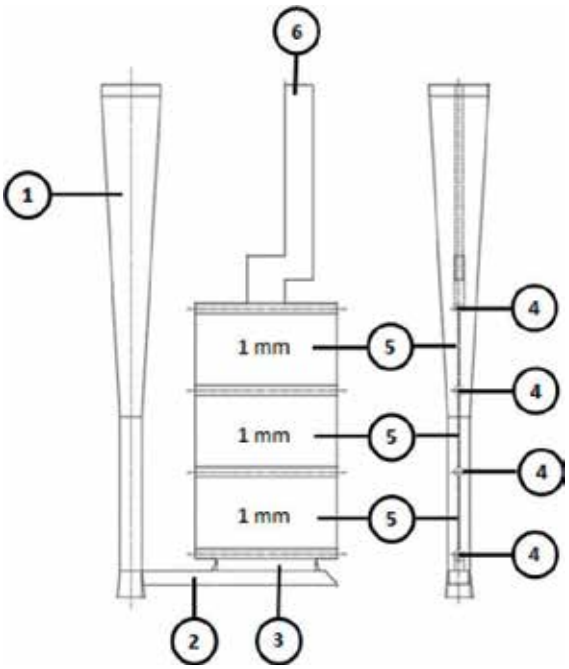

Figure 15. Improved design [34]. 1—Down sprue; 1a—supporting gate; 2—runner; 3—ingate; 4—riser; 5—plate; 6—gas tunnel.

6. Characterisation

Characterisation, especially tensile test, become an important issue in TWDI production since TWDI properties should be same as FCD and thinning process should not change the material properties. ASTM has determined the tensile specimen for TWDI or TWADI, but JIS has not determined which kind of specimen should be used for TWDI or TWADI.

Referring to ASTM Standard, researchers tended to use ASTM E8 [35] as shown in **Figure 16**, for the tensile specimen. While in JIS, several types of tensile specimens can be applied in plate. However, each type of this specimen gave different results. Sulamet-Ariobimo et al. investigated this [36] and decided to use JIS Z2201 No. 5 [37], shown in **Figure 17**. This decision was made based on the findings that fracture propagation in TWDI and nonferrous metals needs wider width.

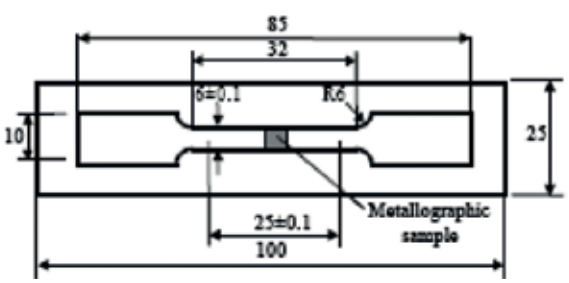

Figure 16. Tensile specimen of ASTM E8 [35].

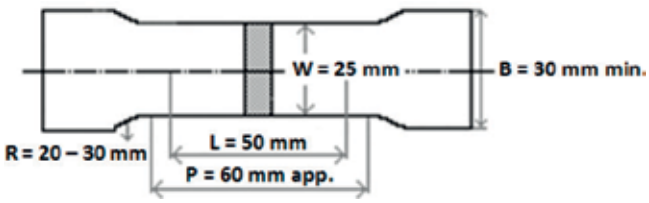

Figure 17. Tensile specimen of JIS Z2201 No. 5 [37].

7. Skin effects

Skin effect [13] or flake graphite rim anomaly [18] is a layer of flake or vermicular graphite formed in outer layer of ductile iron microstructure. This layer tends to appear in sand casting products. The formation of skin effect occurred due to magnesium malfunction. The malfunction of magnesium is caused by several things such as the presence of sulphur or oxygen. Magnesium tends to bind with sulphur which produce MgS or with oxygen which produce MgO. Ruxanda [18] assumed that skin effect was formed due to different level of magnesium content. Aufderheiden [13] found that besides magnesium content, the type of sand also contributed to the formation of skin effect. Sulamet-Ariobimo [38] found that besides magnesium content, cooling rate also influences the formation of skin effect.

Goodrich in Dix [19] stated that skin effect tends to disturb the tensile properties. Ruxanda [18] found difference of magnesium content between bulk and rim area. He concluded that skin effect was formed due to the lack of magnesium. Boonmee [39] supported the Ruxanda's conclusion and concluded that skin effect is formed due to depletion of magnesium. The magnesium depletion is caused by the reaction of magnesium with sulphur and oxygen. Labreque [31] found that although skin effect is detrimental to mechanical properties but up to certain limit, it supports the homogenization of microstructure. Skin effect is an acceptable defect in general casting since it will vanish during the finishing process, but it is vice versa for TWDI. The thickness of TWDI makes it impossible to apply machining process to dispose skin effect. This is the reason why the formation of skin effect in TWDI should be avoided.

8. Conclusion

Light weight components are produced to answer the needs of lower energy consumption. TWDI is produced by applying TWC to ductile iron casting. This will enrich the material preference for lighter weight. TWDI has higher design flexibility than aluminium, which is one of the reasons to choose TWDI rather than aluminium.

During TWDI production, problems occur due to its thickness and liquid treatment process. A vertical design has been made and is able to produce TWDI plates with 1 mm thickness. This design puts the ingate in the thinnest part, which is controverted to the general rule of casting. The casting will be succeeded if the pouring process runs smoothly, while slight interruption will cause failure.

Apart from the regular casting defects, the presence of skin effect is also detrimental to TWDI. In general casting, skin effect can be removed by machining process. This removal process cannot be applied in TWDI.

Author details

Rianti Dewi Sulamet-Ariobimo[1]*, Johny Wahyuadi Soedarsono[2] and Tresna Priyana Soemardi[2]

*Address all correspondence to: rianti.ariobimo@gmail.com

1 Universitas Trisakti, Indonesia

2 Universitas Indonesia, Indonesia

References

[1] Caldera M, Chapetti M, Massone JM, Sikora JA. Influence of nodule count on fatique properties of ferritic thin wall ductile iron. Materials Science and Engineering. 2007;**23**(8):1000-1004

[2] Stefanescu DM, Dix LP, Ruxanda RE, Corbitt-Corburn C, Piwonka TS. Tensile properties of thin wall ductile iron. AFS Transactions. 2002;**02-178**:1149-1162

[3] Soedarsono JW, Suharno B, Sulamet-Ariobimo RD. Effect of casting design to microstructure and mechanical properties of 3 mm TWDI plate. Advance Materials Researchs. 2012;**415-417**:831-837

[4] Soedarsono JW, Sulamet-Ariobimo RD. Effect of casting design to microstructure and mechanical properties of 1 mm TWDI plate. Applied Mechanics and Materials. 2012;**110-116**:3301-3307

[5] Suharno B, Soedarsono JW, Sulamet-Ariobimo RD. The effect of plates position in vertical casting producing thin wall ductile iron. Advance Materials Researchs. 2011;**277**:66-75

[6] Sulamet-Ariobimo RD, Soedarsono JW, Nanda IP. The effect of vertical step block casting to microstructure and mechanical properties in producing thin wall ductile iron. Advance Materials Researchs. 2013;**789**:387-393

[7] Sulamet-Ariobimo RD, Soedarsono JW, Suharno B. Cooling rate analysis of thin wall ductile iron using microstructure examination and simulation. Applied Mechanics and Materials. 2015;**752-753**:845-850

[8] Sulamet-Ariobimo RD. Thin wall ductile iron casting for thin wall austempered ductile iron. [Dissertation]. Indonesia: Universitas Indonesia; 2010

[9] Martinez RA, Boeri RE, Sikora JA. Application of ADI in high strength thin wall automotive part. In: Proceedings of 2002 World Conference on ADI. AFS; 2002

[10] Tomovic M. Designing thin section. Modern Casting. 2003;**93**(5):55-56

[11] Javaid A, Thomson J, Sahoo M, Davis KG. Factors affecting the formation of carbides in thin wall DI castings. AFS Transactions. 1999;**74**:441-451

[12] Showman RE, Aufderheide RC. Getting to the core of thin-walled casting. Modern Casting. 2004;**94**(4):32-34

[13] Aufderheiden RC, Showman RE, Hysell MA. Controlling the skin effect on thin wall ductile iron casting. AFS Transactions. 2005;**5-043**:567-579

[14] Showman RE, Aufderheide RC, Yeomans N. Ironing out thin-wall casting defects, Modern Casting. 2006;**96-7**:29-32

[15] Pedersen KM, Tiedje NS. Temperature measurement during solidification of thin wall ductile cast iron. Part 1: Theory and experiment. Measurement. 2007;**05-200**:1-10

[16] Pedersen KM, Tiedje NS. Graphite nodule count and size distribution in thin-walled ductile cast iron. Materials Characterization. 2007;**09-001**:1-11 (09)

[17] Pedersen KM, Tiedje NS. Temperature measurement during solidification of thin wall ductile cast iron. Part 2: Numerical stimulation. Measurement. 2007;**05-003**:1-8

[18] Ruxanda RE, Stefanescu DM, Piwonka TS. Microstructure characterization of ductile thin wall iron casting. AFS Transaction. 2002;**02-177**:1131-1147

[19] Dix LP, Ruxanda RE, Torrance J, Fukumoto M, Stefanescu DM. Static mechanical properties of ferritic and perlitic light weight ductile iron casting. AFS Transactions. 2003;**03-109**:895-910 (03)

[20] Stefanescu DM, Ruxanda R, Dix LP. The metallurgy and tensile mechanical properties of thin wall spheroidal graphite iron. International Journal of Cast Metal Research. 2003;**16**:319-324

[21] Schrems KK, Dogan ON, Hawk JA. Verification of thin wall ductile iron test methodology. Journal of Testing and Evaluation. 2002;**30**(1)

[22] Schrems KK, Hawk JA, Dogan ON, Druschitz AP. Statistical analysis of the mechanical properties of thin-walled ductile iron casting. 2003. SAE Technical Paper Doc. No. 2003-01-0828

[23] Borrajo JM, Martinez RA, Boeri RE, Sikora JA. Shape and count of free graphite particles in thin wall ductile iron castings. ISIJ International. 2002;**42-3**:257-263

[24] David P, Massone J, Boeri R, Sikora J. Mechanical properties of thin wall ductile iron – Influence of carbon equivalent and graphite distribution. ISIJ International. 2004;**44-7**:1180-1187

[25] Caldera M, Massone JM, Boeri RE, Sikora JA. Impact properties of thin wall ductile iron. ISIJ International. 2004;**44**(4):731-736

[26] David P, Massone JM, Boeri R, Sikora JA. Gating system design to cast thin wall ductile iron plates. International Journal of Cast Metal Research. 2005;**18-5**:1-12

[27] Caldera M, Chapetti M, Massone JM, Sikora JA. Influence of nodule count on fatigue properties of ferritic thin wall ductile iron. Materials Science and Engineering. 2007;**23-8**:1000-1004

[28] Labreque C, Gagne M. Development of carbide free thin wall ductile iron casting. AFS Transactions. 2000;**108**:31-38

[29] Labreque C, Gagne M, Javaid A, Sahoo M. Production and properties of thin wall ductile iron castings. International Journal of Cast Metals Research. 2003;**16**:313-317

[30] Labreque C, Gagne M. Optimizing the mechanical properties of thin-wall ductile iron casting. AFS Transactions. 2005;**05-116**:1-10

[31] Soedarsono JW, Suharno B, Sulamet-Ariobimo RD. Effect of casting design to microstructure and mechanical properties of 5 mm TWDI plate. Applied Mechanics and Materials. 2012;**152-154**:1607-1611

[32] Sulamet-Ariobimo RD, Soedarsono JW, Suharno B. Effect of casting design to microstructure and mechanical properties of 2 mm TWDI plate. Advance Materials Researchs. 2013;**652-654**:2404-2408

[33] Sulamet-Ariobimo RD, Soedarsono JW, Suharno B. Effect of casting design to microstructure and mechanical properties of 4 mm TWDI plate. Advance Materials Researchs. 2013;**702**:269-274

[34] Sulamet-Ariobimo RD, Gemilang Y, Dhaneswara D, Soedarsono JW, Suharno B. Casting design modification to improved casting yield in producing thin wall ductile iron plate. 2017 (in press)

[35] ASTM. E8 Standard Test Methods for Tension Testing of Metallic Materials. Pennsylvania, USA: American Society for Testing and Material; 2000

[36] Sulamet-Ariobimo RD, Soedarsono JW, Sukarnoto T, Rustandi A, Mujalis Y, Prayitno D. Tensile properties analysis of AA1100 aluminium and SS400 steel using different JIS tensile standard specimen. Journal of Applied Research and Technology. 2016;**14**:148-153

[37] JIS. JIS Z2201-2000, Tension Test Pieces for Metallic Materials. Tokyo, Japan: Japanese Standard Association; 2000

[38] Sulamet-Ariobimo RD, Soedarsono JW. Effect of plate thickness and casting position on skin effect formation in thin wall ductile iron. International Journal of Technology. 2016;**3**:375-382

[39] Boonmee S. Ductile and compacted graphite iron casting skin – Evaluation effect on fatique strenght and elimination. [Dissertation]. United State of America: Ohio State University; 2013

Chapter 2

Thermal Analysis of Ductile Iron Casting

Vasudev D. Shinde

Additional information is available at the end of the chapter

http://dx.doi.org/10.5772/intechopen.72030

Abstract

Pure metals solidify with a solidification front that is very well defined and a clearly delineated solid-liquid interface. Ductile cast iron solidification is characterised by a very thin solidified skin and appearance of different phases. The outer skin is formed being very thin in ductile iron; the expansion occurs due to graphite nucleation into the casting forces to the mould walls. With proper care taken while designing and during melt processing stage, quality ductile iron castings can be produced with minimal risering. With recent developments in sensing and storing instruments, it is now possible to see and measure structural transformations within the solidification in ductile iron castings very precisely. The shape of a cooling curve measured by a thermocouple mounted on a thermal analysis sample cup reflects the solidification process of the melted cast alloy for the given solidification conditions. By analysing particular cooling curve, the solidification start, eutectic arrests, recalescence, amount of undercooling and end of freezing temperature temperatures are generated. The thermal analysis data so generated will be used to study composition, soundness, chill and microstructure by analysis of cooling curve. The cooling rates measured in degrees per second at different stages of solidification sequence will be analysed and correlated with the properties of the castings to be produced from the same melt.

Keywords: ductile iron, thermal analysis, solidification, cooling curves, microstructure

1. Introduction

Ductile iron possesses the processing advantages of grey iron, such as low melting point, good fluidity, castability and machinability, and engineering advantages of steel, including high strength, ductility and wear resistance. Achieving the desired quality consistently at low cost in a production foundry is, however, still a challenge. Addition of small amount of cerium or magnesium to molten cast iron changes the shape of graphite from laminar to spheroidal, giving rise to spheroidal graphite iron or ductile iron. The rapid growth in industrial

applications of ductile iron (DI) is driven by its versatility and high performance at low cost. It offers a good combination of tensile strength and ductility. This allows designers to select ductile iron for a wide range of applications. Ductile iron also offers cost savings compared to steel and malleable iron castings through higher yield and thereby lower melting energy. Formation of graphite during solidification leads to lower volumetric shrinkage in ductile iron (compared to steel), necessitating smaller and fewer feeders to prevent the formation of shrinkage defects. Further cost advances can be achieved by eliminating heat treatment of as-cast DI parts.

The near-spherical shape of the graphite nodules distributed evenly in the matrix phase of ductile iron enhances its ductility and impact resistance along with tensile and yield strength equivalent to a low carbon steel. While ferritic ductile iron can be used as 'as-cast', it may also be annealed to increase its ductility and low-temperature toughness. The pearlitic ductile iron has graphite spheroids in a matrix of pearlite, resulting in high strength, good wear resistance, moderate ductility and impact resistance. The most commonly used ferritic-pearlitic ductile iron containing both ferrite and pearlite in matrix offers a good combination of tensile strength and ductility with good machinability and low production costs.

The ductile iron castings are produced in a wide range of weight, from a few grams to a hundred tons or more, greatly varying in shape and size depending on the applications (**Figure 1**). Many forged and fabricated steel components are getting replaced by ductile iron castings, owing to their good combination of mechanical properties such as strength, wear resistance, fatigue strength, toughness and ductility coupled with economic production. The specifications of ductile irons with ferrite/pearlitic matrix with different grades are shown in **Table 1**. They are used in safety parts in automobiles, armatures, pumps and machine tools. They are also used in parts subjected to high pressure, such as pressure containers and hydraulics. Many welded assemblies and forgings used in governor housings, armatures and car parts (like brake calipers and gear housings, hydraulic parts, crankcases and blower buckets) are being replaced by ferritic ductile iron castings.

Figure 1. Ductile iron castings used in automobile, agriculture and sanitation.

Country/region specification	Minimum tensile strength/elongation (N/mm^2/%)								
Europe EN-GS CEN 1563:1997	350-22	400-18	400-10	450-10	500-7	600-3	700-3	800-2	900-2
UK BS2789 1985	350/22	400/18	420/10	450/10	500/7	600/3	700/2	800/2	900/2
USA ASTM A356 1993[1]	60-40-18	60-42-10	65-45-12	70-50-05	80-55-06	80-60-03	100-70-03	120-90-02	
Japan JIS FCD G5502 1995	350-22	400-18	400-10	450-10	500-7	600-3	700-3	800-2	
International ISO 1083 1987	350-22	400-18	400-10	450-10	500-7	600-3	700-3	800-2	900-2
Typical hardness (HB)	<160	130–175	135–180	160–210	170–230	190–270	225–305	245–335	270–360
Typical structures[2]	F	F	F	F & P	F & P	F & P	P	P or T	TM

[1]60-40-18 refers to minimum tensile strength (lbf/in^2)—minimum proof stress (lbf/in^2)—% elongation.

[2]The structures are: F, ferrite; P, pearlite; T, tempered; TM, tempered martensite.

Table 1. Specifications for ductile cast irons [1].

2. Production of ductile iron

Production of thin wall ductile iron (TWDI) castings is challenging due to faster solidification rates in thinner sections, affecting the graphite nodules and matrix phases, which in turn affect the mechanical properties. Ductile iron castings for the applications mentioned earlier are normally produced by sand casting or shell moulding processes, with cores used to create hollow internal sections. Sand casting is the most common process, due to the relatively low cost of production as compared to other manufacturing techniques. The metal composition and micro-constituents in the phases, as well as the cooling rates, control the mechanical properties of these TWDI castings. While the casting wall thickness affects the amount of heat to be transferred, the mould wall thickness affects the rate of heat transfer and thereby the rate of metal cooling during casting solidification. Kasvayee et al. examined localised strain at the location of the first microcrack to form during testing using digital image correlation (DIC) [10]. It has been found that inoculation process influences the microstructure and the fatigue resistance of heavy section pearlitic ductile iron castings [11]. The graphite shape factors were studied on the metallographic samples and evaluated as a function of the chemical composition, and the solid fraction was analysed [12]. The sudden temperature drop of liquid iron shows increased cooling rate, which will affect the solidification and microstructure in thin-walled castings [13].

2.1. Micro-constituent phases

The solidification process in thin wall ductile iron casting involves nucleation of micro-constituent phases such as austenite, graphite and/or carbides. The formation of these phases

depends upon the chemical composition of cast metal, inoculation processing and cooling rate. The chemical composition (especially carbon and silicon) decides whether the DI is hypoeutectic, eutectic, or hypereutectic in nature. The control of chemical composition and inoculation is essential to avoid nucleation of primary carbides. Faster cooling and solidification in thin sections lead to the formation of primary carbides along with austenite dendrites in the structure instead of graphite nodules. The trapping of carbon by formation of carbide restricts the formation of graphite. The inoculation provides more number of nucleating sites on which graphite can grow.

The chemical composition controls the amount of graphite, ferrite and pearlite in the structure. The silicon as a graphitiser facilitates the formation of graphite instead of carbides. The increase in carbon and silicon increases the carbon equivalent of the casting. Addition of elements like copper and manganese decides the amount of pearlite in the matrix. Silicon is a strong solid solution strengthener; it reduces undercooling and avoids carbide formation by nucleating graphite. It increases volume fraction of ferrite and nodule count. Copper is a strong pearlite promoter; its addition up to 1% converts ferritic structure into pearlitic. Arsenic, tin and antimony promote pearlite and carbides and are hence kept to lower limits; their effect can be counteracted by cerium additions [2]. Achieving the desired microstructure in thin castings necessitates controlling chemical composition and cooling rates during solidification.

2.2. Cooling rates

In ductile iron castings, the carbon equivalent should be high (hypereutectic) in the case of very thin-walled components to avoid formation of primary carbides [2]. Thin walls cool faster due to the larger surface area available for heat transfer through mould, influencing the microstructure and mechanical properties of the casting. Design parameters such as the area of the thin wall, its proximity to gate and the availability of an adjacent heavy section influence the process limits of achievable wall thickness [3]. An increase in the number of graphite spheroids can be expected to result in a corresponding increase in the amount of ferrite formed at a given cooling rate and for a given austenite composition. This effect is readily observed in ferrite-pearlite structures of ductile cast irons.

The graphite nodule count and its size distribution are important in deciding the quality of the DI castings. The sufficient number of graphite nodules is required in order to avoid formation of carbides during solidification, especially in thin-walled castings because of the high solidification rate. The total number of particles decreases with increasing plate thickness. Austenite will contract during solidification, but this will be compensated by the expansion of graphite. It is especially important that there is sufficient graphite expansion in the last part of solidification when feeding from an external feeder normally is impossible. Sufficient graphite expansion in the latter stages of solidification is identified by nucleation of graphite nodules, giving many small graphite nodules in the microstructure [4].

The cooling rates and hence the solidification morphology in ductile irons depend on casting wall thickness. The ductile iron microstructures are very sensitive to actual solidification

rate and inoculation processing in casting. The inoculation will provide nucleation sites (substrates) in the melt of specific size such that these nuclei will grow. The high nucleation rate in thin wall ductile iron (due to fast cooling) will thus show more number of graphite nodules in thinner compared to thicker sections. Further, higher growth rates in thicker sections will give less number of graphite nodules, but they will be coarser in size. The solidification rates are also controlled by heat transfer through mould; hence, the use of optimal sand wall thickness to achieve proper cooling rates becomes essential. Thus, the casting geometry (wall thickness), metal composition (especially micro-constituents) and mould configuration (cooling rate) together affect the solidification structure in ductile iron casting production.

2.3. Processing parameters

The properties of as-cast ductile iron are largely driven by liquid metal processing, including melt pretreatment, magnesium treatment and inoculation processing. The melt pretreatment involves controlling the initial sulphur content in the liquid metal so as to facilitate magnesium treatment. If the initial sulphur content is high, then it reacts with magnesium and forms magnesium sulphide, decreasing the effectiveness of magnesium treatment. Also, manganese reacts with sulphur and forms manganese sulphide; hence, Mn:S ratio is to be maintained to control the final properties of the ductile iron.

The magnesium treatment involves addition of magnesium and/or cerium in different forms to facilitate effective melt treatment and achieve spheroidisation of graphite during the solidification of the metal. The most common form is ferro-silicon-magnesium, which allows better magnesium recoveries (than other forms, owing to oxidising properties of magnesium). This helps utilise more amount of magnesium for spheroidisation purpose.

Mg treatment eliminates oxide bi-films and produces compact particles in ductile iron melt. Hence, it is usually followed by inoculation treatment, which increases the number of nucleation sites in ductile iron castings. Graphite nucleates on these particles, and its further growth is controlled by austenite dendrites. The shape and size of these graphite spheroids affect the mechanical properties of castings. The time span between inoculation treatment and pouring has a significant effect on elongation but less effect on the tensile strength and hardness of castings [5].

The ratio of ferrite to pearlite in the matrix and the morphology of graphite influence the mechanical properties of ductile iron castings. This also depends upon the cooling rate during solid-state (eutectoid) transformation, nodule count and alloying elements. The studies of nucleation and solidification help in controlling the final properties of varying thickness ductile iron castings. The ferrite being softer gives higher ductility but lower tensile strength than pearlite. Also, the graphite morphology plays an important role; deviation from spheroidal shape reduces the ductility and impact properties [6].

It is therefore important to understand how the different phases nucleate and grow during solidification in order to be able to control the casting process and achieve the desired set of mechanical properties in varying thickness ductile iron castings.

3. Thermal analysis

Recent developments in thermal analysis instruments make it possible to precisely measure and visualise the events within the solidification of iron samples. Data generated from thermal analysis can be used to study composition, soundness, chill and microstructure. The shape of the cooling curve measured by a thermocouple mounted in a thermal analysis sample cup reflects the solidification process of the melted cast alloy for the given solidification conditions. The cooling rates measured in degrees per second at different stages of the solidification sequence can be analysed and correlated with the properties of the castings to be produced from the same melt. Chronologically, the major parts of the curve are pre-liquidus, austenitic arrest, dendritic growth, eutectic solidification, end of freezing and the austenite transformation region. The normal cooling curve gives basic information about the solidification. Additional information can be obtained from the first derivative (DT/dt) of the curve. The cooling rate which is the first derivative calculated by change in temperature per unit time (dT/dt) in °C/s. The horizontal line is the zero line. If the first derivative is zero, it indicates that heat transferred from the solidifying casting equals the heat generated (evolved) due to phase transformation.

A method of thermal analysis of cooling curve is studied by different researchers. Carbon and silicon content can be estimated from cooling curves when iron is solidified in a tellurium-coated sand cup (the tellurium causes the iron to solidify as white iron rather than grey iron). Silicon is a major alloying constituent in cast irons, which raises the graphite eutectic solidification temperature and lowers the carbide eutectic range. To calculate C% and Si%, the austenite liquidus temperature (TAL) of the ductile base iron and the carbide eutectic temperature (CET) arrest temperatures are used. Once the eutectic composition is determined, the silicon and carbon compositions and carbon equivalent (CE) can be obtained by the following equations [7]:

$$\mathrm{TAL} = 0.556\,(2962 - 212.3\,\mathrm{C}\,\% + 0.25\,\mathrm{Si}\%) \tag{1}$$

$$\mathrm{CET} = 2085.4 - 22.7\,\mathrm{Si}\% \tag{2}$$

The cooling curves generated during solidification of alloys can be further analysed by the use of first-order and second-order derivatives to find out the temperature arrest points. The thermal analysis cooling curves can be used for optimisation of inoculation in ductile iron [8]. The minimum eutectic temperature ($T_{\min}$) should be greater than 1140°C to avoid primary carbides in ductile iron, and the angle at the end of solidification in cooling rate curve (VPS) should be between 25 and 45°C to avoid secondary carbides. Furthermore, computer-aided cooling curve analysis can be used for evaluating latent heat evolved during solidification. Iron castings produced with identical chemical composition can have considerable variations in mechanical properties. With thermal analysis, it is possible to predict such variations and correct the melt before pouring.

The thermal analysis studies explore the effect of inoculation on holding time and fading of graphite nodules in ductile iron castings. The undercooling during solidification known as

recalescence ($T_{max} - T_{min}$) depends on inoculation rate. High T_{min} indicates high inoculation effect and indicates that more graphite is precipitated. High recalescence is an indication of poor inoculation [9]. A lower VPS angle (**Figure 2**) indicates better protection against micro-shrinkage tendencies; however too low VPS angle will produce flake graphite. To compare two cooling curves, the separating distance of the two curves as well as the shape similarity of the curves should be considered. The segment of the thermal analysis curve from the liquidus temperature to the end of the eutectic solidification represents the entire solidification range.

3.1. Solidification cooling curves

The composition of the melt and its processing sequence will reflect in the cooling curve; in other words, cooling curve is a fingerprint of the melt. To predict the final microstructure and mechanical properties, the cup thermal analysis was adopted. Cups of the standard shape made in shell mould are used to pour the melt and generate cooling curves with the aid of small K-type thermocouples inserted in glass tubes at the centre of cup cavity. The contact block of cup stands has points which connect thermocouple wires in the cup after fixing the cup. The extension wire made of NiCr and NiAl connects to the positive and negative ends of the thermocouples, respectively, as shown in **Figure 3**. The extension wires are connected to data-logger instrument to store the time temperature history of the solidifying metal as shown in **Figure 3**. The stored data can be retrieved later to generate the cooling curve.

The melt samples of base iron and inoculated molten iron were tested every hour during the day shift in ductile iron production foundry by pouring cups. It is important to note that the use of identical base metal chemistry is required to compare the efficiency of different amounts of inoculants. The plain test cups without tellurium (Te) are used for pouring the test samples. The samples are poured within 5–7 min after inoculation to minimise variations due to fading. In a series of melt processing trials, particle size and method of addition of inoculant were kept constant; the only varying factor was the amount of inoculant.

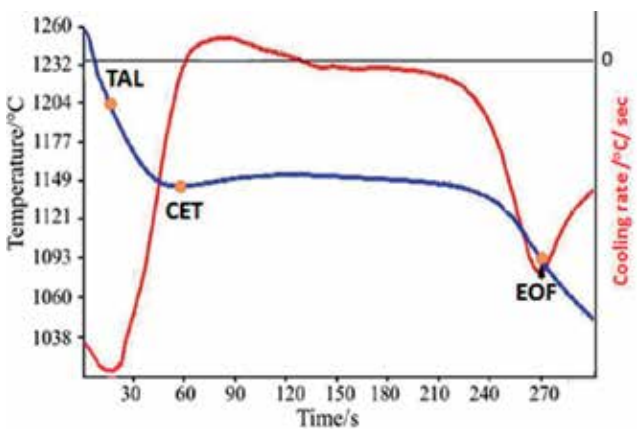

Figure 2. Typical cooling curve and cooling rate in ductile iron [8].

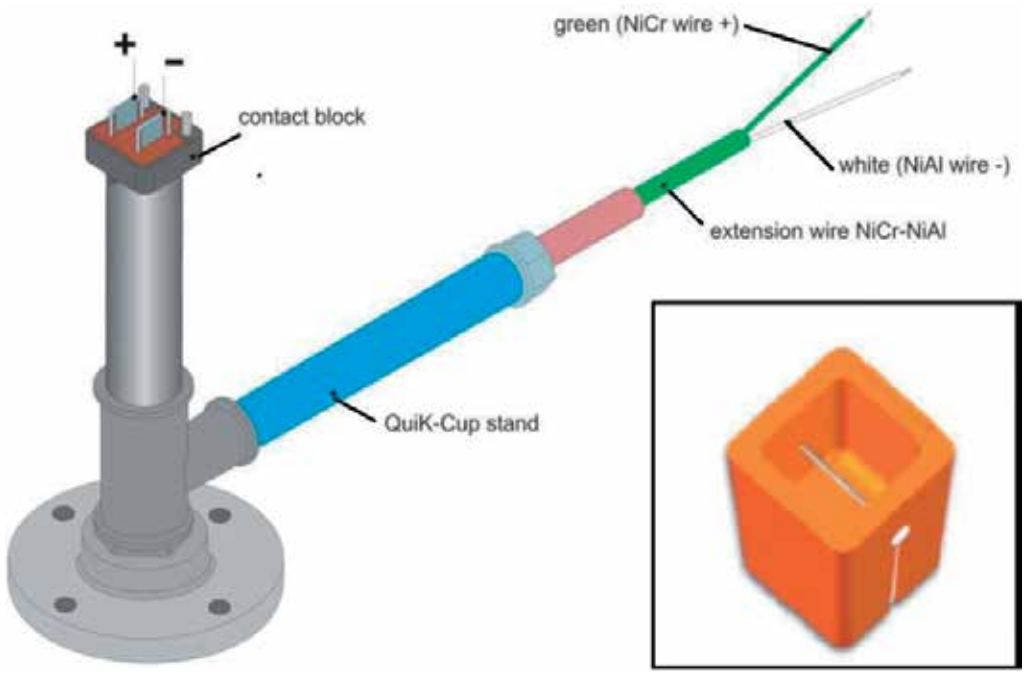

Figure 3. Thermocouple cup holder with extension wires and cup (bottom-right corner).

After testing the inoculated iron, the cooling curves were plotted to analyse the effectiveness of inoculation. The cooling curve analysis includes the liquidus temperature, the eutectic undercooling, the recalescence, the total eutectic freezing zone and the end of freezing. For achieving a smooth and accurate cooling curve, the data is averaged from five consecutive readings. Using this curve, the next data is generated by taking the first derivative. The first derivative is a picture of the actual solidification, and the area it contains is the energy being released by the crystallisation process. The second derivative (if needed) can be used to magnify and detect important events on the overall curve which are indicative at the start or end of a nucleation of a phase in the cooling curve.

The type (inoculant base) and amount of inoculation are varied so as to study its effect on microstructure and properties of ductile iron. By analysing the data generated in the above experiments, the response of these variables on final microstructure of the poured casting can be determined. In the data-logger, the data of the actual temperatures at the tip of thermocouple placed in solidifying metal is stored. The stored data is then retrieved for plotting of time-temperature curve, i.e. cooling curve. The phase transformations during solidification will reflect in the cooling curves and can be identified by calculating a change in the slope by plotting the first derivative of the cooling curve (dT/dt) referred as cooling rate.

The thermal analysis is an effective tool in controlling the melt quality before pouring into actual ductile iron castings. The cooling curve from cup analysis has unique features, affected by melt processing. Five distinct points can be visualised: liquidus temperature (T_{liq}),

minimum eutectic temperature (T_{min}), maximum eutectic temperature (T_{max}), recalescence ($\Delta T = T_{max} - T_{min}$) and end of solidification temperature (TES) and solidification time.

The cooling rate curve with increasing trend passes through zero, marked as eutectic minimum (T_{min}), and, after attaining a peak value, follows a decreasing trend and again passes through zero, noted as maximum temperature (T_{max}). The end of solidification is TES, and cooling rate curve angle at solidus is called VPS. The first peak in cooling rate curve is noted as liquidus temperature (T_{liq}). This is a function of the active carbon equivalent, which shows the integrated effect of all elements that influence solidification process. It indicates the effect of elements which are present in melt, for example C, Si and P, and also some other dissolved elements such as oxygen. It gives more information than carbon equivalent (CE) calculated from chemical analysis. To achieve stable properties in the ductile iron, it is essential that the CE value should be maintained consistently. For hypoeutectic composition (CE < 4.33), the amount of primary austenite is directly proportional to the difference in CE values of eutectic (4.33) and actual melt. Hypereutectic (CE > 4.3) iron will solidify with precipitation of primary graphite (kish graphite) which can give surface defects if proper inoculant is not added. Consequently, this technique can also reveal microstructural information that could not be obtained from the standard metallographic techniques. For example, the amount of austenite cannot be easily determined through classic metallographic techniques because of the solid-state transformations that occur.

The thermal analysis of the ductile iron melts at different processing stages was conducted to study the effect of processing on solidification parameters. The cups were poured with base metal, after addition of FeSiMg alloy in the melt and inoculation processing. Cooling curves were plotted as shown in **Figure 4**. It is observed that inoculation processing increases the overall eutectic temperature and minimises undercooling, i.e. the difference between the minimum and the maximum eutectic temperature ($T_{max} - T_{min}$). The inoculated metal shows a wide range of eutectic freezing.

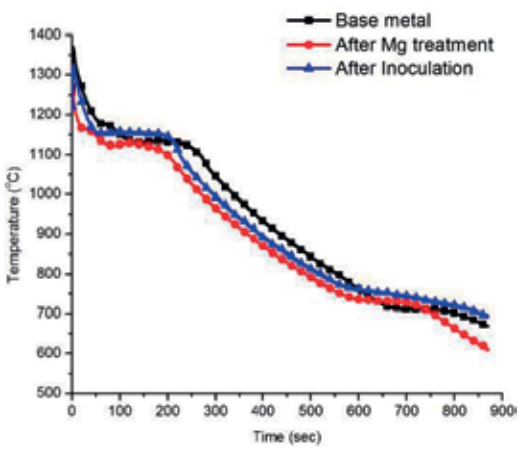

Figure 4. Cooling curves showing effect of melt processing in ductile iron.

Sr. no.	Inoculant type	Si%	Ca%	Ba%	Al%	Zr	Ce%	Fe
1	Ca based	73.34	2.46	–	1.26	1.32	–	Balance
2	Ba based	73.89	1.13	2.84	1.40	–	–	Balance
3	Ce based	72.91	0.96	0.8	0.82	–	1.95	Balance

Table 2. Typical chemical compositions of ductile iron inoculants.

3.2. Effectiveness of inoculation

Ductile iron melts can be inoculated by several methods such as ladle inoculation, in-stream inoculation or mould inoculation. In ladle transfer method, the inoculant is added to the metal as it is transferred from the furnace to the pouring ladle. The turbulence quickly dissolves the inoculant and evenly disperses it throughout the molten bath. For better recovery of the magnesium, inoculation is done in the stream or in the mould. The different nucleation mechanisms are active during the solidification of ductile iron. The solidification behaviour after pouring the metal into the mould can be studied in terms of the heat transfer mechanism in the solidifying metal. The transient temperature data of solidifying metal will be recorded by inserting thermocouples in the casting cavity. These thermal readings are further processed to plot the cooling curves. The analysis of cooling curves will be useful in studying small events occurring during solidification.

For effective and well-controlled inoculation, ferrosilicon of controlled chemical composition is usually used. Active inoculating elements are Ca, Al, Ba, Sr, Zr and Ce; some others are deliberately added in the ferrosilicon alloy. The sample chemical composition of calcium, barium and cerium-based inoculants is shown in **Table 2**. These inoculants were added in varying amounts while transferring the melt from treatment ladle to pouring ladle.

By conducting various trials with different inoculants as mentioned in **Table 2**, the best possible combination could be set for particular foundry processing to determine the optimum addition rate of particular inoculant. The amount of inoculant added could be from 0.05 to 1% of the total weight of liquid metal. With different combinations of melt processing, the cups should be poured to generate the time temperature data for base metal and after inoculation processing. The metal is poured into the cups instrumented with built-in thermocouples. Initially, base metal (without inoculation processing) cup must be poured.

4. Conclusions

The solidification cooling curve, its derivatives, related temperatures and calculated indices are patterns that can be used to assess the melt processing and predict the microstructure and mechanical properties of ductile iron. Inoculation raises both the maximum and minimum eutectic temperatures. The inoculation acts as a deoxidiser, and hence the liquidus temperature of an iron that contains a high amount of oxygen can be reduced by

8–10°C. Both the maximum and minimum eutectic temperatures rises compared to the base metal. The maximum recalescence reduces with an increase in the amount of inoculant. Well-inoculated ductile iron typically shows a recalescence in the range of 2–4°C. Higher recalescence requires more inoculation. Increase in the amount of inoculation decreases the undercooling with an overall increase in the total solidification time. Lower angle of the first derivative at the solidus point indicates high nodule count. It represents the speed with which the cast iron crosses the zone of complete solidification, indirectly measuring the thermal conductivity.

Author details

Vasudev D. Shinde

Address all correspondence to: vasu.metal@gmail.com

DKTE's Textile and Engineering Institute, Rajwada, Ichalkaranji, Kolhapur, India

References

[1] Brown JR. Foseco Ferrous Foundryman's Handbook. Linacre House, Jordan Hill, Oxford: Butterworth-Heinemann; 2000

[2] Pedersen KM, Tiedje NJ. Influence of rare earths on shrinkage porosity in thin walled ductile cast iron. International Journal of Cast Metals Research. 2009;**22**(4):302-305

[3] Hughes ICH. ASM Metals Handbook, Casting. 9th ed. Vol. 15. ASM International; 1992

[4] Skaland T. A new method for chill and shrinkage control in ladle treated ductile iron. In: The 66th World Foundry Congress; Istanbul, Turkey. 2004. pp. 975-987

[5] Pedersen KM, Tiedje NS. Graphite nodule count and size distribution in thin-walled ductile cast iron. Materials Characterization. 2008;**59**:1111-1121

[6] Bockus S, Dobrovolskis A. Peculiarity of producing ferritic ductile iron castings. Materials Science (Medziagotyra). 2004;**10**(1):3-6

[7] Emadi D, Whiting LV, Nafisi S, Ghomashchi R. Applications of thermal analysis in quality control of solidification processes. Journal of Thermal Analysis and Calorimetry. 2005;**81**:235-242

[8] Vaucheret A, Jacquet P, Rossi F, Lagardette P. Optimizing the inoculation of a ductile cast iron using thermal analysis. In: International PhD Foundry Conference; Brno University of Technology, Czech Foundrymen Society. 2009. pp. 1-9

[9] Torrance J, Misterek C, Popovski V. Verification of the dynamic nature of thermal analysis properties in ductile iron. AFS Transactions. 2009;**117**:607-616

[10] Kasvayee KA, Salomonsson K, Ghassemali E, Jarfors AEW. Microstructural strain distribution in ductile iron; comparison between finite element simulation and digital image correlation measurements. Materials Science and Engineering: A. 2016;**655**:27-35

[11] Borsato T, Ferro P, Berto F, Carollo C. Mechanical and fatigue properties of pearlitic ductile iron castings characterized by long solidification times. Engineering Failure Analysis. 2017;**79**:902-912

[12] Stefanescu DM, Alonso G, Larranaga P, Suarez R. On the stable eutectic solidification of iron–carbon–silicon alloys. Acta Materialia. 2016;**103**:103-114

[13] Gorny M. Fluidity and temperature profile of ductile iron in thin sections. Journal of Iron and Steel Research. 2012;**19**(8):52-59

Aluminium Casting

Chapter 3

Depicting Aluminium DC Casting by Means of Dimensionless Numbers

José C. Méndez, Ricardo R. Ambriz,
David Jaramillo and Gabriel Plascencia

Additional information is available at the end of the chapter

http://dx.doi.org/10.5772/intechopen.71893

Abstract

DC casting of aluminium and its alloys is a controlled heat removal solidification process. The rate of heat extraction has strong effects on the microstructure and mechanical properties of the solidified alloy ingots. In view of this strict temperature, control over the ingot as it solidifies should be implemented in order to achieve metal with the best possible properties. In situ direct temperature measurements are complicated; so in this report, the use of dimensionless analysis to predict temperature distributions on the ingots as they are casted is proposed. It is reported that the dimensionless groups that better represent the impact of process variables on the solidification of aluminium and its alloys are the Péclet (Pe) and Biot (Bi) numbers.

Keywords: DC casting, aluminium alloys, dimensionless numbers, solidification, mechanical properties

1. Introduction

Aluminium alloys are widely processed through direct chill (DC) semi-continuous casting. This process was developed almost simultaneously in Europe and in the United States shortly before the Second World War [1].

Nowadays, DC castings can be found in any aluminium casting shop. The process can be described as [2] 'The process involves a short mold of a desired shape to form an ingot by mold cooling. The ingot thus formed is lowered at a predetermined rate and solidification is completed by direct application of water below the mold'.

From the previous description, it is clear that metal solidification strongly depends on cooling water flowrate, casting velocity and mould geometry [3]. Additionally, it is expected that the chemical composition of the cast alloy will influence process parameters [2, 3].

Depending on the aluminium alloy to be casted, different operational problems may arise; for example, consider 1XXX alloys. Given that these alloys are basically constituted of 99% mass aluminium, they require uniform water distribution [2] as well as proper temperature control, since most of the heat loses are attributed to radiation from the metal to its surroundings. Descriptions of problems encountered in DC casting of other aluminium alloying systems can be found elsewhere [2, 4].

As alloying systems get more complex (more components), it becomes more difficult to predict the mechanical properties and structural features of the ingots as they solidify. In view of this, this entry proposes to create a predictive tool to estimate the final alloy properties from dimensionless analysis.

2. Cooling systems in DC aluminium castings

Cooling systems are largely responsible for the solidification of the aluminium ingots. Metal cooling takes place by means of two cooling systems. The primary cooling system is located in the casting mould itself. The mould has a cavity between its walls; thus, cooling occurs as water passes through such cavity. The primary cooling system is used to withdraw the latent heat of solidification; in other words, solidification occurs as a consequence of this cooling system.

The second cooling system consists of water falling from the lower end of the mould. At the bottom of the mould's cavity, there are some holes alongside the length of the mould so water falls from it, forming a water curtain that wets the metal as the ingot is formed. This secondary cooling system removes the sensible heat from the already-solidified ingot. Furthermore, this cooling system completes the solidification of the ingot while it cools down the cast metal. **Figure 1** shows a sketch of the DC casting process.

2.1. Process parameters in DC casting

As sketched in **Figure 2**, during ingot casting three well-defined regions develop: liquid, solid and liquid + solid. The liquid region along with the solid + liquid one is known as sump. The sump is where the actual solidification takes place, and it is bounded between the liquidus and solidus isotherms. The sump itself can be divided into two regions, one known as slurry which is rich in liquid metal and the mushy, which is a mixture between the solid and liquid phases.

Within the sump, as heat is extracted from the liquid, the first solid particles start to appear. These starting solid particles are impinged with liquid metal, leading to a coherent microstructure [1, 5–8]. The microstructure can be altered by changing the process variables.

http://dx.doi.org/10.5772/intechopen.71893

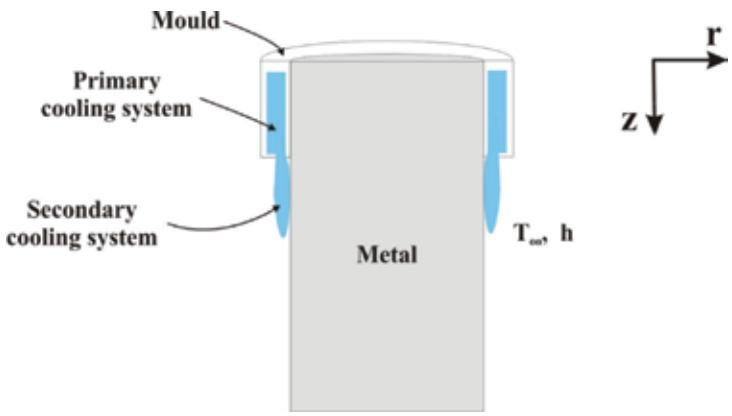

Figure 1. Sketch of an aluminium ingot processed by DC casting.

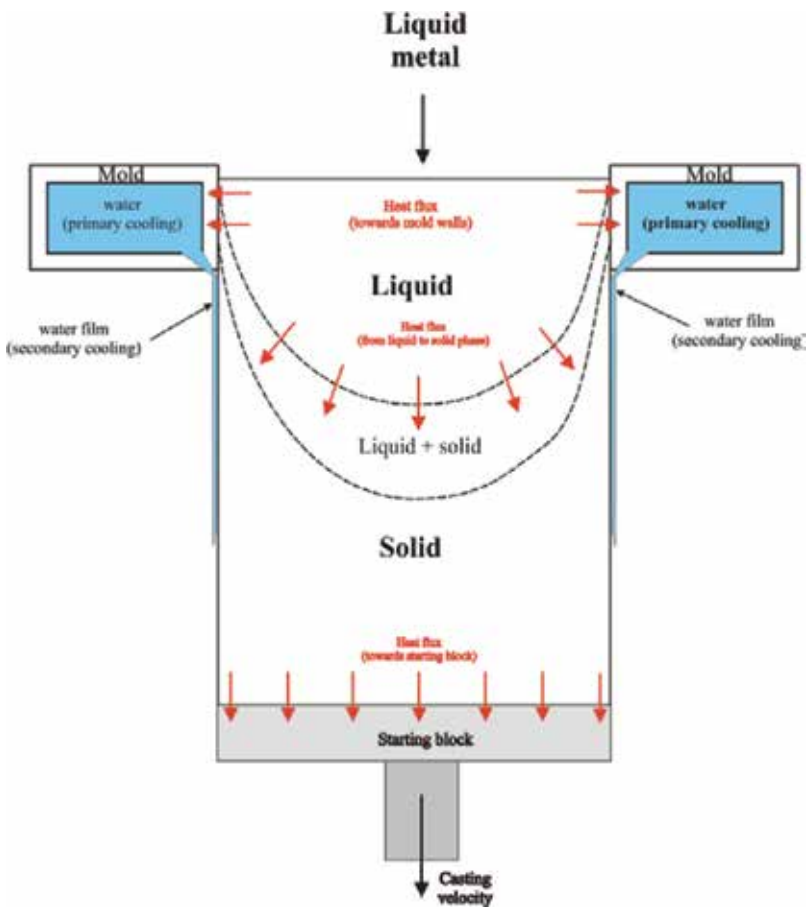

Figure 2. Heat extraction in DC casting; sketch showing main process variables.

The main process variables involved in the DC semi-continuous casting of aluminium and its alloys are:

- Chemical composition
- Cooling water flowrate (cooling rate)
- Casting velocity
- Melt casting temperature (superheat)

2.1.1. Chemical composition

Given the little heat extracted from the liquid phase, most of the heat is withdrawn from the solidification, and the solid phase, thus temperature distribution within the aluminium ingot as it is cooled, might be directly related to the thermal conductivity of the alloy being cast. Depending on the number of alloying elements and the actual aluminium content in the alloy, the liquidus and solidus lines may change accordingly.

Data [9, 10] in **Figure 3** show how the thermal conductivity changes with the aluminium content in different alloys. Such changes directly impact the size and depth of the sump and consequently the local time of solidification; thus, the rate of heat extraction accordingly changes, resulting in modifications to the final microstructure of the solid ingot.

2.1.2. Cooling water flowrate

Cooling water flowrate inside the caster mould is important in the semi-continuous casting of aluminium alloys. Using higher water flow results in higher heat extraction from the melt, and this affects the sump depth.

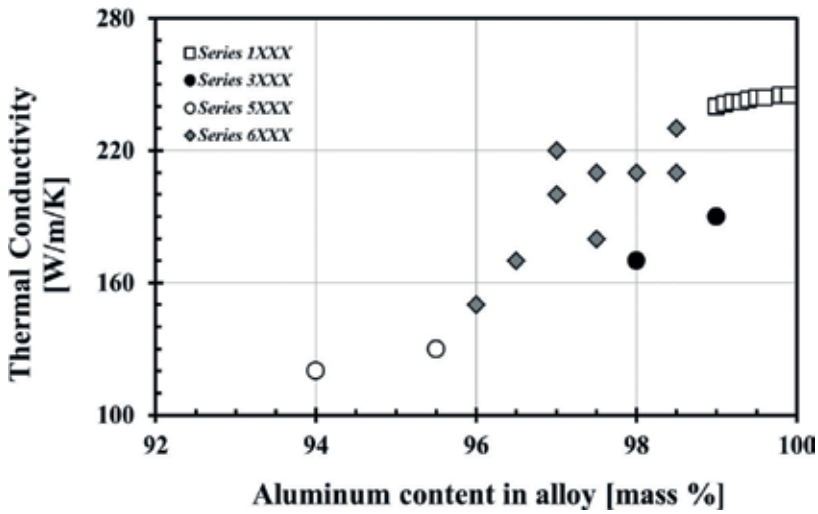

Figure 3. Thermal conductivity of some aluminium alloys [9, 10].

The overall heat balance determines that it must be a minimum water flowrate that can be used during casting to ensure the solidification (enough heat is removed) before the ingot exits the mould, avoiding liquid metal breakout [11, 12].

Increased cooling results in decreasing the sump depth; exhaustive cooling has minimal consequences for the thickness of the solid shell and that of the mushy zone [5]. To prove this, experiments on heated materials (on one side) and cooling down with water spraying on the opposite side of the heating were conducted [13]. From these tests, it was concluded that heat transfer coefficients in the nucleate boiling regime do not change significantly with the water flowrate; however, the cooling flowrate affects the point at which film boiling happens.

Additionally, it has been shown [11, 13] that using cooling water up to 30°C has no effect on the cooling rate of the cast ingot. However, if the cooling water exceeds 70°C, then it may have some negative effects on the depth and thickness of the mushy zone [13, 14].

It has also been found [15] in a stationary laboratory-scale facility that the heat flux is greatly affected by the thermal conductivity of the aluminium alloy. Surface morphology and the initial temperature of the metal sample to be cooled also affect the heat flux. It has been independently concluded [11, 15–17] that the heat flux increases with higher water flowrates, ingots with rougher surfaces and lower cooling water temperature.

In addition to that, it was revealed [18, 19] that there is a strong dependence between temperature distribution and sump depth on casting speed, but also there is a relatively weak dependence on the flowrate of the quenching water striking the outside of the ingot. Furthermore, decreasing the water flowrate by 20% deepens the sump by 4% [19].

2.1.3. Casting velocity

Casting velocity is perhaps the most dominant process variable in aluminium DC casting [5, 16]. Typical values for casting velocities found in industrial shops lie within 3 and 20 cm/min. These velocities depend among other things on chemical composition and ingot size. Also, commercial flowrates are found to be between 0.12 and 0.24 L/min per 1 mm of mould characteristic length [1].

Tests on the casting of magnesium-based alloys [20] showed that casting speed has a large impact on the pool depth. As casting velocity is increased, the metal pool deepens. Casting velocity affects the centre of an ingot the most, with less effect towards the ingot edges. The pool's depth increases proportionally to increments in casting velocity, despite the chemical composition of the casting alloy [14].

Increasing casting velocity conveys into high cooling rates. This is due to high thermal gradients developed inside the ingot. These are provoked by higher energy extraction rates at the water impingement point to keep the system under equilibrium. Faster casting velocities require a corresponding hike in heat flux, as more heat is removed from the ingot [21, 22].

As the casting velocity increases, so does the ingot surface temperature around the secondary cooling, especially at the water impingement point; this affects the water cooling regimes. At the beginning of the casting operation, water film boiling regime occurs, and this increases as the casting approaches steady-state conditions, thus reaching the nucleate boiling regime [22].

Casting velocity can only be increased up to the point in which the cooling water is no longer able to extract heat from the metal surface. If this happens, the ingot shell could remelt, and liquid aluminium may spill and even get in contact with the water. This represents a high risk for an explosion.

2.1.4. Casting temperature

Usually, commercial aluminium alloys are cast between 680 and 730°C; considering that pure aluminium melts at 660°C, the extra heat added to the melt is not as significant as it is in other alloying systems such as alloyed steels.

Casting temperature has very little effect on the overall heat extraction rate; this is because the specific heat of the molten metal at the most represents 7% of the total heat input in the caster. Additionally, the sensible heat of solidification may add another 35–40% of the heat input.

3. Heat transfer in DC aluminium casting

Solidification is the most important process taking place during DC casting. The rate at which solidification occurs directly relates to the roughness of the resulting cast microstructure. The solid microstructure directly relates to the segregation of chemical elements in the alloy matrix, the precipitation of second phases and the occurrence of porosities and inclusions; all of these effects factors into the mechanical properties of the solid metal.

Heat transfer goes from the liquid (hot zone) towards the solid (cold zone). Energy is basically removed by convection and conduction mechanisms. Radiation heat transfer has very little effect on this process and can be neglected. Temperature distribution depends on the balance between heat input and output.

Heat input depends on the amount of thermal energy stored in the melt and the casting rate. The energy content is made up of the specific heat of the liquid (~5–7%), the latent heat of solidification (~30–35%) and the specific heat of the solid (balance) [1, 16]. On the other hand, the solidification of the cast alloys depends on the density of the metal, the casting velocity and ingot size.

As latent heat is removed from the melt, initial solid clusters start to develop in the metal next to the mould wall. The more the extracted heat, the higher the solid fraction present in the melt. As cooling proceeds, the solid fraction increases until reaching full solidification of the metal.

To determine the temperature distribution within the ingot as it is cast, it is necessary to solve the general heat transfer Eq. [23], which for the semi-continuous casting of aluminium has the form [24]:

$$\frac{\partial}{\partial x}\left(k\frac{\partial T}{\partial x}\right)+\frac{\partial}{\partial y}\left(k\frac{\partial T}{\partial y}\right)-u\rho Cp\frac{\partial T}{\partial z}=\rho\cdot Cp\frac{\partial T}{\partial t} \tag{1}$$

In this equation, u is the casting velocity [m/s], ρ is the density of the casting aluminium alloy [kg/m^3], Cp is the heat capacity (at constant pressure) of the aluminium alloy [J/kg/K], k is the

thermal conductivity of the alloy [W/m/K], t is the time [s], x and y are spatial coordinates [m] and T is the temperature [K]. The z coordinate relates to the casting velocity through the casting time, so it can be expressed as $z = u \times time$ [25].

Eq. (1) results from a macroscopic heat balance. The first two terms in Eq. (1) relate to heat conduction within the ingot, whereas the third term is due to heat extraction caused by the ingot motion at the casting velocity.

For calculation purposes it is often assumed that casting proceeds under steady-state conditions and that the heat removed in the z direction is negligible. Thus, heat conduction prevails both in the x and y directions. Additionally, as casting proceeds and the liquid alloy cools down, an additional term involving the latent heat of solidification (ΔH_{solid}) released during phase change from liquid to solid must be added to Eq. (1); this results in

$$\frac{\partial}{\partial x}\left(k\frac{\partial T}{\partial x}\right)+\frac{\partial}{\partial y}\left(k\frac{\partial T}{\partial y}\right) = \rho\cdot\frac{\partial(\Delta H_{solid})}{\partial t} \tag{2}$$

Eq. (2) applies to either the solid or liquid phase, while the thermal conductivity of the metal along with the latent heat of solidification varies with both temperature and position. It is noteworthy that ΔH_{solid} is a function of temperature; thus, Eq. (2) reduces and takes the form

$$\frac{\partial}{\partial x}\left(k\frac{\partial T}{\partial x}\right)+\frac{\partial}{\partial y}\left(k\frac{\partial T}{\partial y}\right) = \rho\cdot\left(\frac{\partial\Delta H_{solid}}{\partial T}\right)\cdot\frac{\partial T}{\partial t} \tag{3}$$

The left-hand side of this expression can easily be related to the convective heat transfer due to water cooling. The term on the right-hand side represents the latent heat removal due to the solidification itself [24]. Eq. (3) can be solved numerically [17, 22, 24, 26–29]. Temperature fields can be computed from this equation as well as stress and deformation fields; however, further discussions on the latter are beyond the scope of this entry.

According to Hakonsen and Myhr [24], heat transfer in aluminium casting operation can be described by using the dimensionless Péclet and Biot numbers. Péclet number represents the ratio of convective to conductive heat transfer [30] and is defined as

$$Pe = \frac{Lu}{\alpha} \tag{4}$$

where L is a characteristic length (geometrical factor) [m], u is the casting velocity [m/s] and α is the thermal diffusivity of aluminium [m^2/s], which is defined as

$$\alpha = \frac{k}{\rho Cp} \tag{5}$$

Similarly, Biot number is defined as the ratio of the internal thermal resistance to the surface film thermal resistance [30]; this is expressed as

$$Bi = \frac{hL}{k} \tag{6}$$

In Eq. (6), h is the heat transfer coefficient between cooling water and aluminium ingot [W/m^2/K]. The other variables in Eqs. (4)–(6) have been already defined.

In view of the former, it has been proposed that Eq. (3) can be rewritten as [24]

$$\frac{\partial^2 T}{\partial X^2} + \frac{1}{Pe}\frac{\partial^2 T}{\partial Y^2} = \Phi \cdot \frac{\partial T}{\partial Y} \tag{7a}$$

$$\frac{\partial^2 T}{\partial R^2} + \frac{1}{R}\frac{\partial T}{\partial R} + \frac{1}{Pe^2}\frac{\partial^2 T}{\partial Y^2} = \Phi \cdot \frac{\partial T}{\partial Z} \tag{7b}$$

Eq. (7a) is defined for Cartesian coordinates, whereas (7b) is for cylindrical coordinates. These last equations are fully expressed in terms of dimensionless variables; thus R, X and Y vary from 0 to 1 and represent r, x and y dimensionless directions, respectively:

$$R = \frac{r}{r_0} \; ; \quad Y = \frac{y\alpha}{y_0 u} \; ; \quad X = \frac{x\alpha}{y_0 u} \tag{8}$$

In addition to the dimensionless parameters in Eq. (8), expression 7a and expression 7b present the Φ parameter which represents the actual solidification process. Φ is a function of temperature and accounts for the release of latent heat and the decrease of the liquid fraction as time increases. This function is represented by

$$\Phi = 1 + \frac{\Delta H_{solid}}{\rho Cp}\frac{\partial(\rho f_l)}{\partial T} \tag{9}$$

In (9) f_l represents the liquid fraction within the solidification range. This fraction depends both on the temperature and the cooling rate. However, in DC casting the cooling rate remains fairly constant, meaning that in fact f_l only depends on the temperature.

It has been observed [1, 24] that in aluminium DC casting, the Péclet number typically lies between 1.4 and 4.5, whereas Biot number varies between 2 and 60. These results mean that both convective heat transfer and conduction have strong influence in the heat extraction.

Having determined that both convective and conductive heat extraction play a similar role, it is now necessary to relate these heat removal modes to the actual process variables, so based on the response of them, the expected solidification microstructure and consequently the final mechanical properties achieved by the final ingot can be predicted. To accomplish that, it becomes necessary to have an accurate estimation of the heat transfer coefficient.

3.1. Estimation of the heat transfer coefficient

Heat transfer coefficient is the key parameter in estimating convective heat transfer. As cooling water passes through the mould, it extracts considerable amounts of heat. The secondary cooling system removes the remaining heat from the molten phase.

The problem associated to the heat transfer coefficient is that this single parameter cannot be calculated directly from a specific equation. It depends on multiple factors that exist during the heat exchange: cooling agent flowrate, system geometry, existing thermal gradient, thermophysical properties, etc. Therefore, to determine the heat transfer coefficient as accurately as possible, this needs to be done from experimental measurements and data fit.

In this regard, many studies have been conducted to have precise estimations of the heat transfer coefficients involved in cooling down the aluminium ingots [7, 8, 13, 31–38].

It has been established [13, 31] that the critical convective heat flux is achieved when transitioning from nucleating to water film boiling regime. This transition directly relates to casting velocity. If this velocity reaches a critical speed, the ingot surface may exceed that of the nucleating-boiling transition, reducing the capability of cooling water to extract heat.

Based on this general observation, it has been suggested that typical heat transfer coefficients in DC casting primary cooling system are in the vicinity of 2000–3000 $W/m^2/K$ [32, 33].

Independent experiments have provided different expressions to determine the heat transfer coefficient as a function of different process variables. Santos et al. [34] proposed that the heat transfer between aluminium and a water-chilled mould coefficient varies with time as

$$h = 2000 \times t^{-0.17} \tag{10}$$

The time in Eq. (10) refers to the residence time of the melt in the mould. Eq. (10) is valid in the interval $0 < t < 250$ s.

A similar analysis was conducted by Aweda and Adeyemi [35]. They studied the heat transfer coefficient in squeeze casting of aluminium. They found that in the caster mould, the heat transfer coefficient between the melt and the mould is a direct function of the metal temperature and also the squeeze pressure. Assuming a pressure of 0 in the DC caster, there is no external applied force in the caster. The correlation for the heat transfer coefficient as a function of temperature is

$$h = 2.679T + 988.921 \tag{11}$$

Such correlation is valid for temperatures above 660°C.

Figure 4, shows how the heat transfer coefficient changes with these variables. In either case, the heat transfer coefficient decreases with time by exchanging heat with the surroundings (temperature dependency) or by extending its residence tie in the mould (time dependency). In any case, the heat transfer coefficient values are in the same order of magnitude.

Correlations (10) and (11) do not account for cooling water flowrate effect. To account for this variable, a series of experiments were conducted [36, 37]. From this setup, it was found that by measuring temperature across the ingot, it is possible to back calculate the values of the heat transfer coefficient during the solidification of the aluminium. From the computations

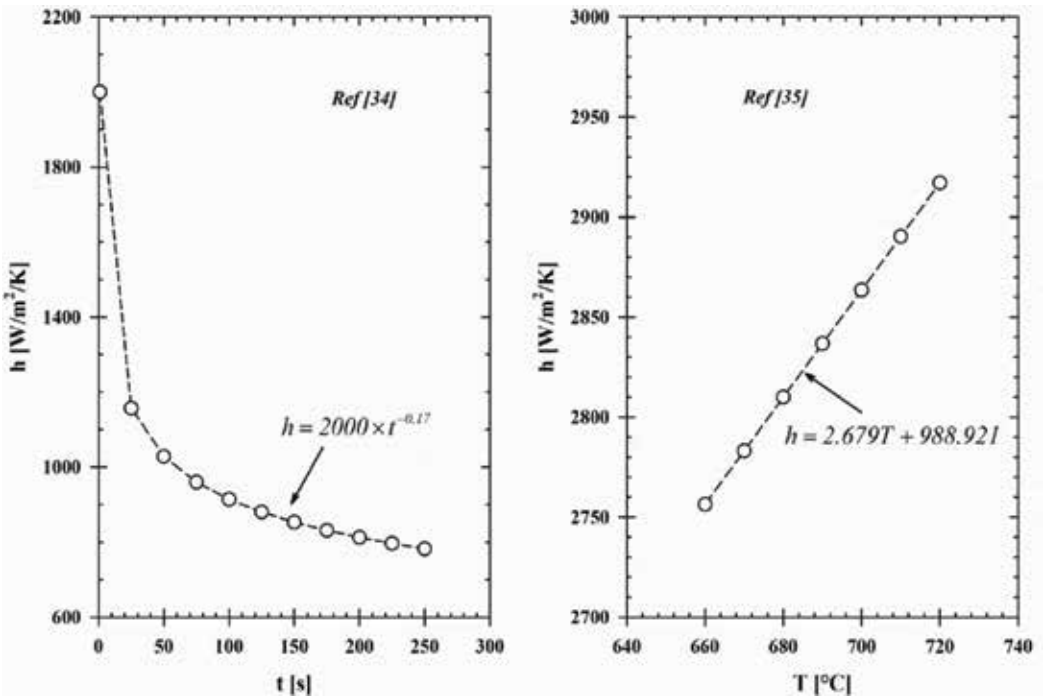

Figure 4. Effect of holding time on the mould [34] and that of the metal temperature in the mould [35] on the heat transfer coefficient during the solidification of an aluminium ingot.

made, it was found that the heat transfer coefficient during the DC casting of aluminium varies between 10^3 and 10^7 W/m^2/K, which is considerably higher than the values computed with Eqs. (10) and (11).

To determine the accuracy of the values reported, it was decided to evaluate another heat transfer coefficient correlation proposed by Sleicher and Rouse [38]:

$$h = \frac{k_{water}}{D}(5 + 0.015\, Re^{0.82}\, Pr^{0.83}) \tag{12}$$

Eq. (12) was obtained after conducting many experiments to quantify convective heat transfer in enclosed channels. In applying Eq. (12), it is assumed that cooling water flowrate within the mould wall is in the turbulent regime. In relationship (12), D is the diameter of the water channel; Re is the water Reynolds number at the cooling water temperature; Pr is the Prandtl number of water (~ 7) at the mould; and k_{water} (0.591 W/m/K) is the thermal conductivity of the water.

From **Figure 5**, it can be seen that by increasing the water flowrate within the mould, it increases the heat exchange rate (higher h value), thus reducing the mould's temperature. This is well established in the continuous casting of steel but has not been studied thoroughly in DC casting of aluminium and other light metals (**Table 1**) [31].

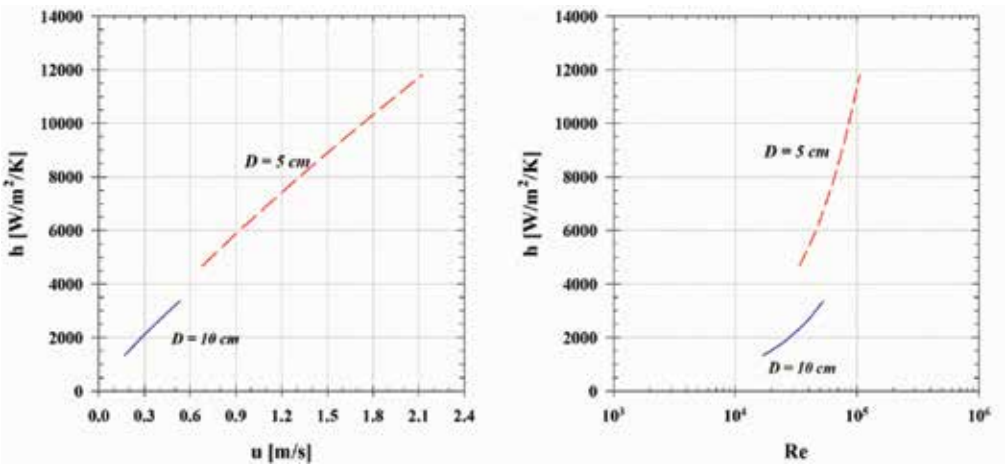

Figure 5. Estimation of the heat transfer coefficient as proposed by Sleicher and rouse [38] as a function of water velocity (u) and Reynolds number (Re).

Water flowrate [L/min]	Water velocity [m/s]	Re	D [m]	h [W/m²/K]
80	0.17	1.69×10^4	0.1	1337
100	0.21	2.11×10^4	0.1	1599
120	0.25	2.54×10^4	0.1	1852
150	0.32	3.17×10^4	0.1	2219
175	0.37	3.70×10^4	0.1	2513
200	0.42	4.23×10^4	0.1	2801
80	0.68	3.38×10^4	0.05	4675
100	0.85	4.23×10^4	0.05	5602
120	1.02	5.08×10^4	0.05	6496
150	1.27	6.34×10^4	0.05	7788
175	1.49	7.40×10^4	0.05	8829
200	1.70	8.46×10^4	0.05	9844

Table 1. Process variables used in Eq. (12) to estimate the heat transfer coefficients shown in **Figure 5**.

4. Estimation of Pe and bi numbers and their effect on the DC casting process

Estimation of Pe and Bi numbers according to Eqs. (4) and (6), respectively, was conducted for different water channel diameters. This is shown in **Figure 6**.

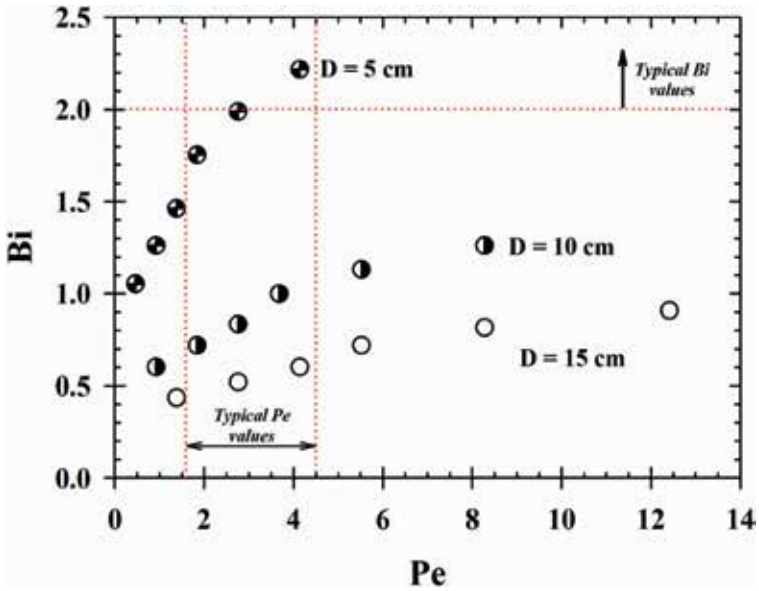

Figure 6. Bi versus Pe plots for different casting conditions and water channel diameters.

Figure 6 indicates typical Pe and Bi values reported in literature [1, 24]. As it can be observed in such figure, a significant amount of data fits well in the reported Pe interval; however, in terms of Bi number, only a few data lie within the observed values.

Péclet number directly relates to the casting velocity, whereas Biot number depends on the heat transfer coefficient.

To increase the value of Biot number, it would be necessary to increase the heat transfer coefficient which in turns means to increase the cooling water flowrate (Re in Eq. 12). If more water is added to the mould (primary cooling system), it may induce thermal stresses due to faster heat extraction rate; such thermal stresses may in turn affect the solidification structure henceforth the mechanical properties of the resulting cast alloy.

On the other hand, if Pe increases it would mean that the casting velocity could be too fast to allow for the initial solidification of the ingot, risking remelting of the initial solidification front and possible leaking of liquid metal. To counteract this effect, more cooling water should be added to the mould to extract as much heat as possible. These effects induce different metallurgical defects that hinder the quality of the solid metal.

The Bi versus Pe diagram represents a compromise between the amount of cooling water added to the mould and the casting velocity. These two process variables have the higher impact on the solidification of the alloys obtained by DC casting. The proper balance between these two variables ensures that a proper temperature distribution within the ingot establishes as it solidifies. Furthermore, such temperature field minimizes the probability of attaining poor mechanical properties and other defects associated to imbalances between these variables.

Acknowledgements

The authors would like to thank COFAA-IPN and SIP-IPN for funding this project.

Author details

José C. Méndez, Ricardo R. Ambriz, David Jaramillo and Gabriel Plascencia*

*Address all correspondence to: g.plascencia@utoronto.ca

CIITEC – Instituto Politécnico Nacional, Cd. de México, México

References

[1] Grandfield JF, McGlade PT. DC casting of aluminium: Process behaviour and technology. Materials Forum. 1996;**20**:29-51

[2] Dieffenbach RP. Practical problems in casting Aluminium D.C. ingot. In: Edgeworth TG, editor. Light Metals, 1971. TMS; 1971. pp. 707-709

[3] Méndez C, Sánchez CC, Salas E, Ríos M, Plascencia G, Jaramillo D. Effect of process parameters on the microstructure of aluminium. Kovove Materialy Metallic Materials. 2014;**52**(1):19-27. DOI: 10.4149/km 2014 1 19

[4] DG Eskin. Physical Metallurgy of Direct Chill Casting of Aluminium. CRC

[5] Nadella R, DG Eskin, Du Q, Katgerman L. Macrosegregation in direct-chill casting of aluminium alloys. Progress in Materials Science. 2008;**53**:421-480

[6] Bergmann WJ. Solidification in continuous casting of Aluminium. Metallurgical Transactions. 1970;**1**:3361-3364

[7] Prasad A, Bainbridge I. Experimental determination of heat transfer across the metal/gap in a direct chill (DC) casting mold - part I. Metallurgical and Materials Transactions A. 2013;**44**(A):456-468

[8] Prasad A, Bainbridge I. Experimental determination of heat transfer across the metal/mold gap in a direct chill (DC) casting mold - part II: Effect of casting metal, and other casting parameters. Metallurgical and Materials Transactions A. 2013;**44**(A):3099-3113

[9] Metals Handbook, Vol. 2. 10th ed. ASM International: Metals Park, OH, USA; 1990. 3470 pp

[10] Smithells CJ, editor. Metals Reference Book. 7th ed. Oxford, UK: Butterworth—Heinemann; 1992. p. 1794

[11] Méndez C. Analysis of the Semi-Continuous Casting System for Aluminium Alloys Castings. National Polytechnic Institute: Mexico City; 2012. 150 pp

[12] Ortega RE. Direct Chill and Fusion™ Casting of Aluminium Alloys. Waterloo, ON, Canada: University of Waterloo; 2012. 120 pp

[13] Grandfield J, Hoadley A, Instone S. Water cooling in direct chill casting: Part I, boiling theory and control. In: Grandfield JF, Eskin DG, editors. Essential Readings in Light Metals. 1st ed. USA: TMS; 2016. pp. 681-688

[14] Livanov VA, Gabidullin RM, Shipilov VS. Continuous casting of aluminum alloys. Meta. 1977:98-110

[15] Wells MA, Li D, Cockcroft SL. Influence of surface morphology, water flow rate and sample thermal history on the boiling-water heat transfer during direct-chill casting of commercial Aluminium alloys. Metallurgical and Materials Transactions B. 2001;**32**(B):929-939

[16] Méndez C, Sánchez CC, Plascencia G, Rubio MA, Jaramillo D. Thermal assessment of the casting operation at IMASA shop. In: Johnson JA, editor. Light Metals, 2010. TMS; 2010. pp. 715-719

[17] Méndez C, Rios M, Barrón MA, Torres AA, Plascencia G, Jaramillo D. Effect of the cooling rate on the microstructure of Aluminium bars continuously casted. In: Bilodeau M, Galliene D, editors. Light Metals 2010. Vancouver, B.C. Canada: The Metallurgical Society of CIM; 2010. pp. 33-40

[18] Prasso DC, Evans JW, Wilson IJ. Heat transport and solidification in the electromagnetic casting of Aluminium alloys: Part I. Experimental measurements on a pilot-scale caster. Metallurgical and Materials Transactions B. 1995;**26**(B):1244-1251

[19] Prasso DC, Evans JW, Wilson IJ. Heat transport and solidification in the electromagnetic casting of Aluminium alloys part II: Development of a mathematical model and comparison with experimental results. Metallurgical and Materials Transactions B. 1995;**26**(B):1282-1288

[20] Hao H, Maijer DM, Wells MA, Cockcroft SL, Sedaiko D, Hibbins S. Development and validation of a thermal model of the direct chill casting of AZ31 magnesium billets. Metallurgical and Materials Transactions A. 2004;**35**(A):3843-3854

[21] Eskin DG, Savran VI, Katgerman L. Effects of melt temperature and casting speed on the structure and defect formation during direct-chill casting of an al-cu alloy. Metallurgical and Materials Transactions A. 2005;**36**(A):1965-1976

[22] Weckman DC, Niessen P. A numerical simulation of the D.C. continuous casting process including nucleate boiling heat transfer. Metallurgical and Materials Transactions B. 1982;**13**(B):593-602

[23] Szekely J, Themelis NJ. Rate Phenomena in Process Metallurgy. 1st ed. USA: John Wiley; 1971. pp. 150-170

[24] Hakonsen H, Myhr OE. Dimensionless diagrams for the temperature distribution in direct-chill continuous casting. Cast Metals. 1995;**8**:147-157

[25] Brimacombe JK, Samarasekera IV, Lait JE, Volume CC. Heat Flow, Solidification and Crack Formation. Warrendale, PA, USA: The Iron and Steel Society; 1984. pp. 20-30

[26] KN Lie YH, Chen MT, Tsai A. Control system analysis pf a direct-chill cast process of Aluminium ingots by an inverse method. International Journal of Applied Science and Engineering. 2014;**12**:257-274

[27] Drezet JM, Rappaz M, Grun GU, Gremaud M. Determination of Thermophysical properties and boundary conditions of direct -chill cast Aluminium alloys using inverse methods. Metallurgical and Materials Transactions A. 2000;**31**(A):1627-1634

[28] Thévoz P, Desbiolles JL, Rappaz M. Modeling of Equiaxed microstructure formation in casting. Metallurgical Transactions A. 1989;**20**(A):311-322

[29] Drezet JM, Rappaz M. Modelling of ingot distortions during direct chill casting of Aluminium alloys. Metallurgical Transactions A. 1996;**27**(A):3214-3225

[30] Szekely J, Evans JW, Brimacombre JK. The Mathematical and Physical Modeling of Primary Metals Processing Operations. 1st ed. USA: Wiley; 1988. xx p

[31] Sengupta J, Thomas BG, Wells MA. The use of water cooling during the continuous casting of steel and aluminum alloys. Metallurgical and Materials Transactions A. 2005;**36**(A):187-204

[32] A Prasad JA, Taylor IF. Bainbridge. The measurement of heat flow within a DC casting mould. In: Grandfield JF, Eskin DG, editors. Essential Readings in Light Metals V2. 1sted. USA: TMS. 2016. pp. 659-664

[33] Kuwana K, Viswanathan S, Clark JA, Sabau A, Hassan MI, Saito K, Das S. Calculation of heat transfer coefficients at the ingot surface during DC casting. In: Kvande H, editor. Light Metals 2005. USA: TMS; 2005. pp. 989-993

[34] Santos CA, Quaresma JMV, Garcia A. Determination of transient interfacial heat transfer coefficients in chill mold castings. Journal of Alloys and Compounds. 2001;**319**:174-186

[35] Aweda JO, Adeyemi MB. Experimental determination of heat transfer coefficients during squeeze casting of aluminium. Journal of Materials Processing Technology. 2009;**209**:1477-1483

[36] Bakken JA, Bergström T. Heat transfer measurements during DC casting of aluminium. Part I: Measurement technique. In: Grandfield JF, Eskin DG, editors. Essential Readings in Light Metals V2. 1st ed. USA: TMS; 2016. pp. 646-652

[37] Jensen EK, Johansen S, Bergström I, Bakken JA. Heat transfer measurements during DC casting of aluminium. Part II: Results and verification for extrusion ingots. In: Grandfield JF, Eskin DG, editors. Essential Readings in Light Metals V2. 1st ed. USA: TMS; 2016. pp. 653-658

[38] Sleicher CA, Rouse MW. A convenient correlation for heat transfer to constant and variable property fluids in turbulent pipe flow. International Journal of Heat and Mass Transfer. 1975;**18**:677-683

Chapter 4

Castability and Characteristics of High Cerium Aluminum Alloys

David Weiss

Additional information is available at the end of the chapter

http://dx.doi.org/10.5772/intechopen.72830

Abstract

This chapter describes the development and the castability of near eutectic aluminum-cerium (Al-Ce) alloy systems. These alloys have good mechanical properties at high temperatures and are very castable. The castability of the binary systems is as good or better than the aluminum-silicon system with some deterioration as additional alloying elements are added. In alloy systems that use cerium in combination with common aluminum alloying elements such as silicon, magnesium, and/or copper, the casting characteristics are generally better than the aluminum-copper system. Alloying with magnesium increases room temperature strength considerably.

Keywords: aluminum, high-temperature alloys, intermetallic, cerium, casting alloys

1. Introduction

Recent research and development work has shown that cerium containing binary Al-Ce and ternary Al-Ce-Mg alloys have the potential to be used for high-temperature use in a number of automotive components [1–3]. In the 1980s, it was shown that powder metallurgy (hot pressing and forging) can be used to produce an Al-4 wt% Ce alloy component that had high-temperature mechanical properties (300 MPa at 230°C) that exceeded the best aluminum commercial aluminum casting alloys [4]. Microstructure and mechanical properties of Al-Ce-Ni alloys containing up to 16 wt% Ce and 8 wt% Ni had been studied by Belov et al. [5]. Shikun et al. reviewed the effect of Ce additions up to 4 wt% on the solidification range, solidification volume change, and cast microstructure [6]. New development work has taken place since 2010 in the Al-Ce system because of a potentially large impact on the economics of rare earth mining if large amounts of cerium could be consumed. A significant amount of data on solidification characteristics and mechanical properties of Al-Ce alloys followed by prototyping to demonstrate the castability of the alloys has been completed [1–3]. While some investigation of thermal treatments is described here, the alloys generally do not require

thermal treatment. The alloys are primarily solid solution and intermetallic strengthened and do not require heat treatment to develop properties. Homogenization has proved to be beneficial in some alloys.

2. Casting characteristics

Figure 1 shows a Thermo-Calc calculated Al-Ce phase diagram [2]. It has a eutectic composition at about 10 wt% Ce with a eutectic temperature of 640°C. Hypo- and hyper-eutectic alloys contain the intermetallic compound Al_{11} Ce_3. Sims et al. focused on Al-12Ce, Al-12Ce-0.4 Mg, and Al-12Ce-4Si-0.4 Mg alloys and evaluated their castability, microstructure, and mechanical and physical properties [1]. Test bars were given the T6 heat treatment (8 h at 537°C, water quenched and then artificially aged at 155°C for 3 h). Castability of the Al-12Ce alloy met or exceeded the castability of commercial Al-Si casting alloys. Addition of 0.4% Mg had no adverse effect on casting castability. However, addition of 4 wt% silicon greatly inhibits the fluidity of the alloy. Influence of lower amount of Si on castability has not been evaluated. No hot tearing was observed when cast into a 6-arm hot tear mold. SEM images of the three alloys are shown in **Figure 2** in both as-cast and heat-treated conditions together with XRD data for phase analysis. **Figure 2a** shows the FCC aluminum (gray) and the intermetallic Al_{11} Ce_3 (white), which has an orthorhombic crystal structure. Although this is a hyper-eutectic alloy, no primary crystallization is observed. Heat treatment modified the cast microstructure containing interconnected lath-like structure to particle-like structure. Microstructure of the Al-12Ce-0.4 Mg alloy shows additional primary crystals of cubic Al_3Mg_2 phase in the as-cast condition, as shown in **Figure 2b**. Microstructural modification of the ternary alloy is similar to that of the binary alloy after heat treatment. The as-cast microstructure of the quaternary Al-12Ce-4Si-0.4 Mg alloy is characterized by the FCC aluminum and the intermetallic Al_{11} Ce_3

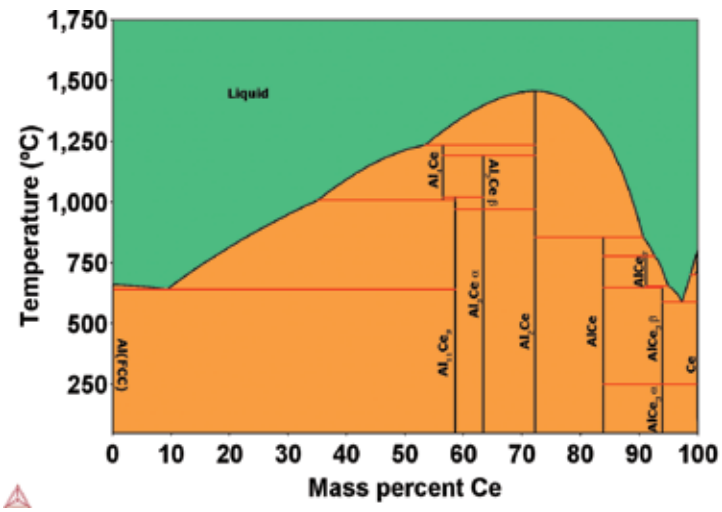

Figure 1. Thermo-Calc calculated Al-Ce phase diagram.

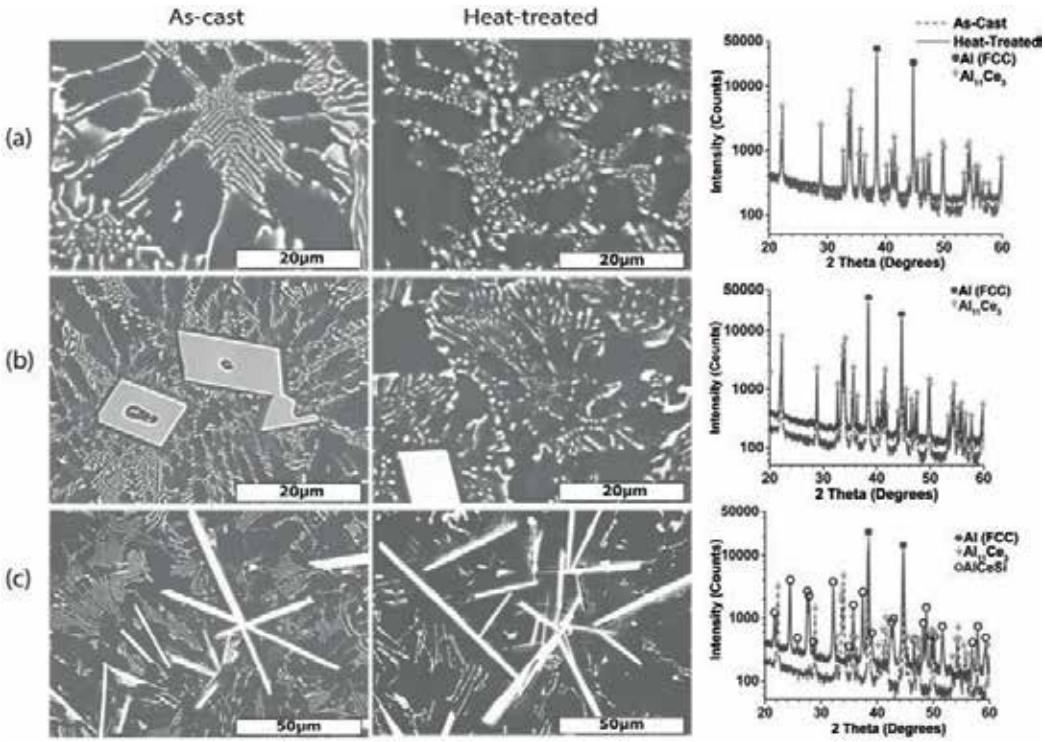

Figure 2. (a) As-cast and heat-treated SEM images of Al-12Ce with accompanying XRD spectra and phase information. (b) As-cast and heat-treated SEM images of Al-12Ce-0.4 Mg with accompanying XRD spectra and phase information. (c) As-cast and heat-treated SEM images of Al-12Ce-4Si-0.4 Mg with accompanying XRD spectra and phase information.

since Si remains in solid solution, **Figure 2c**. However, the $Al_{11}Ce_3$ shows both primary and eutectic solidification in the as-cast state. A new phase, intermetallic AlCeSi phase appears after T6 heat treatment.

3. Mechanical properties

Room temperature mechanical properties of these binary, ternary, and quaternary alloys are summarized in **Table 1** for the as-cast and heat-treated conditions. The ductility of the binary Al12Ce alloy is high despite the presence of the intermetallic phase $Al_{11}Ce_3$. UTS and yield strengths are decreased after heat treatment; but the ductility has doubled. There is marked

	As-Cast				T6 Heat Treated		
Alloy	UTS (MPa)	Yield (MPa)	Yield (4 point flexural testing)	Elongation(%)	UTS (Mpa)	Yield (Mpa)	Elongation (%)
Al-12Ce	161	57	82	13.5	131	47	26.5
Al-12Ce-0.4Mg	200	78	106	6	224	62	8.5
Al-12Ce-4Si-0.4Mg	141	75	155	2	252	128	8.5

Table 1. Room temperature mechanical properties (MPa) for Al-Ce alloys.

increase in UTS and yield strength of the ternary Al12Ce-0.4 Mg alloy over the binary alloy due to the dispersion of the Al_3Mg_2 particles in the aluminum matrix. However, the elongation is reduced by more than 50%. The decrease in elongation may be due to the presence of the large primary Al_3Mg_2crystals. Heat treatment reduces the yield strength, although there is some increase in the ductility. The quaternary Al-12Ce-4Si-0.4 Mg alloy has relatively low UTS and elongation in comparison with the binary and ternary alloys. However, its response to T6 heat treatment is similar to AlSiMg alloys, which are strengthened by the formation and precipitation of Mg_2Si. In the heat-treated condition, this alloy had the best tensile strength of the initial group of alloys tested.

Weiss and Rios determined the mechanical properties of five binary Al-Ce alloys containing 6, 8, 10, 12, and 16% Ce by using the ASTM B108 test bar mold for permanent mold casting [2]. Among these five alloys, the first two belong to the hypoeutectic group, the last two to the hypereutectic group, and the 10% Ce alloy has the eutectic composition. Mold filling was influenced by the Ce content. The hypoeutectic and eutectic alloys filled the mold cavity completely at 750°C pouring temperature and 400°C mold temperature. Mold filling became difficult with further increases in Ce content. At 12% Ce, metal temperature was increased by 25°C to fill the mold cavity. This mold filling behavior is similar to binary Al-Si alloys. At 16% Ce, the mold did not fill completely. Optical micrographs for hypoeutectic Al-6Ce and hypereutectic Al-16Ce are given in **Figures 3** and **4**. The presence of large crystals of the intermetallic $Al_{11}Ce_3$ phase is evident in the Al-16Ce alloy microstructure. By contrast, a very fine interconnected eutectic microstructure is evident for the hypo-eutectic Al-6 alloy.

As-cast mechanical properties of the five binary Al-Ce alloys (hypoeutectic, eutectic, and hypereutectic) are reported in **Table 2**, together with those for the Al-5Si type alloy 443. The room temperature mechanical properties were not high enough for many commercial applications. They also did not have a positive response to the T6 heat treatment. In order to evaluate the effect of other alloying elements on the mechanical properties of binary Al-8Ce alloys,

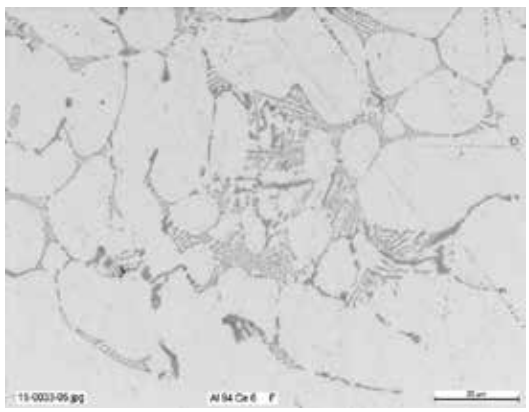

Figure 3. As-cast microstructure of Al-6Ce.

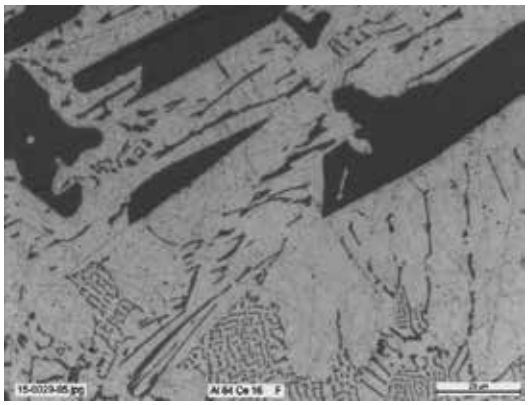

Figure 4. As-cast microstructure of Al-16Ce.

	Tensile, as Cast	Yield, as Cast	% E, as Cast
Al-16Ce	144	68	2.5
Al-12Ce	163	58	13.5
Al-10Ce	152	Test Error	8
Al-8Ce	148	Test Error	19
Al-6Ce	103	30	25
443 (Al-5Si)	145	40	2.5

Table 2. As-cast mechanical properties (MPa) of binary compositions in the Al-Ce system.

	Tensile	Yield	% E
Al-8Ce-4 Mg	189	107	3
Al-8Ce-7 Mg	195	151	2
Al-8Ce-10 Mg	227	186	1

Table 3. As-cast mechanical properties (MPa) of ternary compositions in the Al-Ce system.

	Temp	Time (h)	Tensile	Yield	% E	
Al-8Ce-10 Mg	260°C	0.5	137	130	4	
	260°C	336	137	97	5	
	315°C	0.5	97	55	20	
	315°C	216	172	159	1	Tested at 25°C
	260°C	336	159	138	1	Tested at 25°C

Table 4. Elevated temperature properties (MPa) of Al-8Ce-10 Mg.

another 20 alloys containing Si, Mg, Cu, Zn, Ni, Ti, Mn, or Fe were prepared. However, the mold filling capability was reduced for all alloys when added in excess of 1 wt%, except with Mg, even though many of the alloys had improved mechanical properties. The yield strength increased and percentage of elongation decreased with increasing Mg contents for the ternary Al-Ce-Mg alloys (**Table 3**). Mold filling ability remained unaffected. Extensive high-temperature mechanical testing has been carried out. The data shown in **Table 4** are the average of six test bars.

It was noted that room temperature properties were better after long-term exposure at 315°C than at 260°C. This indicates some positive effects from long-term exposure at high temperatures. Thermal treatments have been investigated to improve room temperature mechanical properties.

4. Thermal treatment

Generally, the Al-Ce-Mg alloys are not heat treated. However, at high levels of Mg, there was microstructural evidence of magnesium pools that were not fully dissolved in the matrix (**Figure 5**). Depending on the amount of segregation present, traditional heat treatments were either not effective or resulted in incipient melting of magnesium aluminum phases. A stepped thermal treatment has been developed that homogenizes the alloy through the dissolution of these segregated aluminum pools (**Figure 6**). For the Al-8Ce-10 Mg, this results in a significant increase in elongation with a 10% increase in tensile and yield strength (**Table 5**).

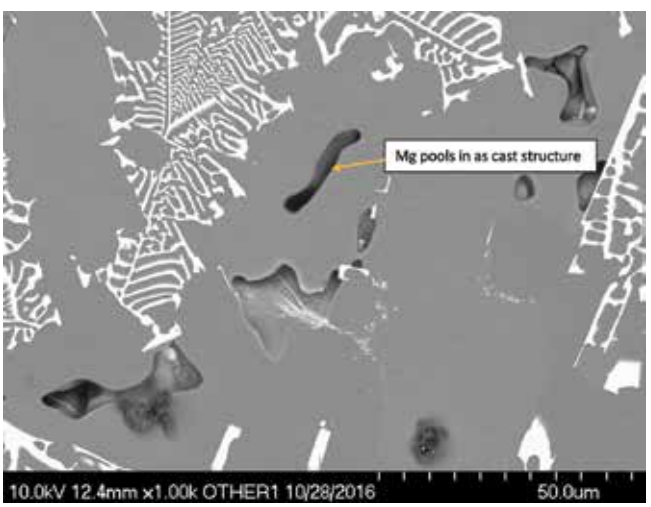

Figure 5. Undissolved magnesium pools in Al-8Ce-10 Mg.

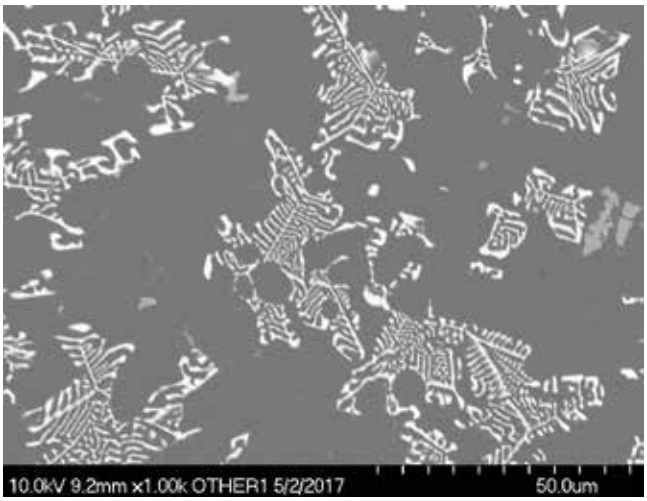

Figure 6. Same sample as shown in **Figure 5** after stepped homogenization treatment.

	Tensile	Yield	% E
As Cast	227 MPa	186 MPa	1%
-T4	248 MPa	199 MPa	2%

Table 5. Comparison of properties in as-cast with T4 condition (Al-8Ce-10 Mg).

5. Prototyping and production

Considering the good castability and good mechanical properties of the Al-Ce and Al-Ce-Mg alloys, commercial castings such as air-cooled cylinder heads (**Figure 7**) and cylinder heads and rotary engine rotors (**Figure 8**) were prototyped. Extensive work has been done by Oak Ridge National Laboratory by using neutron scattering to measure microstructural changes in an Al-Ce cylinder head in an operating engine. **Figure 9** shows the operating setup. SNS pulsed neutron diffraction of alloy showed that load was borne mainly by the Ce_3Al_{11} intermetallic phase. Parts currently in production in Al-Ce alloys include high performance impeller blades and pistons (**Figure 10**).

6. Applications of high cerium aluminum alloys

Early applications of AlCe alloys have focused on two different areas. The first has been complicated thin wall castings and airfoils that require moderate room temperature properties without heat treating. Most heat-treating processes for aluminum require a water

Figure 7. An air-cooled cylinder head cast in Al-8Ce alloy.

Figure 8. Experimental rotary engine rotor produced in chemically bonded sand with an Al-Ce-Mg alloy.

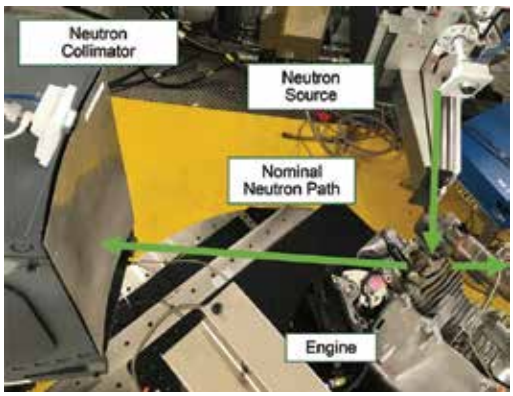

Figure 9. Setup for operating engine neutron scattering experiment.

Figure 10. High performance pistons produced from various formulations of Al-Ce alloys.

quench where significant distortion can occur. This distortion then needs to be corrected by a straightening operation, which can be time consuming and risks damage to the casting. The rapid quench can also induce residual stress into the casting, which reduces its performance or causes difficulty for machining. The second group of applications focuses on high temperature products that operate above the aging temperatures of standard aluminum alloys of about 150°C. These applications include turbocharger components, cylinder heads and pistons.

7. Future prospects of Al-Ce alloys

The basic Al-Ce binary system is a new template for alloy development that is similar in many respects to the Al-Si system. The castability is comparable, and like Si, Ce can form many varieties of potentially useful strengthening structures. Other alloying elements can be used to enhance the performance for specific applications. The roll of transition metals in the improvement of the Al-Ce system is being actively investigated. The impact of other elements, such as Zn, for solid solution strengthening is under development. The lack of solubility, diffusion, or coarsening of the $Al_{11}Ce_3$ intermetallic up to the melting point of the alloy suggests the possibility of a large family of lightweight alloys that demonstrates superior mechanical properties from room temperature up to 500°C.

Author details

David Weiss

Address all correspondence to: david.weiss@eckindustries.com

Eck Industries Inc., Manitowoc, USA

References

[1] Sims ZC, Weiss D, McCall SK, McGuire MA, Ott RT, Geer T, Rios O, Turchi PAE. Cerium-based, intermetallic-strengthened aluminum casting alloy: High-volume co-product development. Journal of Materials. 2016;**68**(7):1940-1947

[2] Weiss D, Rios O. Low density and temperature tolerant alloys for automotive applications. March 2017 SAE International, 2017-01-1666

[3] Weiss D. Development and casting of high cerium content aluminum alloys. AFS Proceedings of the 121st Metalcasting Congress. 2017. Paper No. 17-013

[4] Griffith WM, Sanders RE, Hildeman GJ. Elevated temperature aluminum alloys for aerospace applications (high-strength powder metallurgy aluminum alloys). In: Proceedings of a Symposium Sponsored by the Powder Metallurgy Committee of the Metallurgical Society of AIME. February 17–18, 1982

[5] Belov NA, Evgeniya AN, Eskin DG. Casting alloys of the Al-Ce-Ni system: Microstructural approach to alloy design. Matrials Science and Engineering, A. 1999;**271**(1):134-142

[6] Sikum X, Rongxi Y, Zhi G, Xiang X, Chagen H, Xiuyan G. Effects of rare earth Ce on casting properties of Al-4.5Cu alloy. Advanced Materials Research. 2010;**135**:1-4

Section 3

Special Casting Techniques

Chapter 5

Casting and Applications of Functionally Graded Metal Matrix Composites

Williams S. Ebhota and Tien-Chien Jen

Additional information is available at the end of the chapter

http://dx.doi.org/10.5772/intechopen.71225

Abstract

This chapter discusses the concepts, casting techniques and applications of functionally graded materials metal matrix composites (FGMMCs). Considerations were given to bulk functionally graded aluminium matrix composites (FGAACs) production processes. Liquid-metal forging processes of FGAACs fabrication, such as infiltration process, squeeze casting, friction casting or compocasting, stir, and centrifugal casting were discussed. The chapter provides basic concepts of the processes and overview of their processing parameters, such as mould rotational speed; reinforcement particles size and volume; degassing method; melting and pouring temperatures; pressure; and stirrer. The study notes that functionally graded materials (FGMs) are commonly used in automotive, aircraft, aviation, chemical, medical, engineering, renewable energy, nuclear energy, and optics electronics industries.

Keywords: FGMMCs, aluminium matrix, FGMs fabrication techniques, centrifugal casting, stir casting, ceramics reinforcements, squeeze casting, infiltration process, compocasting

1. Introduction

Man has always found materials critical to his existence and advancement. As time progresses, he is often faced with challenges that usually change his opinion and ways of doing things. Material is not left out in this evolution, which most times facilitates the improvement of knowledge and technology. Value addition to engineering natural materials became desirable in man's quest to add more meaning to both his life and those of the people around him. This is a result of the dissatisfaction and challenges that accompanied the use of materials in their natural forms. The engineering of materials for specific characteristics dates as far back

as 1000 BC, in which straw and mud were used as forms of composites [1]. Refinement of these composites have advanced over time; for example, fibre glass reinforced plastics composites, which are more superior, were introduced four decades ago. In very little time, many limitations were found in fibre reinforced plastics, the majority of problems being attributed to delamination. This delamination shortcoming, coupled with the need of materials to satisfy functional requirements, led to another breed of advanced materials: functionally graded materials (FGMs). The advent of FGMs was a major breakthrough in addressing material properties abrupt change in traditional composite, associated with large inter-laminar stresses leading to delamination [2]. These heterogeneous materials with gradually varied properties have replaced homogenous materials in some critical applications. The base (matrix) material of FGM can be metal or non-metal. Metallic matrix FGM is termed as functionally graded metal matrix composites (FGMMCs). Engineers and scientists are increasingly interested in the research and fabrication of heterogeneous FGMMCs for specific use.

This group of materials can be categorised as advanced materials in the family of engineering composites. Functionally graded material comprises of two or more component phases with continuous and gradually changing composition [3, 4]; they are characterised by continuous transitions in the material's microstructure and composition in a specific direction [5]. FGM gradually vary over volume in both microstructure and composition, resulting in subsequent alterations in the material properties.

1.1. Types of FGMs

Functionally graded materials can be classified based on the material gradient types, as shown in **Figure 1**: fraction gradient, shape gradient; orientation gradient; and size gradient.

Functionally graded material structural unit is regarded as a material ingredient or element. Material ingredients are like biological cells such as tissues and other examples are presented in **Table 1**.

Although the type of this advanced material was developed by engineers and scientists, FGMs are also found in nature. Examples of naturally occurring FGMs are bone, teeth, bamboo and tree human skin. The grading of the human bone is shown in **Figure 2**.

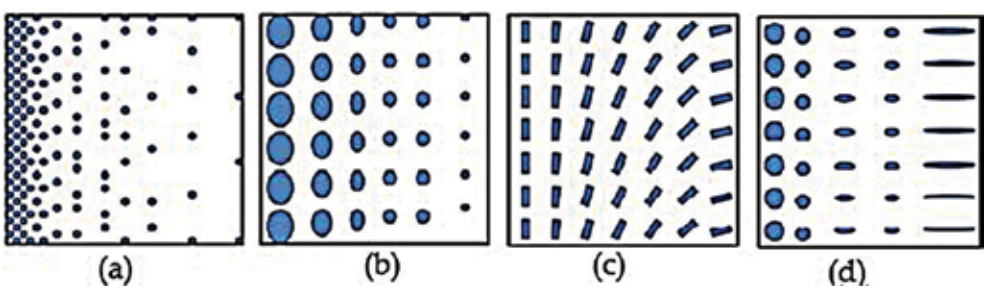

Figure 1. Types of FGMs based on gradient: (a) gradient with fraction; (b) gradient with size; (c) gradient with orientation; and (d) gradient with shape [2].

Chemical	Inorganic, organic, ceramic, metal, and polymer
Physical	Electronic state, ionic state, crystalline state, dipole movement, magnetic movement, band gap, potential well, and barrier
Geometrical	Granule, rod, needle, fibre, platelet, sheet, pole, texture, and orientation
Biological	Complex macromolecule, organelle, cell, and tissue

Table 1. Various material ingredients that can compose FGMs [6].

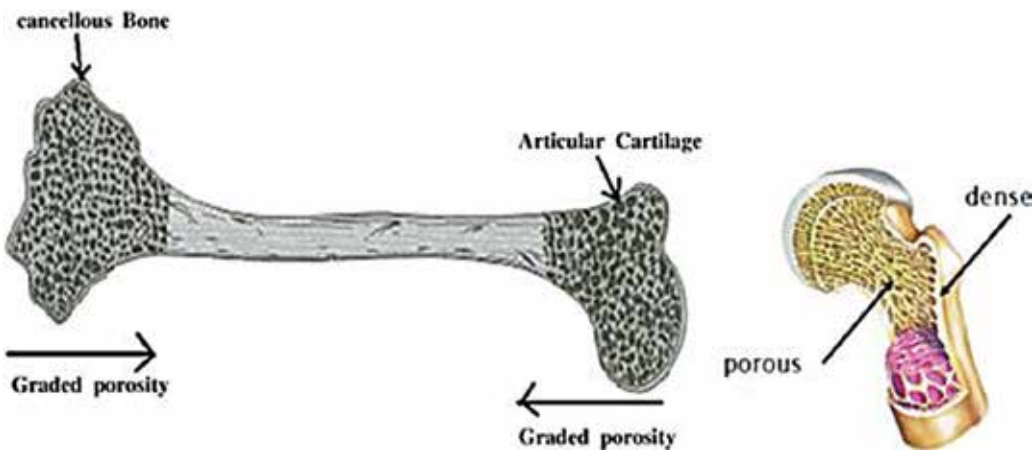

Figure 2. The naturally occurring FGMs human bone.

2. Historical background

2.1. Evolution of FGMs

Functionally graded materials were originally presented as a group of superior composite materials with a single continuous or discontinuous inclination with regard to composition and microstructure as shown in **Figure 3** [7, 8]. The concept of structural gradients was first developed from composites and polymeric materials in 1972. Different methods of applying gradients in in filament concentration, composition and in polymerisation, coupled with application areas of graded structures were proposed. Though many of FGMs' principle theoretical studies were reported in the 1970s, the influence of these works was not felt proportionately. This was due to the inadequate actual investigative studies on the manufacturing techniques and evaluation of the graded structures.

Present day FGMs were developed from the study of composites and polymeric material in 1972 by Bever and Duwez. The study investigated the properties of global material and re-evaluated the potential application of graded composites [10, 11]. In the same year, Shen and Bever studied the structure and properties of polymeric materials having spatial gradients

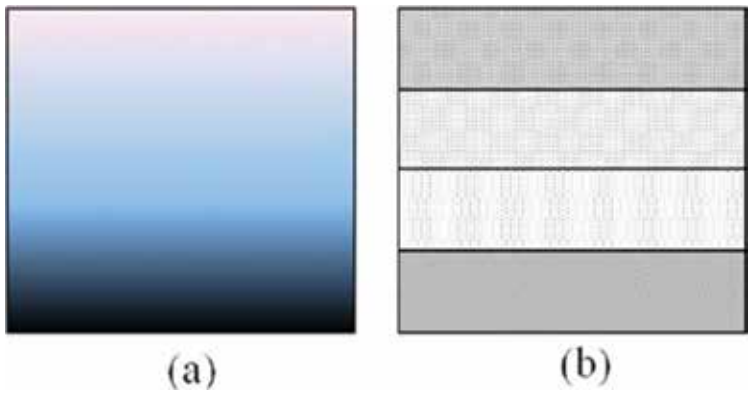

Figure 3. Functionally graded material structure types: (a) continuous and (b) discontinuous [9].

and their potential applications. The study declared that alteration of the chemical formation of monomers, morphology or supramolecular structure and the molecular makeup of the polymers may affect the graduation of polymeric material. However, the study failed to consider the design, fabrication and evaluation of the gradient of the structure [10].

The development of modern day FGMs began in the mid-1980s in Japan. The Japanese engineers were confronted with difficulty in finding a material suitable for a particular barrier in a space project, hypersonic plane. The barrier requires a thickness less than 10 mm and thermal working conditions of 1000 K and 2000 K of inside and outside temperatures respectively. This necessity pushed the engineers to FGM fabricate the barrier using FGM concept [12]. In the development of ceramic coatings and joints for the reusable rocket engine, the application of continuous texture control was suggested in 1985 [13]. This is to minimise the thermal stress and to increase the adhesion strength. These types of graded materials were named functionally gradient materials in 1986, which later became functionally graded materials with acronym FGM. The first FGMs national symposium was organised in Sendai, Japan in 1990 [14]. From 1987 to 1991, the FGM technology became very popular and several production techniques were developed. The early manufacturing processing methods include chemical vapour deposition (CVD), plasma spraying, powder metallurgy, self-propagating high-temperature synthesis (SHS), and galvanoforming. Since 1991 to the present date, these earlier FGM processing methods have been re-evaluated and modified and new one developed. These fabrication techniques have been categorised in various ways by several authors. Miyamoto et al. in 1999, grouped the processes into four main categories: layer, melt, bulk and preform processes [6]. These FGM techniques of production eliminated traditional composite delamination problem, caused by the sharp interface that is mainly responsible for the failure in the composites.

2.2. Functionally graded materials (FGMMCs)

Functionally graded metal matrix composites (FGMMCs) belong to a group of advanced material termed functionally graded materials (FGMs). The uniqueness of FGMs is that they smoothly change properties and composition spatially and vary from any single material that form them. They are materials that are specially engineered in a controlled manner for specific

mechanical or chemical properties for both harsh working environments and optimal performance. This category of high performance materials is described as knowledge-based multifunctional materials (KMMs). They are applied in thermomechanical and high impact loading, high strain rates, high temperature, and aggressive chemical environments. Such environments are associated with turbomachinery, aerospace, automotive, chemical, microsensors, electronic devices, biological implants, and household appliances. Functionally graded materials are a major category of KMM materials. Functionally metal matrix composites (FGMMCs), such as Al-Si-SiC, possess both high wear resistance and high bulk toughness. The structure of FGMMC is continuously or discretely altering the mechanical and thermal properties at the macroscopic or continuum scale. These spatially varied properties are achieved by varying certain process parameters of the reinforcements, such as type, size, shape, and dispersion pattern.

3. Concept of FGMMCS

This category (FGMMCs) of materials was an offshoot of the traditional composite materials, considered as advanced engineering materials. Composites are normally formed by combination of two or more different materials with individual physical and chemical properties in solid forms. However, composite material is characterised by an abrupt interface and a weak interfacial bond between the combining materials. This results in sharp property changes and, as a consequence, eventual failure under harsh working conditions, such as high temperature and high impact load. This failure is attributed to disintegration of reinforcement from the matrix; this type of failure is called delamination [15]. The sharp interface and the gradual change of a traditional composite and FGM are shown in **Figure 4a** and **4b,** respectively. The differences between composite and FGM are presented in **Table 2**.

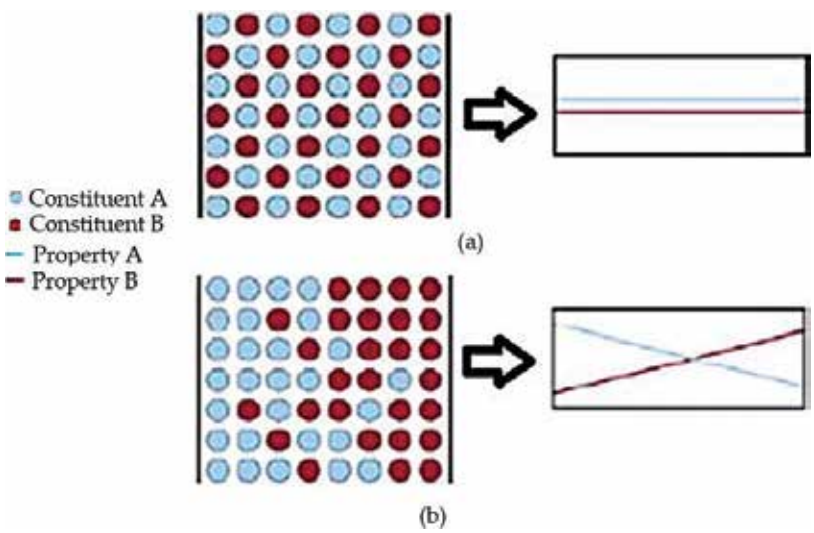

Figure 4. Material of two phases [16]: (a) traditional composite—constant composition and properties; (b) FGM—gradual change in composition and microstructure gives a gradient in properties.

Traditional composite	FGM
Abrupt interface between combining materials, causes sharp properties change	Smooth transition between combining materials
Delamination occurs under extreme working conditions	Very good interfacial bond between materials, so delineation is avoided
Matrix charge, weakness and strength of the combining materials are equally distributed	Properties of the combining materials are spatially distributed is possible
All the part is a bit thermal conductive and the matrix lost a bit of hardness	One side is largely hard and the other side is largely thermal conductive

Table 2. The differences between composite and FGM.

The concept of FGM substitutes the abrupt interface of traditional composite materials with gradually changing interface and this eliminates the shortcomings that accompany the sharp interface. Subsequently, the chemical composition is altered at the interface, which ultimately improves the mechanical properties of the composite. Properties of FGM vary spatially; they are location-dependent in the bulk structure of the material. Functionally graded materials are engineered to possess changing properties, such as varying magnetic, thermal, mechanical, chemical composition, and electrical properties, changing microstructural and atomic arrangement. **Figure 5** shows the model of FGM object gradient, bi-linear material variation and thermal stress relaxation.

3.1. Production methods of FGMs

The development of FGMs production methods witnessed a tremendous push in the last two decades, resulted in several FGMs fabrication methods, as presented in **Table 3**. These production methods are in both chemical and mechanical forms, and their applications are guided by the type/state of raw materials, facility availability and functional properties

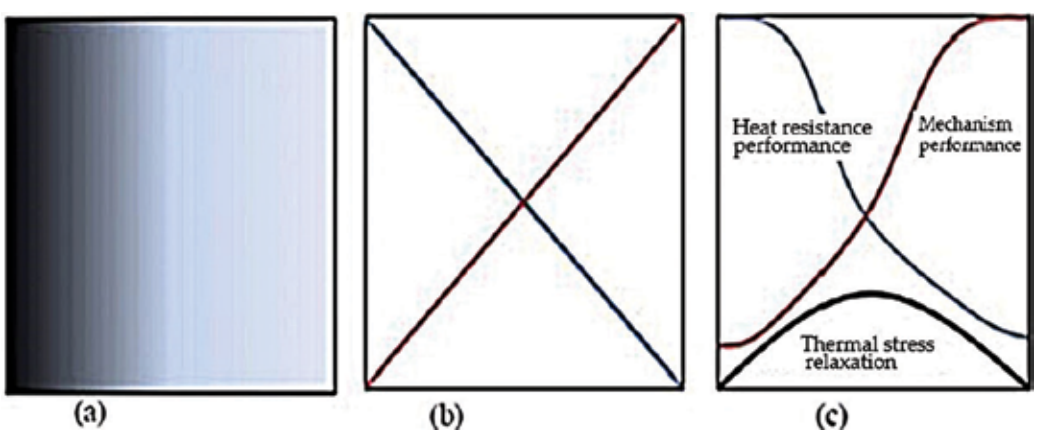

Figure 5. Model of FGM (a) FGMs object; (b) bi-linear material variation; and (c) thermal stress relaxation [2].

Method	Type	Group of FGM
Vapour deposition technique	Chemical vapour deposition (CVD) and physical vapour deposition (PVD)	Thin surface coating
Powder metallurgy (PM)	Stepwise Compositional Control: powder stacking, sheet lamination and wet powder spraying Continuous composition control: centrifugal powder forming (CPF), impeller dry blending, centrifugal sedimentation, electrophoretic deposition and pressure filtration/vacuum slip casting	Bulk
Melting processes	Centrifugal casting, sedimentation casting infiltration processing, thermal spray processing	Bulk
Material prototyping/solid freeform (SFF) Fabrication	Laser based processes: laser cladding, melting, laser sintering, selective 3D-printing and selective laser	Bulk
Other methods	Plasma spraying, electrodeposition, electrophoretic, ion beam assisted deposition (IBAD), self-propagating high-temperature synthesis (SHS)	Thin coating

Table 3. FGM fabrication methods and their applications [18–21].

required. This development led to the emergence of many attractive engineering materials applied in the automotive and aviation sectors. These methods may be broadly categorised into the following [17]:

Constructive process: in this process the engineer determines the phase replacement within the formation.

Transport based process: This process depends on an appropriate and the created in situ reactions of processes during material production.

Also, FGMs are categorised based on products thickness or size into [4, 22]:

i. **Thin FGM**: Thin FGMs are relatively thin surface coatings or thin sections, formed by chemical or physical vapour deposition (CVD/PVD), self-propagating high-temperature synthesis (SHS), plasma spraying, etc.

ii. **Bulk FGM**: Bulk FGMs are fabricated by the following methods centrifugal casting, powder metallurgy, squeeze casting, solid freeform technology etc.

Constituents are the basic building cellblocks of a FGM, made up of matrix, particulates, interphase, precipitates and any other additives, which are identified in the material's microstructure. Constituents in FGM structure are usually described by their chemical composition, volume fraction, size, morphology and orientation within the material. In a broader perspective, FGM is formed by the combination of at least two different materials, which may be metal–metal, metal-ceramic, polymer-ceramic, etc. The structure of FGM is broadly divided into two, the matrix and the reinforcement.

3.2. FGM matrix

The matrix is a monolithic material that forms the surrounding medium or structure, while the reinforcement is the constituent embedded in the matrix. Non-metal and metal matrices form functionally graded non-metal matrix composites (FGMMCs) and functionally graded metal matrix composites (FGNMMCs) respectively. Plastics, polymers and light metals such as aluminium, magnesium, brace, bronze, and titanium are widely used matrices for composite. Cobalt and cobalt–nickel alloy matrices are usually used in elevated temperature applications.

3.3. Reinforcement

Reinforcement is a material embedded in a matrix, which provides the material with the needed structural and physical properties, such as friction coefficient, wear resistance, thermal conductivity, etc. [23]. The reinforcement can be classified into continuous and discontinuous. Standard metalworking techniques, such as forging, extrusion, or rolling can be used to work on discontinuous FGMMCs that are isotropic (uniform in all orientations). Further, polycrystalline diamond tooling (PCD) is required to machine isotropic discontinuous MMCs using conventional techniques. Continuous reinforcement applies monofilament and form anisotropic structure in FGMs. This reinforcement alignment plays a role the strength behaviour of the material. Single, defect-free crystal filament of material is known as monocrystalline whisker. Whisker materials, having very high tensile strength (10–20 GPa), such as graphite, silicon-carbide, silicon, alumina and iron are commonly used as reinforcements in FGMMCs. **Table 4** presents other FGM reinforcements that are used.

3.4. Hybrid composite

In a MMC, there are at least two constituents: one material is a metal matrix, and another a reinforcement, which can be metal or a non-material. A metal matrix composite formed by two different or more reinforcements is termed hybrid composite. Examples of hybrid composites are Al6061-SiC-Graphite, Al6061-SiC-TiB_2, CNTs-Mg-Al, Al6061-SiC-MWCNT, etc., where SiC is silicon-carbide; MWCNT is multiwall carbon nanotubes; TiB_2 is titanium diboride; and CNTs is carbon nanotubes. CNTs-Mg-Al and Al6061-SiC-MWCNT are also called metal matrix nanocomposites.

Metal matrix	Reinforcement
Aluminium	Nitrides: BN, ZrN, TiN
Brace	Carbides: SiC, TiC, ZrC
Bronze	Borides: ZrB_2, TiB_2, SiB_2
Titanium	Oxides: Al_2O_3, MgO, TiO_2, ZrO_2
Magnesium	Silicides: $MoSi_2$
Cobalt	Intermetallic: Fe_3Al, FeAl, NiAl, Ni_3Al, Ti_3Al, TiAl

Table 4. Metal matrices and reinforcing materials used in FGMMCs.

4. Functional graded aluminium alloy matrix composites (FGAAMCS)

Basically, FGMMC composed of metal matrix phase and reinforcement phase, such that the elastic modulus and hardness differ from the metallic phase to the ceramic phase. In this chapter, FGMs formed by aluminium alloy matrix and ceramic particles reinforcements are regarded as functionally graded aluminium alloy matrix composites (FGAACs). Since the Japanese engineers' breakthrough in the hypersonic space plane project in the 1980s, several investigative studies on FGAACs have been performed and reported. Studies on the different aspects of FGAACs are ongoing, which include design of the different composition, characterisation, modelling, optimisation and development of FGMs fabrication techniques [24–28].

4.1. Fabrication techniques of FGAACs

Over the years, several FGAACs production techniques—that is, the processes of combining aluminium alloy with ceramic material—have been designed, developed and used. Despite the various FGAACs achievements that have been reported, further development is still expected. The increase need for FGAACs is due to the lightweight materials demands from the rapidly growing industrial applications of FGMs in the automotive and aerospace industries [29–31]. Apart from the lightweight advantage, the possibility of determining the mechanical and chemical properties of FGAACs, through the alteration of microstructure, also account for the growing interest. Production of a material with high wear resistance at a high temperature is possible by reinforcing the matrix with ceramic material along the part where bulk toughness required [32].

Among the various FGM fabrication techniques, the melting/casting based processes, (**Table 5** refers), will be discussed in this chapter. These techniques include the squeeze casting method, centrifugal casting method, sedimentation casting infiltration, vibration casting, compocasting, stir casting, sequence casting, and pressure casting.

4.2. Squeeze casting

Squeeze casting technique (SCT) is a liquid-metal forging method that involves the solidification of liquid metal under pressure in a closed dies placed in between hydraulic press plates.

Parameters	Range
Casting temperatures—depend on the part geometry and the alloy.	6–55°C above the liquidus temperature
Tooling temperatures ranging	190–315°C
Pressure levels	50–140 MPa
Pressure duration	Varying from 30 to 120 s
Lubrication-for aluminium, magnesium, and copper alloys	Spray of good grade of colloidal graphite lubricant on the warm dies prior to casting.

Table 5. Squeeze casting parameters [34–37].

This process creates a fast heat transfer scenario that produces a fine-grain and pore-free casting. The casting mechanical properties are similar to that of a wrought product. Squeeze casting process has been classified into four basic steps in the fabrication of FGMs by Ghomashchi and Vikhrov in a review study as follows [33]: pouring of a molten metal into the mould, closing the mould, application of pressure and cast ejection. A more detailed series of operational step is depicted in **Figure 6**.

However, for quality casting, these following processing variables should be considered in squeeze casting method: melting temperature (Tm), degassing method, die temperature (TD), delay time (tD), pouring temperature (Tp), applied pressure (P) and humidity (Hd). Additional parameters to consider in the case of FGMMCs fabrication include the temperature of the ceramic particles (Tc), the rate of at which particles are added to the molten metal (ta), stirring time (ts) and speed (tv) of the mixture. Values for some of the SCT parameters are presented in **Table 5**. In the squeeze casting method, casting properties, such as hardness, density, and secondary dendrite arm spacing, depend mainly on the effects of these processing parameters. **Figure 6** shows the input-output model of a SCT.

The many advantages of SCT rest in its production of casting with low gas porosity and shrinkage; improved mechanical properties through rapid solidification; good surface quality and performance of good preformation infiltration. The process can be automated to yield near net shape, high-quality parts, with minor post production processes. Squeeze casting technique is widely used for the fabrication of aluminium, magnesium alloys and FGMMCs. A schematic of SCT die set-up is shown in **Figure 7**.

4.3. Infiltration method

Infiltration is one of the FGMMCs fabrication techniques, which involves the soaking of a preformed dispersed phase (fibres, particles, woven) in a molten metal. This is to allow the spaces between the dispersed phase inclusions to be filled. Infiltration requires two stages: initiation of flow depicted by the dynamic wetting angle, and advancing the flow in the preform capillaries.

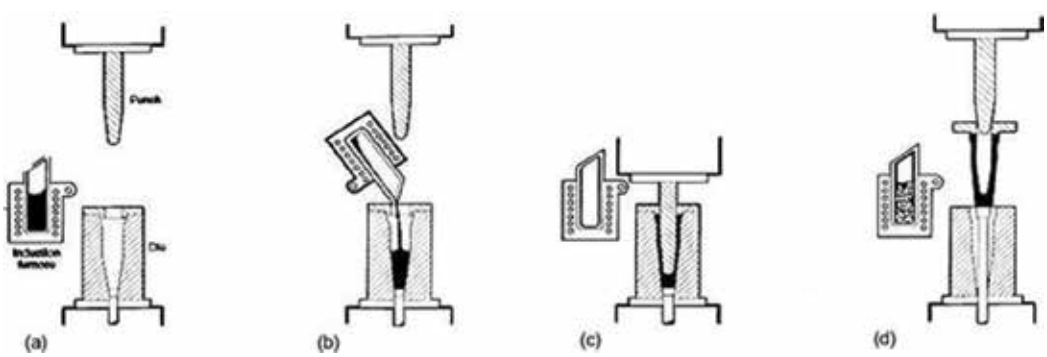

Figure 6. Schematic in squeeze casting process operations [34]: (a) melt charge, preheat and lubricate tooling; (b) pour melt into the die cavity; (c) close tooling, allow melt to solidify under pressure; and (d) ejecting the casting, and felting and die cleaning.

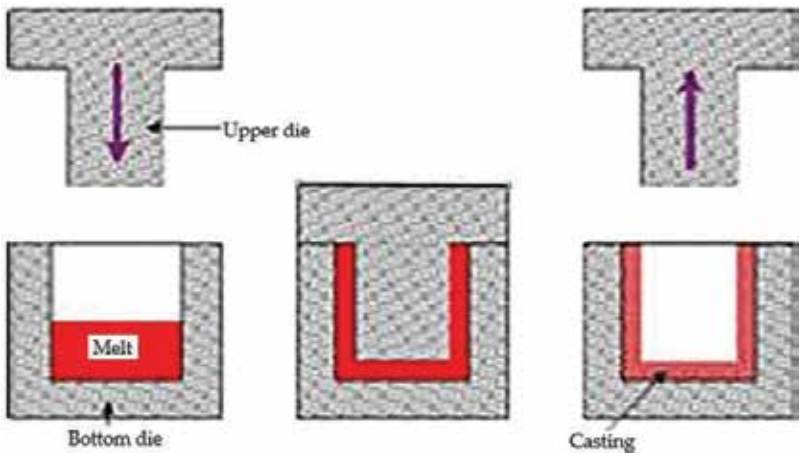

Figure 7. Schematic of SCT die set-up for melt [38].

Infiltrating a preformed porous body with molten metal is normally accomplished by applying pressure or a vacuum to facilitate penetration of the liquid metal into the voids. Also, this process can be achieved through a pressureless infiltration process—that is—without the application of external force. The external force required for infiltration operation can be provided by a hydraulic or mechanical press with a heater or from gas pressure. Infiltration methods are classified based on sources of external force: pressureless infiltration method; gas pressure infiltration method; pressure die infiltration method; and squeeze casting infiltration method.

Several successful studies on pressureless infiltration have been reported, and the process has been modelled in many studies [39–41]. According to capillary law, the infiltration pressure threshold, $P_{0'}$ is [42]:

$$P_0 = 6\,\lambda\gamma_{lv}\cos\theta\left(\frac{V_p}{(1-V_p)D}\right) \tag{1}$$

Oh, Cornie, and Russell, in their study, defined capillary pressure or infiltration threshold pressure (P_0) in terms of pore fraction of powder compact and particulate size [43]:

$$P_0 = \frac{6\,\lambda\gamma_{lv}\cos\theta(1-\omega)}{D\omega} \tag{2}$$

where θ is the contact angle; λ is the geometry depended factor (assumed to be 1.4); γ_{lv} is the tension of liquid-vapour surface; D is the mean diameter of the particles; Vp, is the volume fraction of the particulates; and ω is the void fraction in the preform.

4.4. Gas pressure infiltration method

Gas pressure infiltration method (GPIM) is a FGMMCs fabrication process by forcing a molten metal to penetrate a preformed dispersed phase using a pressurised gas. This method is

applied in the manufacturing of large composite components. The method is suitable for non-coated fibres due to short interaction time of the fibres with the hot metal and ensures low destruction of the fibres. **Figure 8** shows the schematic of a GPIM set up.

Boczkowska et al. in 2013, studied the impact of infiltration method on the mechanical properties and microstructure of FGAACs [45]. The FGMMCs specimens were produced by GPIM and pressure-vacuum infiltration at the same conditions of Tp = 7000C, P = 4 MPa, tD = 5 min. The infiltration methods were applied to pressure on aluminium alloy melt to penetrate porous Al_2O_3 ceramics preforms. The chemical composition of the aluminium alloy is presented in **Table 6**.

The ceramic preforms were produced by sintering of RA-207LS Al_2O_3 powder, provided by Alcan Chemicals. The aluminium oxide used chemical composition is presented in **Table 7**. The preforms have similar porosity, of about 72 vol%, at same level and three types of polyurethane sponges, varying density and size of pores (60, 45 and 30) were used. This resulted to the production of varying pore sizes, from 300 to 1000, preforms.

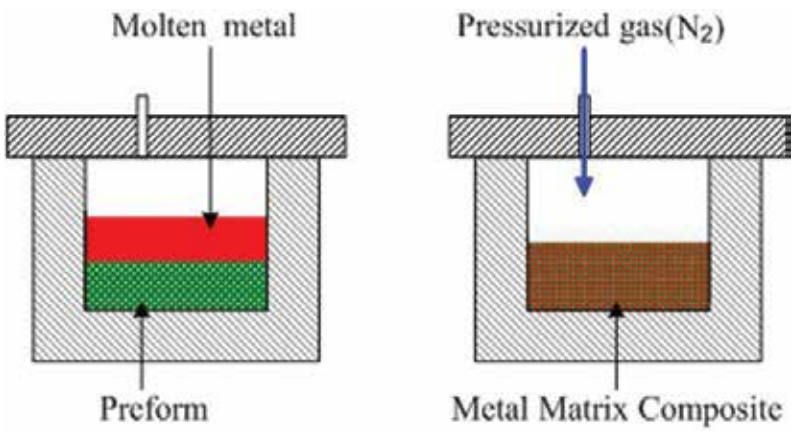

Figure 8. Schematic of a GPIM set-up [44].

Oxide	Al_2O_3	MgO	CaO	Fe_2O_3	SiO_2	Na_2O
wt.%	99.8	0.04	0.02	0.03	0.04	0.07

Table 6. Chemical composition of the aluminium oxide.

Element	Al	Si	Fe	Mn	Cu	Mg	Ni	Zn	Ti
wt.%	83.81	12	0.44	0.16	1.08	1.28	1.06	0.14	0.03

Table 7. AK12 cast aluminium alloy's chemical composition.

The study observed that:

i. The Preforms with the smallest size of pores shown better degree of infiltration in in both infiltration methods.

ii. The specimens from both methods showed higher compressive strength, hardness, and Young's modulus.

iii. Composites fabricated by GPI smallest pores size preform possessed better mechanical properties.

iv. The compressive strength, Young's modulus and hardness improvements were proportional to the increase of the specific surface section of the interphase frontiers.

Per the study, the flow of metal within the preforms hangs on the size of capillary; the pressure difference along the length of capillary; the preserving time of molten metal state in the capillary; and the alloy's dynamic viscosity.

4.5. Pressure die infiltration

Pressure die infiltration method (PDIM) involves the forcing of MMCs liquid phase to penetrate into a preformed dispersed phase placed in a die by applying die casting technology. The molten metal, is ejected through the spruce, under the pressure of a movable plunger to penetrate the preform. The schematic of PDIM is shown in **Figure 9**.

4.6. Squeeze casting infiltration

Squeeze casting infiltration method (SCIM) is similar to the squeeze casting technique used for pure metals and their alloys. In SCIM, however, a hydraulic or mechanical press is required to

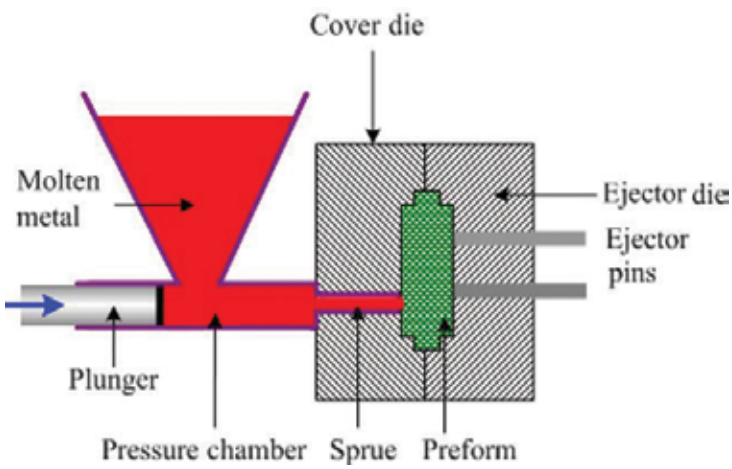

Figure 9. Schematic of PDIM.

apply external force on the melt to penetrate the preform pores. As shown is **Figure 10**, the press may be with or without a heating unit; however, one with a heating unit is preferred. The heating unit is used to heat up and to keep the die at a required temperature before pouring. In additional to SCT processing parameters, preform temperature (Tf) is a factor to be considered in SCIM.

4.6.1. Preform

Preform is a rigid, porous body, containing a discontinuous of one or mixture more reinforcement materials. Production of a preform has three fundamental steps [46]: processing of liquid powder, pressing and shaping, and sintering the preform. The concept behind a preform is the combination of a ceramic powder slurry and a sacrificial organic pore forming agent (PFA) that will undergo pyrolysis. The thermochemical decomposition of organic in the absence of oxygen at high temperatures is termed pyrolysis. The blend of ceramic powder slurry and PFA is pressed and sintered to pyrolyse the PFA in order to form preform voids. The properties of a preform can be controlled by the following processing parameters: the type of pore forming agent (PFA), the green pressing pressure and the green sintering temperature. Examples of PFAs are carbon fibres (PF) and cellulose particles (PC). **Table 8** presents some PFAs and their sintering temperature.

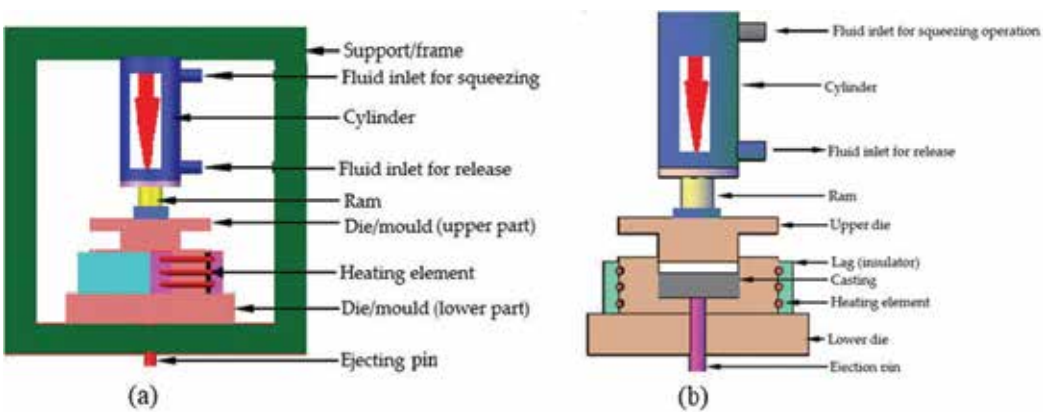

Figure 10. Schematic of hydraulic or mechanical press: (a) SCIM assembly with heating unit and (b) SCIM exploded diagram.

Ceramics	Pore forming additives	Sintering temperature (°C)
AO	PF	1500
AO	PC	1600
Al_2O_3	Glassy frit binder (AG)	1000

Table 8. Sintering temperatures for different preform formation [47, 48].

In a study, ceramic preforms were produced by compressing a blended Al_2O_3 Condea CL 2500 powder and PFA in the form of carbon fibres and followed by sintering [49]. The chemical composition of Al_2O_3 Condea CL 2500 powder is presented in **Table 9**. The profile of the sintering process is presented in **Figure 11**.

4.7. Centrifugal casting

The filling of a rotating mould with a molten metal and allowing the melt to solidify before the spinning is stopped describes fabrication of FGM by centrifugal casting technique (CCT). The rotation creates force that pushes the molten metal outwards from the rotating axis. This process creates a centrifuge in a fluid and separate the fluid's constituents into regions based on density difference. The denser constituent migrates to the outer region. This method was first used by a Brazilian, Dimitri Sensaud DeLavaud, in 1918 [50]. Subsequently, this concept has been adapted in the casting of FGMs, aluminium alloys, corrosion and heat-resistant steels, copper alloys, etc. Its use is also found in the production of non-metal such as plastics, ceram-

Diameter D50 μm	Mean mass concentration of elements, wt.%					
	Al_2O_3	Fe_2O_3	CaO	SiO_2	Na_2O	Others
1.80	99.80	0.02	0.01	0.01	0.05	0.10

Table 9. Chemical composition and particle diameter of Al_2O_3 Condea CL 2500 powder [49].

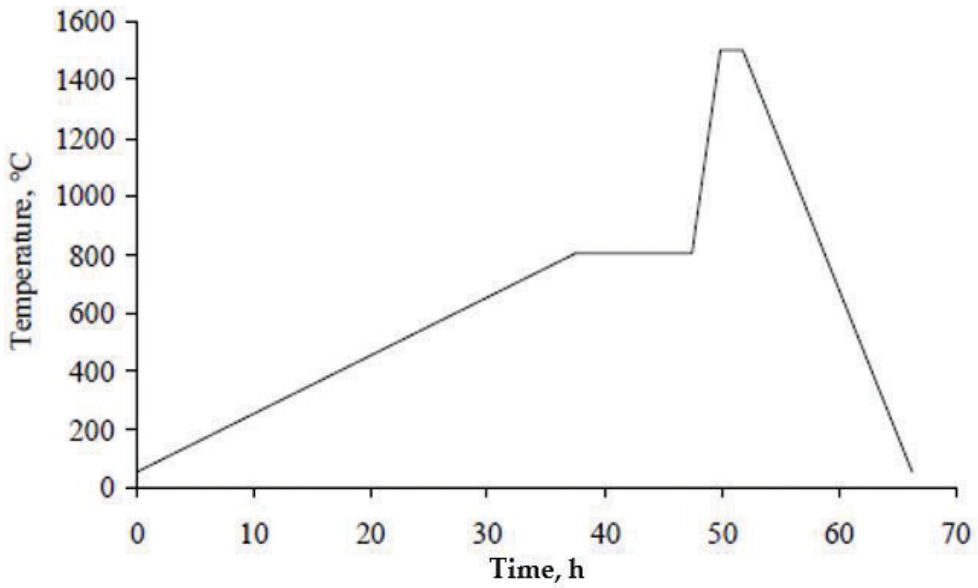

Figure 11. Temperature performance during the sintering process [49].

ics, glasses, and practically every material that is based on liquid or slurries forging method. A schematic of a centrifugal casting machine is shown in **Figure 12**.

In the centrifugal casting of hypereutectic Al-Si alloys, such as A390–5%Mg, the outer region is formed by fibrous silicon. The large α-aluminium dendrites and large primary silicon occupy the inner region due to similarity in their densities. Such castings are regarded as FGAACs. The fabrication of FGMs by CCT is characterised by the discontinuous distribution of reinforcements in a radially graded pattern. The metal matrix and reinforcement density difference cause segregation in which the particles with higher density move to the outer region and lower density particles migrate to the inner surface. The grading defines the functionality and can be controlled and improved by processing variables such as centrifugal rotation speed, molten metal alloying temperature, particle size and volume, mould temperature, and cast geometry [51].

4.7.1. Classification of CCT

The centrifugal casting process can be classified according to mould arrangement and angle inclination of mould to either vertical or horizontal planes [50], as shown in **Figure 13**; and based on the liquidus temperature of the matrix alloy. There are two types of centrifugal methods based on the liquidus temperature [52]: the ex situ or solid-particle centrifugal method; and the centrifugal in situ method.

4.7.2. Forces acting on particle in a melt

In CCT, the force generated primarily depends on the speed of mould rotation. Considering a vertical centrifugal casting, a particle suspended in molten metal is subjected to four types of

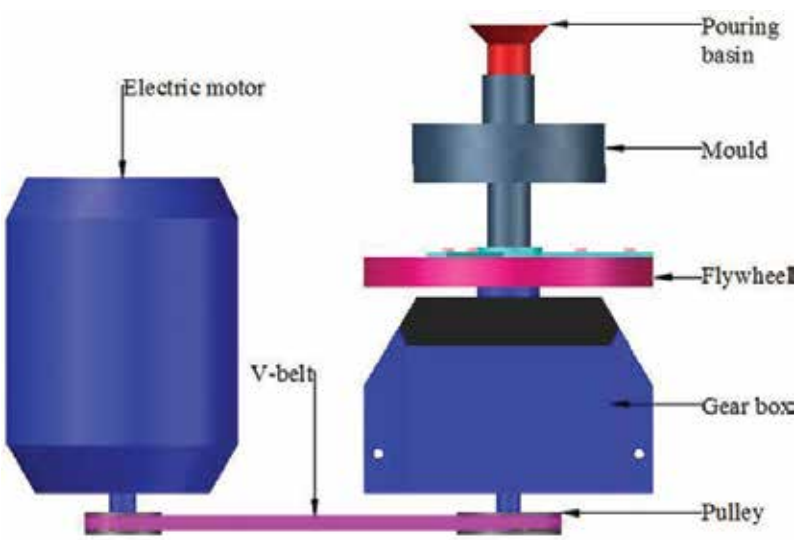

Figure 12. Schematic of a vertical centrifugal casting machine [46].

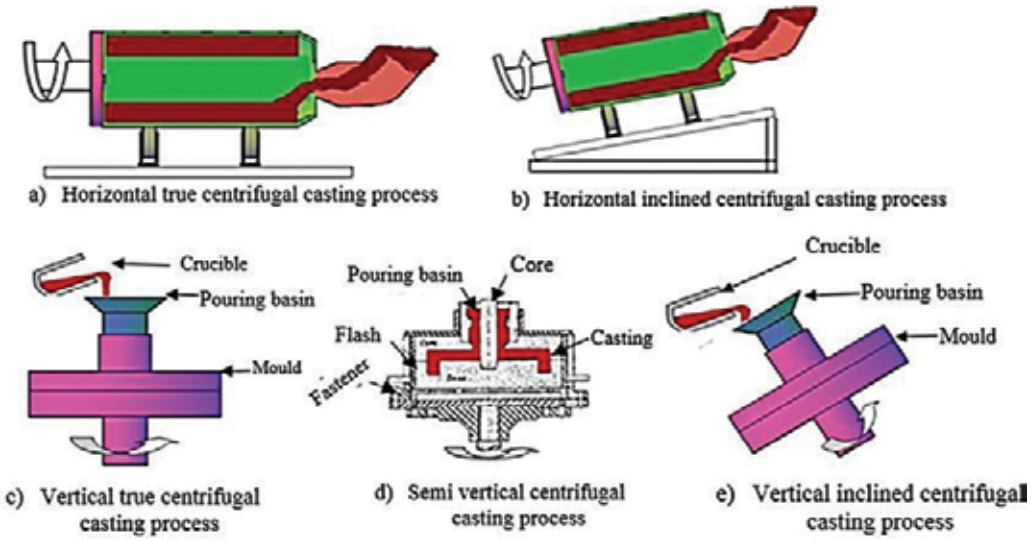

Figure 13. Classification of centrifugal casting methods based on mould rotation [50].

forces, as represented in **Figure 14**: centrifugal force caused by mould rotation, FC; drag force due to viscosity effect, FD; gravitational force, FG; and repulsive force or van der Waal forces caused by solid–liquid interface movement, FL. Force of gravity is often neglected because it is very small compared to centrifugal force [53–55].

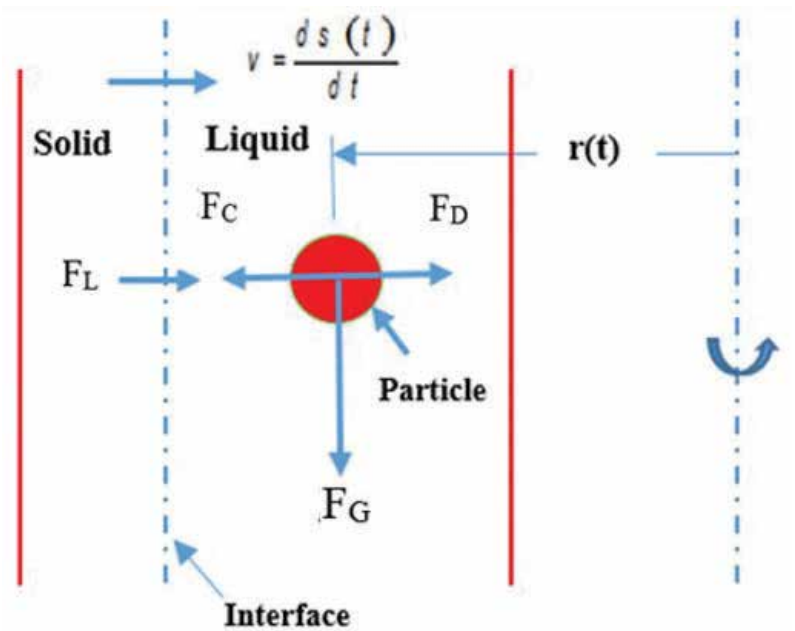

Figure 14. Forces acting on a particle moving in molten metal.

Force balance equation, F_{net}.

The force balance expression, F_{net} is estimated as:

$$F_{net} = F_C - F_D - F_L \tag{3}$$

The FL is linked to the particles within a solid–liquid interface or solid wall. The dynamic Fnet that is not induced by solid wall/interface is:

$$F_{net} = F_C - F_G \tag{4}$$

The Fnet equation assuming that the fluid flow is laminar (Re ≤ 1) is:

$$4/3 * \pi * R^3 * \rho_p(d^2 r/dt) = 4/3 * \pi * R^2(\rho_p - \rho_m)\,\omega^2 * r - 6 * \pi * R * \mu(dr/dt) \tag{5}$$

The solution of Fnet without FL of a particle at a given position moving at uniform velocity at any given time, t, is:

$$r(t) = r_0 \exp\left[\frac{4\,\omega^2(\rho_p - \rho_m)\,R^2\,t}{18\mu}\right] \tag{6}$$

Where r0 = position of the particle at time t = 0.

4.7.3. Application of CCT

In a study, Ramadan and Omer fabricated FGAACs of varying fraction volumes of boron (1.2% to 1.85% wt), dispersed in Al, Al-Cu, and Al-Si alloys matrixes respectively, using CCT [56]. It was observed that B could only dissolve in aluminium alloys sufficiently at elevated temperature. Consequently, the source of boron, B_2O_3, was mixed with aluminium alloys at 1400°C and held for 30 minutes. Centrifugal casting was performed at 800°C. The study reported that two regions were identified without smooth gradient, as shown in **Figure 15**, outer zone with AlB2

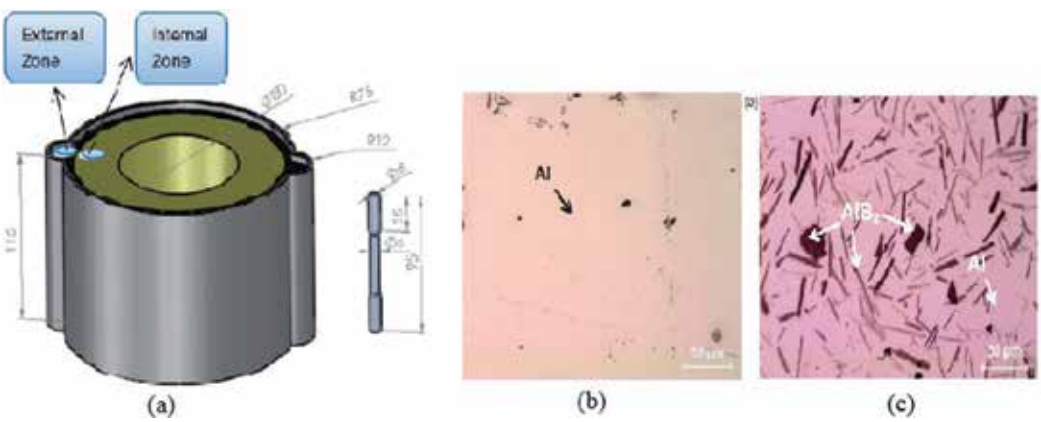

Figure 15. (a) Centrifugal casting mould for Al-AlB_2 FGAAC (a) internal area and (b) external area [56].

surplus and inner zone with AlB2 deficit. Further, hardness of 64% and strength increase were observed with reinforcement particles volume fraction increase at the outer region.

In an investigative study, a complex shape component, a Pelton turbine bucket, was produced from FGAACs using CCT [57]. Functionally graded materials specimen, A356 alloy and A356–10%SiCp, were given T6 heat treatment. The study reported that the concentration of SiCp particles was higher at the inner periphery of the bucket. This was attributed to the Pelton turbine bucket mould design and arrangement. The heat treated specimens shown an appreciable hardness increase. The Pelton turbine bucket mould configuration is shown in **Figure 16**.

4.8. Stir casting

The liquid state technique of fabricating MMCs by mechanical means of mixing of molten metal matrix with the reinforcing particles (dispersed phase) is termed as stir casting. The schematics of a stir casting set-up as well as a complete stir casting facility are shown in **Figure 17**. This method has been described as the simplest and the most effective technique of liquid state production. The stir casting is made up of liquid phase (matrix) and the dispersed phase, which is limited to 30 vol. %. Gravity may cause the reinforcement to segregate due to dispersed and matrix phase density difference. Furthermore, dispersed particles (fibres) form local clouds (clusters). These reasons are why the dispersed phase is not uniform (homogeneous). However, the uniformity of the dispersed phase may be improved when stirring process is conducted in a semi-solid state and this process is called Rheocasting.

The introduction of particles into the melt is an important step in FGAACs fabrication and can be achieved in multiple ways. These methods include inserting particles by an injection gun; adding the particles to the melt stream during pouring; pushing particles into the molten metal with a reciprocating piston; spraying atomised particles and molten metal on a substrate, vortexing, and so on. Vortexing is regarded as the most effective approach towards inserting particles into the molten metal and ultimately dispersing and suspending the dispersed phase in the slurry. The introduction of stirring process is done after the matrix has melted. Vigorous

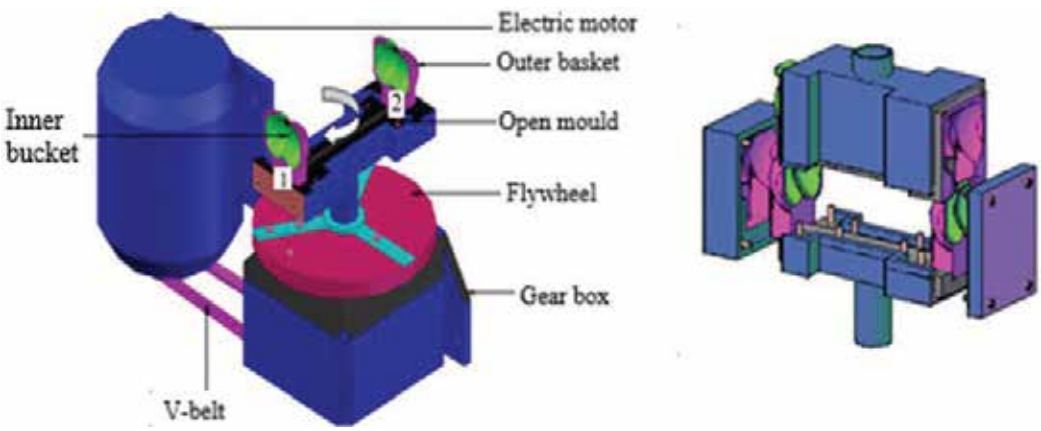

Figure 16. Centrifugal casting machine showing the configuration of the mould [57].

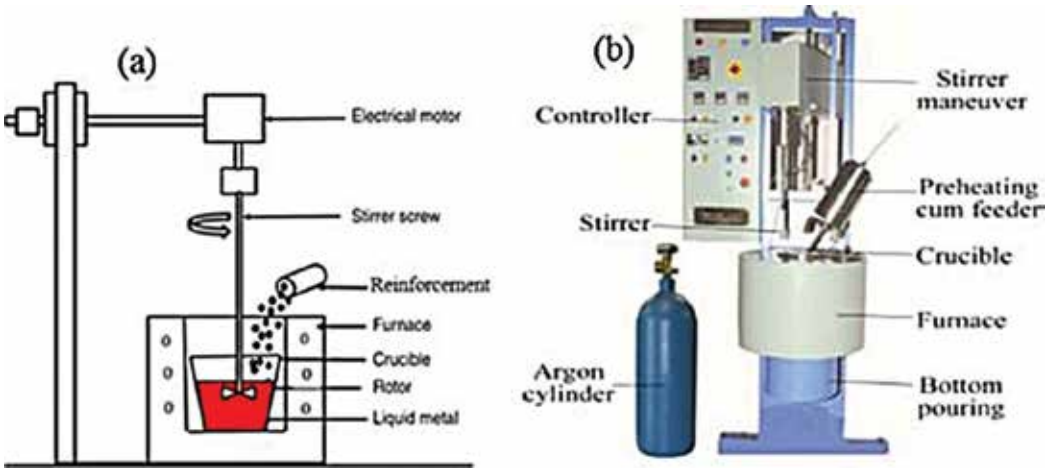

Figure 17. (a) A schematic stir casting set-up and (b) a complete stir casting facility [58].

stirring is required for the formation of vortex at the matrix melt surface. The particles are inserted into the matrix through the vortex and stirred for few minutes before the slurry mixture is poured into the mould. Stir casting is affected by certain variables, such as stirring time, pouring temperature, pouring rate, stirrer blade angle, and gating systems [58, 59].

4.9. Compocasting

Many wettability enhancement methods have been introduced and some of these methods include the use of wettability agents and fluxes, preheating, oxidation and ceramic coating [60, 61]. The application of some of these techniques is expensive. However, the compocasting method is an economical technique to improve wettability [62]. Compocasting, or slurry casting, is a liquid state process in which the dispersed phase is added to a solidifying melt under a vigorously agitation. This method prevents agglomeration and the gravity induced reinforcement segregation by mechanically entrapping the dispersed phase in the semi-solid slurry. Further, the reinforcing particles are better distributed, and gives lower porosity casting [63, 64]. The better wettability between the matrix and the dispersed phase, and matrix alloy lower volume shrinkage are accountable for the lower porosity.

Compocasting liquid state process technology is undergoing review and the investigative study on the process is expanding due to its increase in applications. Gladston et al. produced AA6061-RHAp, rice husk ash particle composite, via the compocasting method [61]. Formation of intergranular distribution of particles and the enhancement of macro hardness and ultimate tensile strength of RHA particles of FGAAC were observed. Poor mechanical properties of Al-Si alloys have been attributed to the challenges of homogeneous dispersion of SiCp particles and the non-uniform distribution of coarse Si fibres in the matrix. The use of an accumulative roll bonding (ARB) technique, which operates on the concept of the compocasting technique, eliminates these setbacks [65]. This was used to produce MMC with finer and spheroidal Si particles; minimised porosity; no Si and SiC particles free zone; better matrix-particle bonding; and evenly dispersed Si and SiCp particles. The schematic of ARB is shown in **Figure 18**.

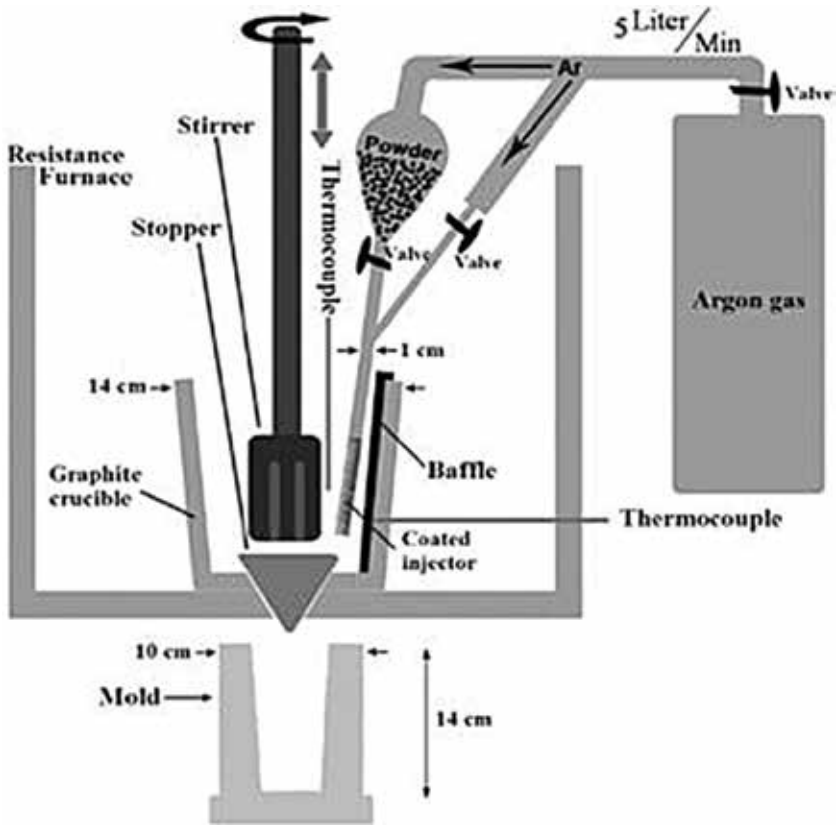

Figure 18. Schematic of ARB set-up [65].

5. Effects of wettability and porosity in FGMs

5.1. Wettability

Several barriers prevent FGAACs from performing in their full potentials, and one paramount among them is insufficient wetting of reinforcing particles by molten aluminium. The spreading of a liquid on the solid surface is defined as wettability and has been linked to close contact between a liquid and a solid. The way in which the dispersed phase is wetted by melt is a sign of success of particle insertion into the matrix in FGAAC fabrication. The aluminium oxide layer which covers molten aluminium and/or the inherent silicon oxide that covers SiC particles is responsible for the inadequate wetting of SiC particles by molten aluminium. Reactive elements, such as Ti, Zr, Ca, Mg, etc. are added to metal matrix to stimulate wettability of matrix on reinforcements.

The relation between bonding force of the matrix and the particles was described by Young Dupre's equation in terms of contact angle (θ) as depicted in **Figure 19** as follows [66]:

$\theta - 0^{o}$ (Perfect wettability); $\theta - 180^{o}$ (no wetting); $0 < \theta < 180^{o}$ (partial wetting).

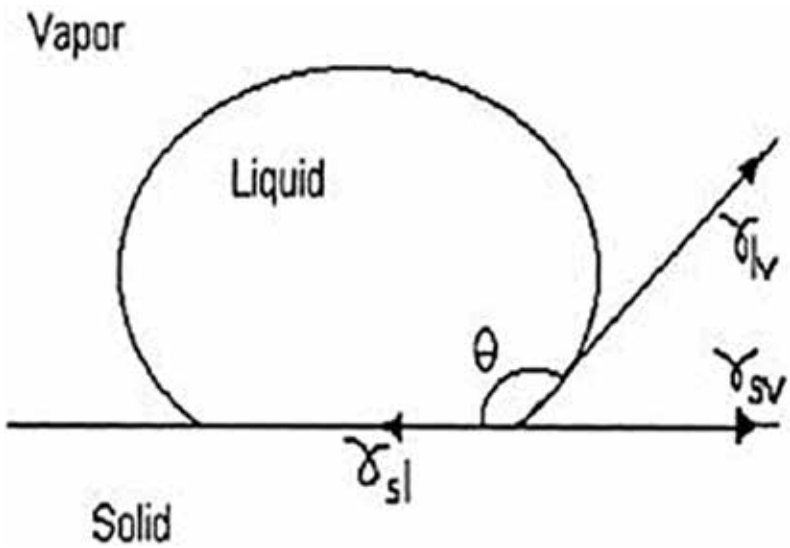

Figure 19. Schematic showing the contact angle between the liquid phase and the solid phase [59], where γ_{sv} is the solid–vapour; γ_{sl} is the solid–liquid interfacial energy; and γ_{lv} is the liquid–vapour interfacial energy.

5.2. Porosity

Porosities are often seen as defects in engineering materials, unless the materials are deliberately designed to have pores for functionality, such as in biomedical materials, where porosity is useful for permeation of medical compounds. Other applications of porosity include filters, catalyst supports and furnace lining bricks. FGAAMCs are made dense to minimise porosity and to improve the mechanical properties of the materials. Damping capacity, the Poisson ratio, tensile and compressive strengths and Young's modulus of elasticity are inversely proportional to porosity. Porosity formation is caused by vapour from surfaces of reinforcement, air bubbles in a matrix melt, shrinkage during solidification and gas entrapment and hydrogen evolution [67]. Series of manufacturing techniques have been invented and appraised to minimise porosity in cast FGMs and these include: vacuum casting, casting under pressure, inert gas bubbling past the liquid metal, rolling of material after casting to close the voids, compressing, and addition of hexachloroethane to melt [68].

6. Applications areas of FGMS

The FGM concept is described as a systematic process of combining incompatible functions such as wear and corrosion resistance, thermal, toughness and machinability into a single part. This has expanded the application of FGMs in many sectors. Two FGMs in commercial status are high performer cutting tools, namely, tungsten carbide/cobalt and a razor blade of iron aluminium/stainless steel (FeAl/SS) FGM [6]. **Table 10** presents FGMs application areas.

Sectors	Applications
Engineering	Cutting tools, machine parts, engine components, etc.
Medical	Biomaterials: implants, artificial skin, drug delivery system
Energy	Thermionic and thermoelectric converters, fuel cells and solar batteries
Aerospace	Space plane nose, combustion chamber protective layer, body components, etc.
Automotive	Crown of piston, cylinder liners, exhaust valves and valve seating
Nuclear	First wall of fusion reaction, fuel pellets
Optics	Optical fibre, lens
Chemical plants	Heat exchanger, heat pipe, slurry pump, reaction vessel
Electronics	Graded band semiconductor, substrate, sensor

Table 10. Application areas of FGMs.

7. Conclusion

This chapter presents an overview of the bulk FGMs production techniques, their evolution, principles and applications. The fabrication processes discussed include squeeze casting, compocasting, infiltration process, stir casting, and centrifugal casting. The chapter observed that despite the tremendous development in developing FGMs and their production technologies, challenges still abound in getting the desirable material without certain material attributes being a trade-off. The use of some of these methods for mass production is challenging from cost of fabrication perspective. However, the combination of techniques seems to be satisfactory as stir casting with compocasting, stir casting with squeeze casting processes. Several FGAAMCs laboratory investigations have revealed that processing parameters to consider are peculiar to the type of fabrication method used. However, reinforcement particle size, and casting temperature seem to be common to all the methods.

Author details

Williams S. Ebhota* and Tien-Chien Jen

*Address all correspondence to: willymoon2001@yahoo.com

Mechanical Engineering Department, University of Johannesburg, Johannesburg, South Africa

References

[1] Tarlochan F. Functionally graded material: A new breed of engineered material. Journal of Applied Mechanical Engineering. 2013;**1**:1-5

[2] Rezaei Mojdehi A, Darvizeh A, Basti A, Rajabi H. Three dimensional static and dynamic analysis of thick functionally graded plates by the Meshless local Petrov–Galerkin (MLPG) method. Engineering Analysis with Boundary Elements. 2011;**35**(11):1168-1180

[3] Shailendra KB, Ritesh S, Prabhat RM. Functionally graded materials: A critical review. International Journal of Research (IJR). 2014;**1**:289-301

[4] Knoppers GE, Gunnink JW, Van Den Hout J, Vliet WPV. The Reality of Functionally Graded Material Products. Presented at the International Solid Freeform Fabrication Symposium. Texas: University of Texas at Austin; 2004

[5] Ebhota WS, Inambao FL. Principles and baseline knowledge of functionally graded aluminium matrix materials (FGAMMs): Fabrication techniques and applications. International Journal of Engineering Research in Africa. 2016;**26**:47-67

[6] Miyamoto Y, Kaysser W, Rabin B, Kawasaki A, Ford R. Functionally Graded Materials: Design, Processing and Applications. US Kluwer Academic Publishers; 1999

[7] Lannutti JJ. Functionally graded materials: Properties, potential and design guidelines. Composites Engineering. 1984;**4**:18-94

[8] Shukla A, Jain N, Chona R. A review of dynamic fracture studies in functionally graded materials. Strain. 2007;**42**:76-95

[9] Saifulnizan J. Application of Functionally Graded Materials for Severe Plastic Deformation and Smart Materials: Experimental Study and Finite Element Analysis; PhD. Department of Engineering Physics, Electronics and Mechanics, Graduate School of Engineering, Nagoya Institute of Technology, Japan; 2012

[10] Shen M, Bever MB. Gradient in polymetric materials. Materials Science and Engineering. 1972;**7**:741-746

[11] Bever MB, Duwez PF. Gradient in composite materials. Materials Science and Engineering. 1972;**10**:1-8

[12] Niino M, Hirai T, Watanabe R. The functionally gradient materials. Japan Society for Composite Materials. 1987;**13**:257-264

[13] Niino M, Kumakawa A, Watanabe R, Doi Y. Fabrication of a High Pressure Thrust Chamber by CIP Forming MethodMetal powder report 41, 663, 9.1986

[14] Ankit BM, Khushbu CP. A review of stress analysis of functionally graded material plate with cut-out. International Journal of Engineering Research & Technology (IJERT). 2014;**3**

[15] Wang SS. Fracture mechanics for delamination problems in composite materials. Journal of Composite Materials. 1983;**17**:210-223

[16] Dalal R. Thermal Analysis of Functionally Graded Material (FGM) Plate Using Finite Element Method (FEM)M. Tech. Murthal: Mechanical Engineering, Deenbandhu Chhotu Ram University of Science and Technology; 2016

[17] Siti NSJ, Faizal M, Dewan MN, Shah NB. A review on the fabrication techniques of functionally graded ceramic-metallic materials in advanced composites. Scientific Research and Essays. 2013;**8**:828-840

[18] Besmann TM. Proceedings of the Thirteenth International Conference on Chemical Vapor Deposition vol. 96-5. Pennington, New Jersey, USA: The Electrochemical Society, Inc., 1996

[19] Groves JF, Wadley HNG. Functionally graded materials synthesis via low vacuum directed vapor deposition. Composites Part B: Engineering. 1997;**28**:57-69

[20] Hutmacher DW, Sittinger M, Risbud MV. Scaffoldbased tissue engineering: Rationale for computer-aided design and solid freeform fabrication systems. Trends in Biotechnology. 2004;**22**:354-362

[21] Mumtaz KA, Hopkinson N. Laser melting functionally graded composition of Waspaloy and zirconia powders. Journal of Materials Science and Engineering. 2007;**42**:7647-7656

[22] Rasheedat MM, Esther TA, Mukul S, Sisa P. Functionally Graded Material: An Overview. In: Proceedings of the World Congress on Engineering, WCE, London, UK, 2012

[23] Jiang R, Chen X, Ge R, Wang W, Song G. Influence of TiB2 particles on machinability and machining parameter optimization of TiB_2/Al MMCs. Chinese Journal of Aeronautics 20-04-2017. 2017

[24] Ibrahim A, Mohamed F, Lavernia E. Particulate reinforced metal-matrix composites–A review. Journal of Materials Science. 1997;**26**:1137-1156

[25] Rajan TPD, Jayakumar E, Pai BC. Developments in solidification processing of functionally graded aluminium alloys and composites by centrifugal casting technique. Transactions of the Indian Institute of Metals. 2012;**65**:531-537 01-12-2012

[26] Rajan TPD, Pai BC. Developments in processing of functionally gradient metals and metal–ceramic composites: A review. Acta Metallurgica Sinica (English Letters). 2014;**27**:825-838

[27] El-Galy IM, Ahmed MH, Bassiouny BI. Characterization of functionally graded Al-SiCp metal matrix composites manufactured by centrifugal casting. Alexandria Engineering Journal 27-03-2017. 2017. DOI: http://dx.doi.org/10.1016/j.aej.2017.03.009

[28] Tsiatas GC, Charalampakis AE. Optimizing the natural frequencies of axially functionally graded beams and arches. Composite Structures. 2017;**160**:256-266 15-01-2017

[29] Vieira AC, Rocha LA, and Gomes JR, Influence of Sic Particles Incorporation on the Microstructure and Tribological Behaviour of Functional Graded Al/SiCp Composites. In: Proceedings of the IV Iberian Congress on Tribology, Ibertrib, Bilbao, Spain, 2007

[30] Erdemir F, Canakci A, Varol T. Microstructural characterization and mechanical properties of functionally graded Al2024/Sic composites prepared by powder metallurgy techniques. Transactions of Nonferrous Metals Society of China. 2015;**25**:3569-3577

[31] Vieira AC, Sequeira PD, Gomes JR, Rocha LA. Dry sliding wear of Al alloy/SiCp functionally graded composites: Influence of processing conditions. Wear. 2009;**267**:585-592

[32] Watanabe Y, Kawamoto A, Matsuda K. Particle size distributions in functionally graded materials fabricated by centrifugal solid-particle method. Composites Science and Technology. 2002;**62**:881-888

[33] Ghomashchi MR, Vikhrov A. Squeeze casting: An overview. Journal of Materials Processing Technology. 2000;**101**:1-9

[34] Total Materia (2007, 23-07-2017). Squeeze Casting Process: Part one. Available: http://www.totalmateria.com/page.aspx?ID=CheckArticle&site=ktn&NM=172

[35] Li R, Liu L, Zhang L, Sun J, Shi Y, Yu B. Effect of squeeze casting on microstructure and mechanical properties of hypereutectic Al-xSi alloys. Journal of Materials Science and Technology. 2017;**33**:404-410 01-04-2017/

[36] Wang F, Ma Q, Meng W, Han Z. Experimental study on the heat transfer behavior and contact pressure at the casting-Mold Interface in squeeze casting of Aluminum alloy. International Journal of Heat and Mass Transfer. 2017;**112**:1032-1043 01-09-2017/

[37] Jahangiri A, Marashi SPH, Mohammadaliha M, Ashofte V. The effect of pressure and pouring temperature on the porosity, microstructure, hardness and yield stress of AA2024 Aluminum alloy during the squeeze casting process. Journal of Materials Processing Technology. 2017;**245**:1-6 01-07-2017/

[38] Kopeliovich D. Squeeze Casting; 2012(25-07-2017)

[39] Ibrahim IA, Mohamed FA, Lavernia EJ. Particulate reinforced metal matrix composites — A review. Journal of Materials Science. January 01 1991;**26**:1137-1156

[40] Meier A, Javernick DA, Edwards GR. Ceramic-metal interfaces and the spreading of reactive liquids. JOM. February 01 1999;**51**:44-47

[41] Gupta M, Ibrahim IA, Mohamed FA, Lavernia EJ. Wetting and interfacial reactions in Al-Li-SiCp metal matrix composites processed by spray atomization and deposition. Journal of Materials Science. December 01 1991;**26**:6673-6684

[42] Bear J. Dynamics of Fluids in Porous Media. New York: American Elsevier Publishing. Co; 1972

[43] Oh SY, Cornie JA, Russell KC. Wetting of ceramic particulates with liquid aluminum alloys: Part I. Experimental techniques. Metallurgical Transactions A. 01-03-1989;**20**:527-532

[44] D. Kopeliovich. 2012, (26-07-2017). Liquid State Fabrication of Metal Matrix Composites. Available: http://www.substech.com/dokuwiki/doku.php?id=liquid_state_fabrication_of_metal_matrix_composites

[45] Boczkowska A, Chabera P, Dolata AJ, Dyzia M, Oziębło A. Porous ceramic–Metal composites obtained by infiltration methods. Meta. 2013;**52**:345-348

[46] Ebhota WS, Karun AS, Inambao FL. Principles and baseline knowledge of functionally graded aluminium matrix materials (FGAMMs): Fabrication techniques and applications. International Journal of Engineering Research in Africa. 2016:47-67

[47] Staudenecker D. Development of Porous Ceramic Preforms and Manufacture of Metal-Ceramic Composites: Diploma FH Aalen. FH Aalen, Germany; 2001

[48] Bernd AH. Pressure Infiltration Behaviour and Properties of Aluminium Alloy - Oxide Ceramic Preform CompositesDoctor of Philosophy. School of Metallurgy and Materials, The University of Birmingham, UK; 2009

[49] Dobrzañski LA, Kremzer M, Nowak AJ, Nagel A. Aluminium matrix composites fabricated by infiltration method. Archives of Materials Science and Engineering. 2009;**36**:5-11

[50] Sufei W, Steve L. ASM handbook: Centrifugal casting. ASM International. 2008;**15**:667-673

[51] Ebhota WS, Karun AS, Inambao FL. Centrifugal casting technique baseline knowledge, applications, and processing parameters: Overview. International Journal of Materials Research. 2016;**107**:960-969

[52] Watanabe Y, Sato H, Fukui Y. Wear properties of intermetallic compound reinforced functionally graded materials fabricated by centrifugal solid-particle and in-situ methods. Journal of Solid Mechanics and Materials Engineering. 2008;**2**:842-853

[53] Balout B, Litwin J. Mathematical Modeling of particle segregation during centrifugal casting of metal matrix composites. Journal of Materials Engineering and Performance. 2012;**21**:450-462

[54] Emila P, Dipak M, Mehrotra SP. Mathematical Modeling of particle segregation during centrifugal casting of metal matrix composites. Metallurgical and Materials Transactions. 2006;**37A**:1675-1687

[55] Rempel AW, Worster MG. Particle trapping at an advancing solidification front with interfacial-curvature effects. Journal of Crystal Growth. 2001;**223**:420-432

[56] Kayikci R, Savaş Ö. Fabrication and properties of functionally graded Al/AlB2 composites. Journal of Composite Materials. 2015;**49**:2029-2037

[57] Ebhota WS, Karun AS, Inambao FL. Investigation of functionally graded aluminium A356 alloy and A356-10%SiCp composite for hydro turbine bucket application. International Journal of Engineering Research in Africa. 2016;**26**:30-46

[58] Jebeen MJ, Dinaharan I, Joseph SS. Prediction of influence of process parameters on tensile strength of AA6061/TiC Aluminum matrix composites produced using stir casting. Transactions of Nonferrous Metals Society of China. 2016;**26**:1498-1511

[59] Hashim J, Looney L, Hashmi MSJ. Metal matrix composites: Production by the stir casting method. Journal of Materials Processing Technology. 1999;**92-93**:1-7

[60] Ashok KB, Murugan N. Metallurgical and mechanical characterization of stir cast AA6061-T6-AlNp composite. Materials and Design. 2012;**40**:52-58

[61] Allwyn KGJ, Mohamed SN, Dinaharan I, David RSJ. Production and characterization of rich husk ash particulate reinforced AA6061 aluminum alloy composites by compocasting. Transactions of Nonferrous Metals Society of China. 2015;**25**:683-691

[62] Ceschini L, Minak G, Morri A. Tensile and fatigue properties of the AA6061/20 vol.% Al_2O_3p and AA7005/10 vol.% Al_2O_3p composites. Composites Science and Technology. 2006;**66**:333-342

[63] Dinaharan I, Nelson R, Vijay SJ, Akinlabi ET. Microstructure and wear characterization of aluminum matrix composites reinforced with industrial waste fly ash particulates synthesized by friction stir processing. Materials Characterization. 2016;**118**:149-158 01-08-2016

[64] Hoziefa W, Toschi S, Ahmed MMZ, Morri A, Mahdy AA, El-Sayed Seleman MM, et al. Influence of friction stir processing on the microstructure and mechanical properties of a compocast AA2024-Al_2O_3 nanocomposite. Materials & Design. 2016;**106**:273-284 15-09-2016

[65] Amirkhanlou S, Roohollah J, Behzad N, Mohammad RT. Using ARB process as a solution for dilemma of Si and SiCp distribution in cast Al-Si/SiCp composites. Materials Process Technology. 2011;**211**:1159-1165

[66] Narciso J, AIonso A, Pamies A, Garcia-Cordovilla C, Louis E. Wettability of binary and ternary alloys of the system Al-Si-Mg with SiC particulates. Scripta Metallurgy. 1994;**31**:1495-1500

[67] Aqida SN, Ghazali MI, Hashim J. Effects of porosity on mechanical properties of metal matrix composite: An overview. Jurnal Teknologi. 2004;**40**:17-32

[68] Larry LH. Bioceramics. Journal of the American Ceramic Society. 1998;**81**:1705-1728

Chapter 6

Evaporative Pattern Casting (EPC) Process

Babatunde Victor Omidiji

Additional information is available at the end of the chapter

http://dx.doi.org/10.5772/intechopen.73526

Abstract

The chapter provides details of operations and activities in evaporative pattern casting (EPC) Process. The process was developed in the year 1956 to tackle some of the inadequacies of the traditional sand casting processes but has in itself some challenges that should be taken care of if sound castings would be obtained. The challenges come mainly from the evaporative pattern employed as pattern material in the process. The material makes the process to be sensitive to process variables such that proper and adequate control should be ensured to have castings of sound integrity. Some of the known process variables are pouring temperature, refractory coating, vibration and pattern and molding materials. In the whole the EPC is known to have edge over the traditional sand casting methods.

Keywords: pattern, molding, casting, variables and coating

1. History of evaporative pattern casting (EPC) process

Evaporative pattern casting (EPC) Process is a sand molding process that makes use of evaporative patterns produced industrially by steam molding or machined out from a block of expandable polystyrene foam (EPS) [1, 2]. The pattern is buried in the sand mold and the melted casting material is poured into the mold without removing pattern, unlike the traditional sand casting method that makes use of wooden, plastic and metallic pattern which is removed from the mold before molten metal is advanced.

It was in 1956 that Shroyer made a documentation of his work on EPC where green sand was used as the molding material [3]. The author machined a shape from expanded polystyrene (EPS) and supported it inside a flask with bounded sand. Another researcher called Flemmings

came up in 1964 to use unbounded silica grains for the process [1]. Foundry men later came to differentiate between the two; calling the first the full mold and the second the lost foam processes. The subtle difference only lied in the use of bounded (green) sand and loose sand.

The process became known to foundry men in 1958 and many trade names have been formed to describe it [3]. They include styrecast, replicast, full mold, lost foam and evaporative process. A distinguishing feature of this type of sand process is that an evaporative pattern made of polystyrene foam is used [4]. It is coated with a coating developed from a refractory material usually silica or zircon sand before being buried in the mold. It is not removed from the mold once it is buried.

After 1964, some works have been done by researchers to understand the variables that affect the process. Some works in the automotive industry have also been done. General motors have produced a number of automotive components with the method. This started in the year 1980 and they are still in the use of the process. The full mold process unlike the conventional sand casting process uses patterns and pouring system, which retains the pattern in the mold, thus justifying the title full mold [5]. The term 'evaporative' stands as a family name for all the trade names that have so far been coined out for evaporative pattern casting processes. This is because the pattern evaporates when there is contact between it and liquid metal; all the features are replicated [6].

2. Introduction

By evaluation and practices, the process is known to take care of intricate and complex shapes without the use of cores; this is not achievable in traditional sand casting methods. The surface finish of the castings produced has an edge over the ones of green sand method. Very slender elements are produced with ease using EPC which is very difficult in other sand casting methods. Precision in terms of dimensional accuracy is better [7].

With the trend in the automotive industries; where engine blocks and cylinder heads are made with aluminum alloy, the evaporative pattern casting process has found a place for effective production. This has opened up endless research opportunities aimed to improve on the use of metal alloy components obtained by EPC.

Patterns used in EPC process are produced locally by machining them from blocks of polystyrene material and industrially by steam molding of the beads. The ones produced industrially are for mass production. The commonly used pattern material is expandable polystyrene (EPS). Polyalkylene carbonate (PAC) is used to manufacture ferrous castings [3]. Another material that is used for EPC is the poly methyl methacrylate (PMMA). Metal tooling with techniques that have been developed for industrial packaging is used. Precision machine tools are required for EPC process. The tooling material is aluminum alloy. It is used because of its exceptional properties which are not found in other alloys. The properties include good thermal conductivity, good erosion resistance, fair strength, light weight and good surface finish upon machining.

http://dx.doi.org/10.5772/intechopen.73526

The process of producing pattern material is regarded as polymerization. In local development of EPC Process, the patterns are cut manually using knives, blades, pre-heated wire etc. and then smoothened out by emerald paper. At times when parts are to be joined together, the use of glue is employed. Juice from rubber plant can as well be used to join patterns. After the production of the pattern and it is assembled with the gating system, it is coated with refractory material which may be wet (slurry) or dry. The coating provides a barrier between the flowing motel metal and the molding sand to prevent metal penetration. Other benefits are offered. An example is the quality of casting surface produced.

The gating system assembled with the pattern is informed by the weight of the casting to be poured. Immediately the pattern that is coated is dry, it is taken and buried in the mold. Care is taken so that the coating layer is not peeled off. Molding sand is packed into the molding flask and rammed carefully so that the pattern is not distorted and the mold is poured. After solidification, shake out process follows and cleaning of the casting is done. The molding sand is entirely reclaimable. The process offers many benefits to both the casting producers and users in terms of time reduction and low cost in the production of the patterns and low cost of purchase of pattern materials.

Mold production entails the placement of the coated pattern assembly in green sand and rammed to obtain compaction of the grains. In the full mold, green sand is used as molding material. Things required in mold production are: molding sand, molding boxes, pattern and vibration. Following vibration, the mold is prepared for casting, which may simply involve the location of a pouring basin above the sprue entrance. However, to prevent fluidization/erosion of the sand during pouring, caused by the evolved gaseous pattern decomposition products, mold weights may be necessary, or the top of the box may be covered with a plastic sheet and a soft vacuum applied [3].

When pouring the liquid metal into prepared molds, it must flow full right from the pouring cup on top of the sprue in the gating system down to the mold cavity [8]. This offers advantages in that the mold would not collapse, the sprue evaporates completely, air aspiration is avoided and sound casting is obtained. The pouring rate is determined by the density of the foam, permeability of the sand and casting material. Gating design is therefore done carefully to achieve sound castings. The elements of gating system include pouring cup, down sprue, sprue base well, runners, ingates and risers. Careful design of each of these elements brings about soundness in castings. The gating ratio is informed by the type of material to be cast. For aluminum alloys, non-pressured gating ratios like 1:2:4, 1:3:3 or 1:4:4 is used [8]. This refers to the cross-sectional areas of the choke, runners and ingates. For the ferrous materials, pressurized gating ratios are used like 4:3:1, 2:1:8, 1:1:4 and 1:2:1 [8].

Once liquid metal is poured in EPC mold both physical and chemical reactions start to occur. EPC is known to be influenced by many variables. The combination of these variables determines whether sound casting would be obtained. The process begins by mold filling with the liquid metal, followed by transfer of heat energy from the liquid metal to the evaporative pattern in the mold. The flow of liquid metal to make contact with the pattern is also observed and when it eventually makes contact, decomposition of the foam begins, leading to pyrolysis

products [2]. Pressure in the mold is built up as a result of these products and reactions. The pressure determines what quality of the casting that would be obtained [9, 10].

As a unique technique to produce integrated components which otherwise must be cast in several parts, it has drawn great interest from both academia and industry [10]. Efforts have been made over the years to understand variables and physico-chemical activities that significantly affect the process and initiate means of monitoring and controlling them. These research efforts have enabled rapid growth of EPC production around the world [6]. This has cumulated to the increase of the products of the process in the automotive and similar industries. Researches are still on-going to maximize the benefits.

It has been observed that the EPC offers many advantages over the traditional/conventional casting processes. One of the advantages is that it eliminates the requirements of cores for internal structures because foam patterns which are produced by steam molding in industrial set-up or machined from a block of polystyrene are shaped desirably to bring out the casting. This machining method also allows several parts to be assembled and makes complex casting designs possible. Other advantages include increased dimensional accuracy, saved material and costs as castings produced with the process require minimal fettling.

In EPC Process the molding sand is reusable because no binders are used, which makes EPC a more environmentally friendly process [11]. This process also eliminates issues like dewaxing and mold firing that occurs in the lost wax process. It has been shown that the mechanical properties of lost foam castings and full-mold castings have cutting edge over those of other sand castings [11]. Other attractive features include near-net-shape casting, elimination of parting lines and excellent surface finish. **Table 1** shows a comparison among the various casting processes on labor cost, equipment and surface finish. Studies show that all ferrous and nonferrous metals have been successfully cast using EPC process.

Type of process	Labor cost per unit	Equipment cost	Surface finish μ m CLA	Accuracy mm	Minimum section mm
Sand (green)	Medium	Low	500–1000	±2.5	5.0
Shell	Low	Medium	100–300	±0.25	2.5
Centrifugal	Low	Medium	100–500	±0.7	8.0
Investment	High	Medium	25–125	±0.06–25	0.6
Die casting gravity	Low	Medium	100–250	±0.4 + 0.05 per 25 mm	2.5
Die casting low press	Low	Medium	40–100	±0.05 + 0.05 per 25 mm	1.2
continuous	Low	High	100–200	±0.12 per 25 mm	8.0
EPC	Low	Low	60–300	±0.05 + 0.05 per 25 mm	1.0

Source: [10].

Table 1. Summary of casting processes.

One outstanding advantage that EPC process offers is that there is minimal number of rejected castings. It could then be inferred that there is a saving on cost of purchase of furnace fuel used in firing and melting and energy to remelt the scraps or rejected products is reduced. The casting material is also optimized as it does not end in scraps; sound castings are produced with them.

In overall evaluation EPC should be preferred to the traditional casting methods. Therefore in where energy supply is not adequate the foundry engineer could make use of the EPC for these afore mentioned benefits and the rapid production of the patterns with less energy expended unlike the patterns used in the conventional methods where large amount of energy is expended.

With the advantages and benefits that the process offers, not all foundries are known to embrace it. However, predictions have been made that soon very many foundries would use the process; looking at it from the perspective of automotive industries. It is believed that if the process parameters that affect the EPC process are properly monitored and controlled and there is proper gating system design and melting and pouring practices, defect free castings should be obtained [5].

In order to obtain castings with good surface finish free from defects researchers both in industries and academia are giving attention to both experimental, modeling and theoretical studies of the variables known to influence the process [2, 6, 12–17]. It has been recognized that the pyrolysis products are the main source of defects in EPC [11, 18].

The EPC process is very sensitive and known to be complex because of the very many variables that affect it. Experiments and research efforts have not been able to adequately quantify certain parameters like the heat transfer coefficient existing between the liquid metal flow and the decomposing foam. Therefore a range of the coefficient has been proposed to be 40–160 W/m^2 K [10, 19].

According to Mohammed [20] computational models and simulations have been developed to further understand the interactions of various variables in EPC process in order to help reduce defect formation in the castings [9–11, 21–24]. Since the heat transfer from the molten metal to foam pattern plays a very important role, models without sufficient consideration of the foam pyrolysis process do not capture the effect of process parameters on the defect formation in the castings.

3. Evaporative pattern casting (EPC) process steps

Clegg [3], Acimovic-Pavlovic [12] and Kumar et al. [6] outlined the basic steps in the EPC Process. All the activities are diagrammatically illustrated in **Figure 1**. It is of interest to see the steps simply outlined but every step needs to be carefully monitored and controlled because of the physico-chemical interactions in the steps coupled with the process parameters that are involved for the purpose of producing consistent and high quality castings.

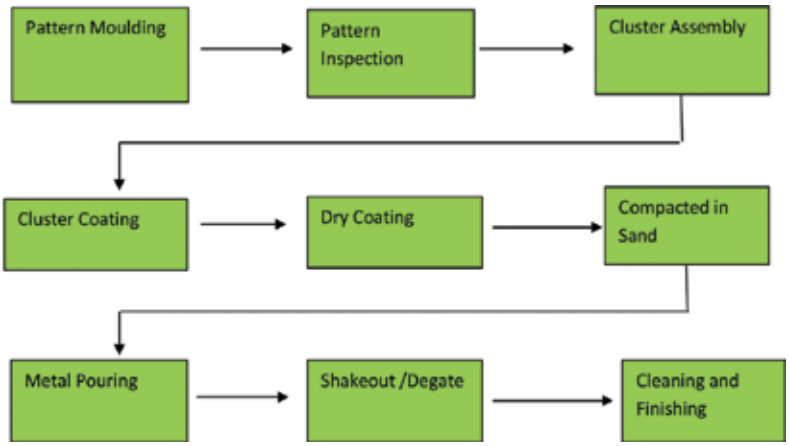

Figure 1. Steps of EPC process. Source: [10].

The very many variables of EPC process grouped into six categories have made the process to react to changes that occur in the system. The combined and individual effects of these variables sometimes produce significant effects on the process and its products [11, 25]. The chain of systems observed to make castings by EPC process are divided into two main classes

a. Evaporative pattern production, assembly and inspection

b. Casting production and inspection

The first division is a six-step operation. The step 1 is the pattern molding. This is done industrially by injection process. Beads of polystyrene foam are injected into molding machine under pressure. The foam material together with the amount of applied pressure for compaction determines the density of the polystyrene pattern that would be employed for casting. This is an industrial option. On the other hand, patterns are machined from a block of polystyrene foam with a device called heated wire. Step 2 is the inspection of the patterns produced industrially or manually. Dimensional accuracy and correctness of the shape are inspected at this level. Distortion of the patterns is avoided. This is paramount to the EPC Process. Many a time, EPC Process involves casting of intricate shapes such that a shape will be broken into segments and patterns will be produced for these segments. The patterns of the segments are joined together with glue. The joining process is referred to as cluster assembly which is step 3. To provide ability to withstand thermal energy from advancing liquid metal and prevent sand penetration in evaporative pattern castings, refractory coating which is made from highly refractory materials is sprayed on the patterns. Step 4 takes care of this. The patterns are left to dry. The drying period is within a matter of seconds; maximum 15 s. This is possible because of the reducer/carrier which is usually methyl alcohol at 99% concentration that is employed in the transfer of the coating to spraying the pattern. The drying process is done in step 5. Step 6 deals with compaction of the coated patterns in the sand mold. The sand mold is prepared with molding sand usually river sand whose grain fineness number has been determined and some other properties which molding materials should have like green strength, refractoriness, hot strength and so on. Immediately the bed is laid, the pattern is put

inside the molding flask then it is filled with molding and backing sand. The pattern is not removed from the mold.

The second division deals with casting production and inspection. Three steps are involved. The step 1 deals with metal pouring. Casting materials are charged into the furnace and allowed to melt. Each metal has its melting temperature. The foundry man takes the melt from the furnace with pouring equipment and pours into the prepared mold. Solidification of the casting takes place inside the mold. Step 2 takes care of shakeout and de-gating of the casting. The process of removing the casting from the mold is the shakeout while removal of sprue, runner bar and ingates from the casting is the de-gating. Step 3 which is the last of all sees to the cleaning and finishing of the casting. Here brushes are employed to clean by removing sand attached to the casting. Unnecessary projections are also cut off.

4. Advantages and disadvantages of (EPC) process

From an environmental and economic perspective, one of the principal advantages of EPC Process is the fact that the casting sand can be reused. This is not so with the traditional green sand casting method as it will require chemical treatment to maintain the properties of the molding sand with will have negative impact of the environment when the sand is finally disposed. The process offers manufacture of complex shapes without the need for cores which must be provided for in production of holes and passages when green sand mold method is used. EPC Process does not present lines that separate molds into several parts which are called parting lines. Based on these afore, researchers have sub mitted that the process reduces machining cost and energy use.

Even with the advantages that researches have outlined which include good surface finish, high dimensional accuracy and reduction in cost of production which make the EPC process to be competitive [26]; it is not without its disadvantages. It is true that the process offers good surface finish but it is subject to the surface of the pattern. The pattern density has significant effect on the quality of casting produced with it. The density values of the patterns vary due to level of compaction of the beads by steam molding. The foams, if not carefully handled may be distorted or permanently damaged. On the whole the disadvantages recorded in the process are associated with the EPS [13, 26].

5. Problems and challenges in EPC process

EPC Process is known to offer many advantages over the traditional sand molding processes like rapid production of patterns and at low costs. However, there are pronounced disadvantages and problems that have been identified. These problems are known to occur because of the sensitivity of the Process to the variables. The chemistry of decomposition of the polystyrene foam which is used as the pattern material is vital in the overall success. The pyrolysis

products therefore must escape from the molds as fast as possible to have castings free of defects.

Some problems are associated with the process majorly referred to as casting defects [10, 27]. The EPS foam pattern undergoes a series of complex reactions: collapse, liquefaction, vaporization and depolymerization. Kumar et al. [6], Molibog [28], Wang et al. [29] and Shivkumar et al. [30] showed that the pyrolysis liquid and gaseous products are potential defect sources like blow holes and the effective elimination of these degradation products is important to produce quality castings. Common EPC defects such as internal porosity, folds and surface defects are all pyrolysis product related.

Variable like refractory coating, pattern density uniformity, and pouring temperature are critical factors affecting formation of defects in the castings. Porosity defects are created when a fast moving metal front engulfs portions of the foam pattern which form voids in the solidified castings. Folds are caused when two streams of molten metal meet and pyrolysis products at the metal front prevent the two streams of metal from fusing. Surface defects are present at the surface of the casting, and are a result of foam pyrolysis products trapped at the metal- coating interface.

6. Applications of evaporative pattern casting process

The application of the EPC process is dynamic. It has been applied in the production of aluminum and its alloys. Iron founding also makes use of the process for production of various products. Magnesium and it alloys are now being cast using the method. The first public recognition of the application of the process was in 1980 when General Motors produced some automobile components with it [6, 7, 31]. Aluminum railway valve body, aluminum cylinder head, pipe fittings and shaft hubs are now being produced by foundries in Canada, Italy, USA and Netherlands [32].

7. EPC process parameters

EPC Process is relatively new and from works of researchers, many process parameters have been known to affect/influence the process. It is also believed to be very sensitive as these variables affect the soundness of the castings produced by it. In both local and industrial applications of the process, difficulties have been encountered [10]. The difficulties have led to casting defects. Some of the process parameters are the patterns, pattern coating, pouring temperature, vibration, gating ratios and geometry of components.

7.1. Patterns in EPC process

Patterns are made of expanded polystyrene foam; poly methyl methacrylate and polyalkylene carbonate [10]. The materials are light in weight. They must be carefully handled after

production to avoid distortion. The expanded polystyrene is used for aluminum and its alloys; it is not used in iron founding because of the defects that it causes for the casting. It is known that the materials have different density values and this has effects on the quality of castings produced [33]. It is then required that there must be consistency in the material used as pattern for consistent quality in terms of the mechanical properties and the microstructures of the castings. It is observed that the pattern used in EPC is in sharp contrast to the ones employed in the traditional sand casting methods where wooden, metallic and plastic materials are used to create cavity in the molds and then removed before pouring casting material into the molds.

7.2. Pattern properties

Xuejun [10], Clegg [3], Kumar et al. [6] and Behm et al. [13] observed that the properties of the pattern significantly affect the casting quality. Xuejun [10] and Liu et al. [34] also showed that to a very large extent, defects caused in castings are attributed to the non-uniformity in pattern density. Consistency should be observed in the properties of the pattern, especially, the density which is a result of the bead compaction [35]. The density affects the flow of molten metal expected to displace the pattern material buried in the sand mold when the compaction of the beads of one side is different from the other side. Instead of having uniform flow of molten metal, the metal tends to flow to low density areas, thus causing folds and foam inclusion in the casting because metal flow faster in the area of low density showing low bead compaction. The decomposition of the patterns may be by scission or unzipping; a number of reactions are involved in this before completion and patterns rejected usually become environmental problems [10, 36, 37].

7.3. Pattern coating

Pattern coating which is a mixture of refractory material and binder or many a times only the refractory material, when applied on patterns, forms a solid layer on the pattern when it is dry. The coating must be permeable to allow gas to escape into the surrounding; otherwise the gas would be trapped, causing defects in the castings [38]. Houzeaux and Codina [31] showed that the escape of the gas from the mold is subject to coating applied on the foam. Chen and Penumadu [11] posited that mold filling times decreased with permeability of the coatings.

Depending on the type of coating, the time to fill the mold with the liquid metal is affected. The gas generated must escape continuously from the mold to avoid defects. The pyrolysis products are the main causes of defects in EPC Process [39]. The release of the gas products should be in a timely manner; if they are too fast, it leads to mold collapse because of pressure drops such that the coating layer is no longer supported and could not therefore bear the weight of the sand. An ideal pattern coating must allow gaseous and liquid foam degradation products to be transported out of the casting in a timely and balanced manner. Variables such as coating material, percent solid, viscosity, liquid absorption capability, coating thickness and gas permeability affect the quality of casting" [10, 16, 20].

The application of the pattern coating must be carefully done on the pattern to ensure that it is consistent [40]. If the coating is applied wet, the wettability must be consistent. If it is applied

dry, the thickness must be consistent [41]. This will allow for controlled liquid absorption and gas permeability. The coating layer provides clean and smooth surfaces on the castings because it is easily removed.

As regards the particle size of the refractory coating, Kumar et al. [2] and Nwaogu and Tiedje [38] had recommended 200 meshes (75 μm) in their research. In reality, the particle size can be reduced to 65 μm. This gives good surface finish to the castings produced with it. The surface roughness obtained in the castings when the coatings are used is subject to the type of casting method employed. With ceramic investment casting process, Singh et al. [42], obtained 2 μm surface roughness but with sand casting method 10 μm to 50 μm was obtained [38].

Usually one of the three methods; spraying, dipping, swabbing, is used to apply the refractory coating to the surface of patterns. Spraying has proved to be the most effective in that uniform spread of the coating is obtained leading to almost uniform thickness. In reality constant thickness cannot be obtained for all patterns. The dipping process will not give uniform spread of the coating. There is great variation in the thickness that would be obtained. In the swabbing, the brush used in the painting makes marks on the pattern thereby reproducing the marks on the castings produced with it.

7.4. Structure and thermal degradation of foam pattern

Polystyrene was discovered in Germany in 1839 by Edward Simon and is a derivative of petroleum produced by polymerization of monomer styrene. The chemical structure of the polystyrene contains only carbon and hydrogen atoms with benzene ring attached to it and it is then classified as hydrocarbon. The chemical formula is $(C_8H_8)_n$. The polymerization process of producing the foam is illustrated in the **Figure 2**. In EPC Process, thermal degradation of the polystyrene occurs at elevated temperature.

Kannan et al. [43], Liu et al. [34], Barone and Caulk [44] and Mirbagheri et al. [9] had studied the thermal degradation of Expanded Polystyrene Foam (EPS) used for EPC Process. The authors had advanced physical and kinetic models for the degradation of the polystyrene foam applied in EPC Process. In the physical model as a result of heat energy transferred from the liquid metal to the solid foam, there were formations of pyrolysis products at the reaction site.

A number of physical models were proposed [14]. The physical models advanced that the composition of the mixture of degradation products is a function of the time that the products reside in the interface before escaping out through the coating and sand [43]. Worthy of note is

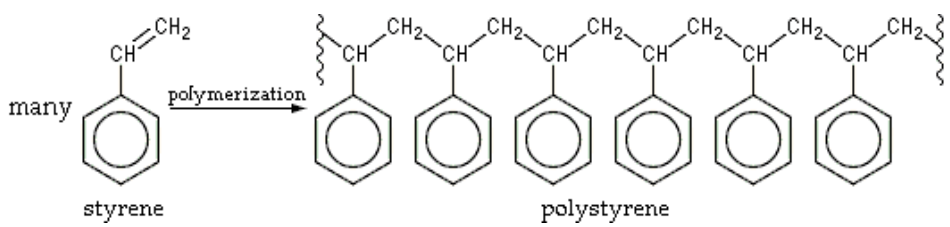

Figure 2. Polymerization process.

the proposal of Molibog [28] who had advanced that there is a three-phase kinetic zone in the metal-foam interface. Molibog's proposal is shown in **Figure 3**.

From the available literature, it was observed that at the initial stage, as temperature increased, the polymer retained its structure without any changes until the temperature reaches the glass transition temperature (T_g). T_g is the temperature at which the molecules begin to vibrate. This is the initial stage of translational movement.

Immediately the temperature is raised above the T_g the molecules of the polymers increase in vibration and its viscosity reduces. A point of collapse of the polymer beads is reached when the temperature is increased further. Partial depolymerization of the polymer chain is achieved as the temperature proceeds. The products of the depolymerization include monomers, dimers and other oligomers [10]. Usually, with EPS, the beads collapse at a temperature about 120°C and its volume decreases to 1/40 of its original size. The degradation process known with the EPS occurs by random scission. The C-C bonds contained in the polymer break down at different locations [45]. It has been noted that at 160°C, the beads which are expanded by team molding to produce the EPS melt, forming viscous substance, consisting of depolymerized products. At various temperatures, the products are formed and they are known to undergo further fragmentations. Finally at about 750°C, the gaseous products formed contain styrene, toluene (C_7H_8), benzene (C_6H_6), ethylene (C_2H_4), acetylene (C_2H_2) and methane (CH_4) [45]. The properties of expanded polystyrene (EPS) and poly methyl methacrylate (PMMA) thermal degradation are summarized in **Table 2** [10].

In iron founding, lustrous carbon defects are known to occur by using EPS as the pattern material. It is to this end that alternative is provided called poly methyl methacrylate (PMMA) as the pattern material. This is capable of eliminating the defects known with EPS. The

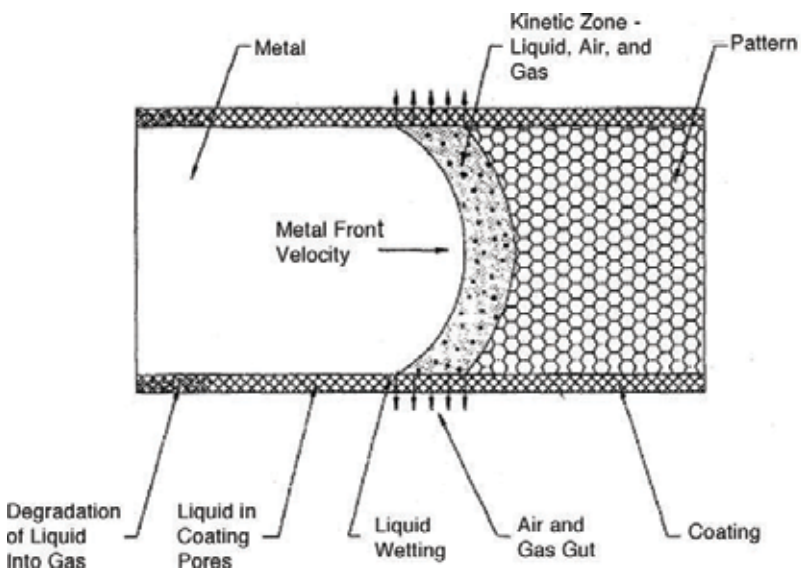

Figure 3. Schematic of the foam degradation process. Source: [43].

properties of the PMMA are included in **Table 2**. The PMMA is known to undergo degradation by a process called unzipping. Research efforts to eliminate completely or at least reduce the lustrous carbon defects of the EPS in iron founding have yielded positive results by the invention of other polymers such as polyalkylene (PAC) and copolymers of the EPS [3].

7.5. Molding practices in EPC process

After the patterns have been produced by injection molding as applied to industrial method or machined out from block of polystyrene, they are assembled with the gating systems design for the patterns and coated with refractory material. Time is given to allow the refractory material to dry. The patterns with the gating systems are then taken and positioned in the molds and supported with green molding sand and rammed carefully. The ramming is necessary to provide rigidity for the molds so that they would not collapse when molten metal is poured. The patterns with the gating systems buried in the molds are not removed like those in traditional sand casting methods. When the liquid metal is poured, the patterns and gating system evaporate leaving only the castings at solidification. The schematic of the pattern-gating system assembly positioned in the mold is shown in **Figure 4**. The thermal energy helps foam patterns to decompose and leaving desired dimensional casting products. As the metal replaces the foam pattern, the process involves a series of complex foam reactions: collapse, liquefaction, vaporization, and depolymerization. The degradation products are vented through the coating layer into the surrounding sand.

The quality of castings in the EPC process is strongly affected by the elimination of liquid and gaseous products produced by the foam pattern [27, 34, 46, 47]. If the foam pattern pyrolysis

Thermal properties	EPS	PMMA
Glass transition temperature (°C)	80 to 100	105
Collapse temperature (°C)	110 to 120	140 to 200
Melting temperature (°C)	160	260
Starting temperature of volatilization (°C)	275 to 300	250 to 260
Peak volatilization temperature (°C)	400 to 420	370
End volatilization temperature (°C)	460 to 500	420 to 430
Heat of degradation (J/g)	912	842
Rate of vaporization at 750°C (Kg/s.m.^{2})	0.77	0.61
Rate of vaporization at 1300°C (Kg/s.m.^{2})	0.18	0.31
Gas yield at 750°C (m^3(STP)/Kg)	0.23	0.273
Gas yield at 1300°C (m^3(STP)/Kg)	0.76	0.804
% Viscous residue at 750°C	61	32
% Viscous residue at 1400°C	15	3

Source: [10].

Table 2. The characteristics of EPS thermal degradation.

http://dx.doi.org/10.5772/intechopen.73526

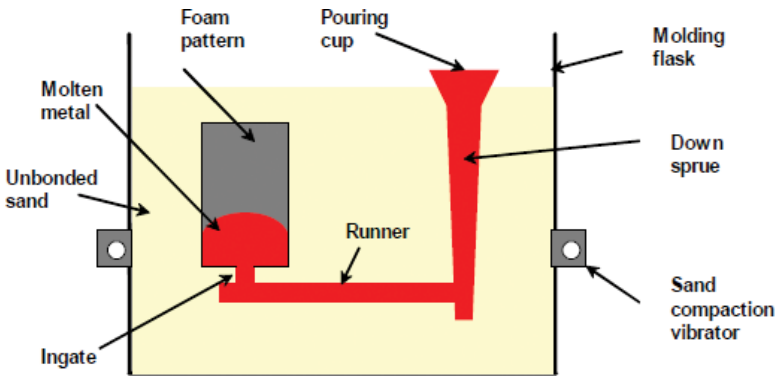

Figure 4. Schematic of molten metal pouring in EPC process. Source: [10].

products cannot be effectively eliminated from the casting, they can cause various defects [19, 48]. After the castings cool down, they are shaken out, de-gated, cleaned and inspected for quality. These final procedures are similar to those used in conventional casting process.

7.6. Vibration

Vibration of the sand around the pattern to obtain the optimum density and compaction of the mold is a critical feature in the successful production of castings by the EPC. The vibration characteristics are critical since the sand must be caused to flow into internal cavities and undercuts for good compaction. The frequency, amplitude and intensity of vibration, direction of movement impacts, shape of the container and the point at which the vibration is applied all influence the quality of the castings. [49] reported that applying vibration during solidification is an effective way for grain refinement. Vibration can modify the solidified microstructure by promoting nucleation and thus reduce the grain size and lead to a homogenous microstructure. The frequency can be of range 10 to 60 Hz, the amplitude ranges from 0.11 to 0.45 while the intensity which is quantified as force ranges from 80 to 12,000 N.

7.7. Characteristic behaviour of molten metal in prepared molds

To eliminate mold erosion in sand molding processes, it is important that gating and feeding system is designed and constructed for the particular casting that would be produced. It is the gating system that will eliminate turbulence that may occur as a result of the pouring of the liquid metal into the prepared mold. It enters the mold by gravity.

In EPC, immediately the liquid metal contacts the buried polystyrene foam, it begins to decompose and violent gas escapes from the mold through vents that have been provided. Physical and chemical reactions begin to take place inside the mold. The gas evolving develops a back pressure to resist the advancing liquid metal; by this a kinetic zone is established. The molten metal displaces the foam because of its high temperature; resulting in pyrolysis products like monomers and emissions toxic to human [13]. All the products formed in the mold have been established as potential causes of defects in castings obtained by EPC process

[6, 43, 45, 49, 50]. Attempts have been made to study comprehensively the behaviour of the liquid metal poured into EPC molds. Some researchers have employed x-rays to study the physico-chemical reactions taking place at the sites. Attempts have been made to model and simulate the interactions that have been known to occur for possible predictions. However, difficulty still exists to quantitatively/qualitatively represent that behaviour of the fluid in the mold.

7.8. Pouring temperature

This refers to the temperature at which the liquid metal is poured into the mold. It is one of the pouring material variables. By experimental determination, it has been established that pouring temperature has significant effects on the mechanical properties of the castings obtained by sand molding processes, EPC inclusive. Usually, it is at high temperature that the casting material is melted in the furnace. Once the casting material melts, the prepared mold is poured. By experiment, it is determined that some aluminum alloys when poured into EPC mold at 650°C, quality casting is obtained [50, 51].

Effects of pouring temperature on the mechanical properties and microstructures of casting can be studied by observing a range of values and levels are taken within the range when the casting material is poured at the levels, opportunity is provided to compare results in terms of visual and mechanical examination of the casting obtained. The visual examination reveals some defects on the surface of the casting if they are existing. Surface roughness can as well be measured. The mechanical examination reveals the mechanical properties in terms of impart, tensile, creep, % elongation, hardness and elasticity [52]. These provide evaluation of the casting to know if it is of good quality. Sometimes the effect of the pouring temperature is examined on the grain refinement.

Each casting material has the temperature range at which it must be poured. Therefore the temperature is measured to determine the pouring range. Usually a k-type chromium-nickel thermocouple is employed to take the measurement. It has a grinded junction. Other forms of thermocouple can be used. The pouring temperature because of the high thermal energy that it has is responsible for the dissociation of H_2O in the molding sand, thereby producing H_2 which escapes from the mold and the decomposition of the evaporative patterns used in EPC process [31].

7.9. The gating system

Molten metal is poured into already prepared mold through a gating system. The gating system designed for a casting is informed by the weight of the casting. There are a number of parts that make up the gating system. Pouring basin is a reservoir at the top of the gating system that receives the stream of molten metal poured from the ladle. Next to the pouring basin is the sprue which usually tapers down to the sprue base well. The sprue usually in the form of a cone has an exit diameter determined by employing the formula for the area of a cone [53].

The sprue base well is usually taken to be five the size of the cross-sectional area of the sprue exit [8]. The choke informs what the cross-sectional areas of the runner bar and ingates will be

by employing the gating ratios. Pressurized and non-pressurized gating ratios are used; pressurized for the ferrous castings and the non-pressurized for the light alloys such as Al-alloys. The runners and ingates convey the molten metal to the cavity of the mold or the polystyrene pattern buried in the mold in the case of EPC Process. Riser is an important part of the gating system. Its function is to feed the casting during solidification so that no shrinkage cavities are formed.

There are many types of gating system designs; top, bottom, side and step. Jain [54] and Rao [8] posited that side gating system enjoys the advantages of both the top and bottom gating designs. However, gating system should be used based on the shape of component to be produced. For example the bottom design is best for the cylinder. **Figures 5–7** show the top, bottom and side or parting line gating designs. These gating systems must be designed, constructed and assembled with the patterns and positioned in the mold ready for the pouring of the liquid metal. Rao [8] provided an insight into the pouring rate of molten metals with respect to their weights poured into already prepared mold. This assists the foundry engineer to determine the rate of flow of liquid metal which can ultimately be used to determine the pouring time. **Table 3** gives the pouring rates of some metals [8].

7.10. Review of specific work on EPC process

Sands and Shivkuman [55] demonstrated the influence of refractory material porosity on mold filling in the EPC process by changing coating thickness. The demonstration showed that mold filling times decreased with the permeability of the coating. From practical perspective, the gas permeability of the refractory coating has been a critical factor in the EPC process for casting soundness control [2].

Behm et al. [13] submitted that EPC process does produce quantities of airborne emissions that are known to be toxic to humans. He further argued that little is known about how individual process variables- coating, pattern thickness, pouring temperature, pouring time, vibration etc. impact the quantity and makeup of these' emissions. This fundamental knowledge may lead to a more environmentally responsible process by reducing the airborne emissions from EPC process. A limitation known with EPC which has not been totally eliminated by experiments is blow hole formation.

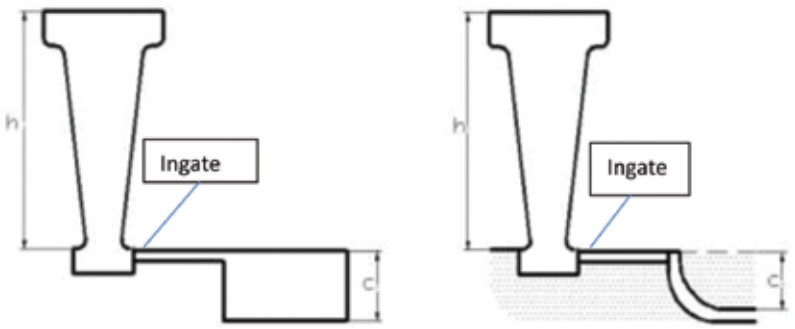

Figure 5. Top gating system.

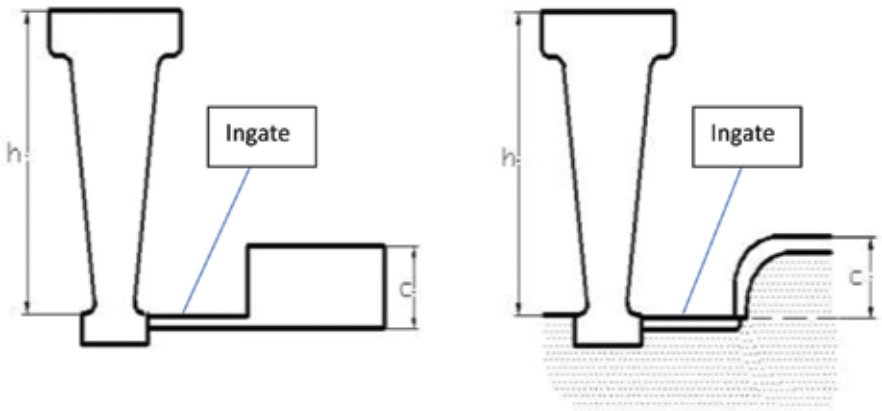

Figure 6. Bottom gating system.

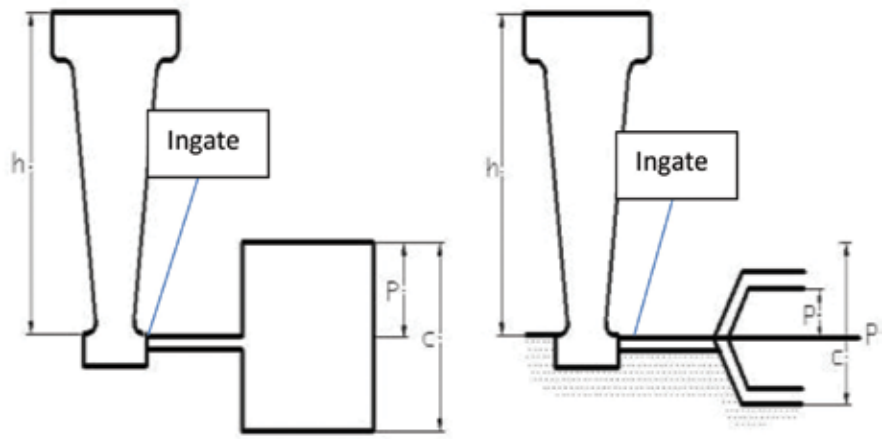

Figure 7. Parting line gating system.

Metal	Pouring rate in Kg/s for castings of mass, Kg			
	Up to 10	**10–50**	**50–100**	**100–500**
Pig iron	1.1	1.5–2.0	3.0–4.0	3.5–6.0
Steel	1.2–1.4	1.9–2.5	4.0–5.0	4.5–7.0
Aluminum alloys	0.25–0.3	0.5–0.7	1.0–1.3	1.2–2.0

Source: [8].

Table 3. Pouring rate of metals.

This provides a platform to make some analysis on the variables that may have weighty results on the soundness that would be produced using EPC Process. In respect of the process parameters that influence the quality of components produced by EPC, gating ratios and geometry of

components were investigated in combination with other parameters like the pouring temperature and grain fineness number (GFN) of molding sand [4, 35]. It was observed that geometry of component as a parameter produced significant effect on the mechanical properties and microstructures of the test castings produced.

8. Pouring and pouring equipment

To achieving soundness in metal casting, more importantly in EPC Process that is susceptible to many variables, pouring of liquid metal into the sand mold is carefully done. In pouring, the liquid metal must be clean and free from slag [54]. The pouring is done such that air aspiration and turbulence are excluded. By this, mold erosion is avoided and defect like metal penetration does not occur. Sound castings are then obtained. The pouring equipment which is the ladle should not be too heavy for the foundry man to carry, otherwise, a mechanical system should be used to carry out the pouring to prevent accident which may occur as a result of inability of the foundry man to carry the equipment.

Author details

Babatunde Victor Omidiji

Address all correspondence to: bomidiji@oauife.edu.ng

Department of Mechanical Engineering, Obafemi Awolowo University, Ile-Ife, Nigeria

References

[1] Clegg AJ. A Review of Recent Developments and Progress. 2000. 10-15. Retrieved on August 10, 2010 from http://www.allbusiness.com/primarymetal

[2] Kumar S, Kumar P, Shan HS. Characterization of the refractory coating material used in vacuum assisted evaporative pattern casting process. Journal of Materials Processing Technology. 2009;**209**:2699-2706

[3] Clegg AJ. Precision Casting Processes. England: Pergamon Press Plc; 1991

[4] Omidiji BV, Owolabi HA, Khan RH. Application of Taguchi's approach for obtaining mechanical properties and microstructures of evaporative pattern castings. The International Journal of Advanced Manufacturing Technology. 2015. DOI: 10.1007/s00170-015-6856-1

[5] Trumbulovic L, Acimovic Z, Gulisija Z, Andric L. Correlation of Technological Parameters and Quality of Castings Obtained by the EPC Method. Materials letters. 2004. Retrieved on August 8, 2010 from www.elsevier.com/locate/matlet

[6] Kumar S, Kumar P, Shan HS. Optimization of tensile properties of evaporative pattern casting process through Taguchi's method. Journal of Materials Processing Technology. 2008;**204**:59-69

[7] Liu Z-L, Pan Q-L, Chen Z-f, Liu X-q, Jie T. Heat transfer characteristics of lost foam casting process of magnesium alloy. Transactions of Nonferrous Metals Society of China. 2006;**16**:78-89

[8] Rao PN. Manufacturing Technology: Foundry, Forming and Welding. New Delhi: Tata McGraw-Hill Publishing Company Limited; 2001

[9] Mirbagheri SMH, Babai R, Dadashzadeh M. Simulation of mould filling in the EPC process. Scientia Iranica, Sharif University of Technology. 2004;**11**(1-2):69-80

[10] Xuejun L. Experimental and computational study of fluid flow and heat transfer in the lost foam casting process, Ph.D Dissertation. Alabama: Auburn University; 2005. Unpublished

[11] Chen X, Penumadu D. Permeability Measurement and Numerical Modeling for Refractory Porous Materials. Schaumburg IL, USA: AFS Tractions, America Foundry Society; 2008. Unpublished

[12] Acimovic-Pavlovic ZS. Condition for Balancing Evaporative Pattern-Refractory Coating-Liquid Metal-Sand System. Vol. 20. Association of Metallurgical Engineers of Serbia, UDC; 2011. pp. 140-146

[13] Behm SU, Gunter KL, Sutherland JW. An Investigation into the Effect of Process Parameter Settings on Air Characteristics in the Lost Foam Casting Process. Houghton, Michigan: Michigan Technological University; 2003. Unpublished

[14] Cai M, Siak J, Powell BR, Nouaime G, Swarin SJ. Physical and chemical analysis of the degradation products of expanded polystyrene patters with short thermal exposure. Transactions of the American Foundrymen's Society. 2002;**110**(2):1463-1481

[15] Hill MW, Lawrence M, Ramsay CW, Askeland DR. Influence of gating and other processing parameters on mold filling in the LFC process. Transactions of the American Foundrymen's Society. 1997;**105**:443-450

[16] Kumar S, Kumar P, Shan HS. Parametric optimization of surface roughness castings produced by evaporative pattern casting process. Materials Letters. 2006;**60**:3048-3053

[17] Liu J, Ramsay CW, Askeland DR. A study of foam-metal-coating interaction in the LFC process. Transactions of the American Foundrymen's Society. 1996;**105**:419-425

[18] Jer-Haur K, Jui-Ching C, Yung-Ning P, Weng-Sing H. Mold filling analysis in lost foam casting process for aluminum alloys and its experimental validation. Materials Transactions. 2003;**44**(10):2169-2174

[19] Kang B, Kim Y, Kim K, Cho G, Choe K, Lee K. Density and mechanical properties of aluminum lost foam casting pressurization during solidification. Journal of Materials Science and Technology. 2007;**23**(6):828-832

[20] Mohammed BA. Lost foam casting of LM6-Al-Si cast alloy, M.Sc. Thesis. Technological University of Malaysia. Unpublished; 2009

[21] Tsai HL, Chen TS. Modeling of evaporative pattern process, part I: Metal flow and heat transfer during the filling stage. Transactions of the American Foundrymen's Society. 1998;**96**:881-890

[22] Sun Y, Tsai HL, Askeland DR. Effect of silicon content, coating materials and gating design on casting defects in the aluminium lost foam process. Transactions of the American Foundrymen's Society. 1996;**104**:271-279

[23] Żółkiewicz Z, Maniowski Z, Sierant Z, Młynski M. Ecological aspects of the use of lost foam patterns. Archives of Foundry Engineering. 2010;**10**:159-162

[24] Żółkiewicz Z, Żółkiewicz M. Pattern evaporation process. Archives of Foundry Engineering. 2007;**7**:49-52

[25] Pacyniak T, Kaczorowski R. Modelling of mould cavity filing process with iron in lost foam method. Archives of Foundry Engineering. 2008;**8**:69-74

[26] Bolton W. Engineering Materials Technology. Jordan Hill Linacre: Butterworth-Heinemann; 1998

[27] Hill MW, Vrieze AE, Moody TL, Ramsay CW, Askeland DR. Effect of metal velocity on defect formation in al LFCs. Transactions of the American Foundrymen's Society. 1998;**106**: 365-374

[28] Molibog TV. Modelling of Metal/Pattern Replacement in the Lost Foam Casting Process. Ph.D. Dissertation. Birmingham: University of Alabama; 2002. Unpublished

[29] Wang C, Paul AJ, Fincher WW, Huey OJ. Computational analysis of fluid flow and heat transfer during the EPC process. Transactions of the American Foundrymen's Society. 1993;**101**:897-904

[30] Shivkumar S, Wang L, Apelian D. The lost-foam casting of aluminium alloy components. Journal of Materials. 1990;**42**(11):38-44

[31] Houzeaux G, Codina R. A finite element model for the simulation of lost foam casting. International Journal of Numerical Methods in Fluids. 2004;**46**:203-226

[32] Brown JR. Foseco Non-Ferrous Foundryman's Handbook. New Delhi: Butterworth Heinemann; 1994

[33] Sharma PC. A Textbook of Production Technology (Manufacturing Processes). New Delhi: S. Chand and Company Ltd; 2008

[34] Liu XJ, Bhavnani SH, Overfelt RA. Simulation of EPS foam decomposition in the lost foam casting process. Journal of Materials Processing Technology. 2007;**182**:333-342

[35] Omidiji BV. Evaporative Pattern Casting (EPC) Process for Production of Aluminum Alloy Components. Ph.D Thesis. Minna: Federal University of Technology; 2014

[36] Caulk DA. A foam melting for lost foam casting of aluminum. International Journal of Heat and Mass Transfer. 2006;**49**:2124-2136

[37] Pletka J, Drelich J. Recovery of expanded polystyrene from coated patterns rejected from lost foam casting. Minerals and Metallurgical Processing Journal. 2002;**19**(1):10-15

[38] Nwaogu UC, Tiedje NS. Foundry coating technology: A review. Materials Sciences and Applications. 2011;**2**:1143-1160

[39] Kabushiki K (2017): Evaporative Pattern Casing Method. Patent Number: W02017135150

[40] Omidiji BV, Khan RH, Abolarin MS. Silica-kaolin mix effect on evaporative pattern castings surface roughness. Achieves of Foundry Engineering, Polish Academy of Sciences. 2016;**16**(3)

[41] Lee K-W, Cho G-S, Choe K-H, Jo H-H, Ikenaga A, Koroyasu S. Effects of reduced pressure and coat permeability on casting characteristics of magnesium alloy in evaporative pattern casting process. Materials Transactions. 2006;**47**(11):2798-2803

[42] Singh B, Kumar P, Mishra, BK. Parametric Optimisation of Casting Surface Roughness Produced by Ceramic Shell Investment Casting Process. National Conference on Advancements and Futuristic Trends in Mechanical and Materials Engineering. Unpublished; 2011

[43] Kannan P, Biernacki JJ, Visco DP. A review of physical and kinetic models of thermal degradation of expanded polystyrene foam and their application to the lost foam casting process. Journal Analytical Application of Pyrolysis. 2007;**78**:162-171

[44] Barone MR, Caulk DA. A foam ablation model for lost foam casting of aluminium. International Journal of Heat and Mass Transfer. 2005;**48**:4132-4149

[45] Shivkumar S, Yao X, Makhlouf M. Polymer-melt interactions during casting formation in the lost foam process. Scrita Metallurgica et Materialia. 1995;**33**(1):39-46

[46] Green JJ, Ramsay CW, Askeland DR. Formation of surface defects in gray iron lost foam castings. Transactions of the American Foundrymen's Society. 1998;**106**:339-347

[47] Kim K, Lee K. Effects of process parameters on porosity in aluminum lost foam process. Journal of Materials Science and Technology. 2005;**21**:681-685

[48] Marlatt M, Weiss D, Hryn JN. Developments in lost foam casting of magnesium. The Minerals, Metals and Materials Society. 2003:141-145

[49] Zhong Z, Zitian F, Xuanpu TB, Pan D, Jiqiang L. Influence of mechanical vibration on the solidification of lost foam cast 356 alloy. China Foundry. 2010;**7**(1):67-75

[50] Trumbulovic L, Gulisija Z, Acimovic-Pavlovic Z, Andric L. Influence of the condierite lining on the lost foam casting process. Journal of Mining and Metallurgy. 2003;**39**(3–4): 1726-1731

[51] Kumar S, Kumar P, Shan HS. Effects of evaporative pattern casting process parameters on the surface roughness of Al-7%Si alloy castings. Journal of Materials Processing Technology. 2007;**182**:615-623

[52] Dieter GE. Mechanical Metallurgy. London: McGraw-Hill Book Company; 1988

[53] Shahmiri M, Kharrazi YHK. The Effects of Gating System on the Soundness of Lost Foam Casting (LFC) Process of Al-Si alloy (A.413.0), 2007;60–65. Retrieved on September 11, 2010 from http//www.foseco/casting.com

[54] Jain PL. Principles of Foundry Technology. New Delhi: Tata McGraw-Hill Publishing Company Ltd; 1997

[55] Sands M, Shivkumar S. Influence of coating thickness and sand fineness on mold filling in the lost foam casting process. Journal of Materials Science. 2003;**38**(4):667-673

Section 4

Metal Matrix Composite Casting

Chapter 7

Fabrication of Aluminum Matrix Composites by Stir Casting Technique and Stirring Process Parameters Optimization

Mohit Kumar Sahu and Raj Kumar Sahu

Additional information is available at the end of the chapter

http://dx.doi.org/10.5772/intechopen.73485

Abstract

Aluminum matrix composites (AMCs) and hybrid aluminum matrix composites (HAMCs) becomes choice for automobile and aerospace industries due to its tunable mechanical properties such as very high strength to weight ratio, superior wear resistance, greater stiffness, better fatigue resistance, controlled co-efficient of thermal expansion and good stability at elevated temperature. Stir casting is an appropriate method for composite fabrication and widely used industrial fabrication of AMCs and HAMCs due to flexibility, cost-effectiveness and best suitable for mass production. Distribution of the reinforcement particles in the final prepared composite regulates the anticipated properties of AMCs and HAMCs. However, distribution of reinforcements is governed by stirring process parameters. The study of effect of stirring parameters in the particle distribution and optimal selection of these is still a challenge for the ever-growing industries and research. In this chapter accurate and precise attempts were taken to explore the effect of stirring parameters in stir casting process rigorously. Further, Optimal values of stirring parameters were suggested which may be helpful for the researchers for the development of AMCs and HAMCs. This chapter may also provide a better vision towards the selection of stirring parameters for industrial production of AMCs and HAMCs comprising superior mechanical properties.

Keywords: stir casting, stirring parameters, aluminum matrix composites, hybrid aluminum matrix, optimization

1. Introduction

Metal matrix composites (MMCs) are those composites in which metals are taken as base or matrix materials and ceramics or organic compounds are used as reinforcements to enhance the properties of the composite as compared to the base metal. Aluminum matrix composites (AMCs), magnesium matrix composites, copper matrix composites are some examples of MMCs which are in demand these days in various applications such as automobile industries, aerospace industries, and electronics industries etc. due to their suitable properties with low cost availability [1, 2]. Nowadays, aluminum matrix composites (AMCs) and hybrid aluminum matrix composites (HAMCs) are most commonly used MMCs [3]. Aluminum matrix composites are those type of composites which contains aluminum or aluminum alloy as base material (matrix) and nonmetals as reinforcements. Reinforcements can be added in weight % or volume % and in various form i.e. particulates, whiskers and fibers. In case of hybrid aluminum matrix (HAMC) more than one reinforcements are added in aluminum matrix. Particles reinforced aluminum matrix composites are used in aerospace, automobile and structural application due very high strength to weight ratio, superior wear resistance, high stiffness, higher fatigue resistance controlled co-efficient of thermal expansion and better stability at elevated temperature, high thermal and electrical conductivity compared to conventional metals and alloys, which makes it suitable for design of an extensive range of components in advanced applications [1, 2, 4–7]. Selection of processing of technique plays a vital role over the property of the composite.

Stir casting is a suitable processing technique to fabricate aluminum matrix composites and hybrid aluminum matrix composites as it is an economical process and preferred for mass production. The first step of stir casting involves melting of aluminum. During melting, aluminum melt reacts with the atmosphere and moisture and forms a layer of aluminum oxide (Al_2O_3) as given by Eq. (1). This layer shields the surface of the melt from further reaction with atmosphere [8].

$$2Al + 3H_2O \Leftrightarrow Al_2O_3 + 6H \tag{1}$$

Stir casting process involves stirring of melt, in which the melt is stirred continuously which exposes the melt surface to the atmosphere which tend to continuous oxidation of aluminum melt. As a result of continuous oxidation, the wettability of the aluminum reduces and the reinforcement particles remain unmixed. Al_2O_3 is a very stable chemical compound, which cannot be reduced under normal conditions and the wettability of melt remains unchanged. To stop the oxidation completely, an inert environment has to be created, which involves lots of complications. Therefore adding wetting agents such as TiK_2F_6, borax and magnesium in the melt is an alternate solution of this problem and widely used for the fabrication of AMCs and HAMCs [9, 10]. Apart from the oxidation problem, achieving homogeneous distribution of particles in the melt is another major problem frequently faced in stir casting process, which is controlled by stirring parameters. Therefore selection of stirring parameters plays major role in stir casting process. Stirring speed, stirring time, impeller blade angle, size of impeller and position of impeller are major parameters, affecting the distribution of the reinforcements in the matrix. Many authors attempted to find effect and the optimal values of stirring parameters.

Hashim et al. [11] used finite element analysis to simulate the fluid flow and investigated optimal values of stirring speed, and impeller position to achieve effective flow patterns to distribute the solid particles in the melt homogeneously. Naher et al. [3] performed Scaled-up stirring experiments with liquids having similar characteristics of aluminum melt and used SiC particles as reinforcements. The experiment was carried out in a transparent crucible and established photographing flow patterns. Ravi et al. [2] investigated effect of mixing parameters through a water model for the fabrication of Al-SiC composite through stir casting. Impeller blade angle, stirring speed, direction of impeller rotation were taken as stirring parameters. Lu and Lu [12] used finite element method to simulate the flow pattern and to find effects of stirring parameters like blade angle, stirring speed, impeller size, and the stirrer geometry over the flow characteristic. Sahu and Sahu [13] used computational fluid dynamics to simulate the fluid flow and optimized stirring parameters like blade angle, impeller size and stirring speed using Grey Taguchi method. This chapter attempt to review the studies conducted on the effect of stirring parameters and optimization of stirring parameters for the fabrication of AMCs and HAMCs through stir casting method.

2. Stir casting

Stir casting is a type of casting process in which a mechanical stirrer is introduced to form vortex to mix reinforcement in the matrix material. It is a suitable process for production of metal matrix composites due to its cost effectiveness, applicability to mass production, simplicity, almost net shaping and easier control of composite structure [14].

Stir casting setup as shown in **Figure 1**, consist of a furnace, reinforcement feeder and mechanical stirrer. The furnace is used to heating and melting of the materials. The bottom poring furnace is more suitable for the stir casting as after stirring of the mixed slurry instant poring is required to avoid the settling of the solid particles in the bottom the crucible. The mechanical stirrer is used to form the vortex which leads the mixing of the reinforcement material which are introduced in the melt. Stirrer consist of the stirring rod and the impeller blade. The impeller blade may be of, various geometry and various number of blades. Flat blade with three number are the preferred as it leads to axial flow pattern in the crucible with less power consumption. This stirrer is connected to the variable speed motors, the rotation speed of the stirrer is controlled by the regulator attached with the motor. Further, the feeder is attached with the furnace and used to feed the reinforcement powder in the melt. A permanent mold, sand mold or a lost-wax mold can be used for pouring the mixed slurry.

Various steps involved in stir casting process is shown in **Figure 2**. In this process, the matrix material are kept in the bottom pouring furnace for melting. Simultaneously, reinforcements are preheated in a different furnace at certain temperature to remove moisture, impurities etc. After melting the matrix material at certain temperature the mechanical stirring is started to form vortex for certain time period then reinforcements particles are poured by the feeder provided in the setup at constant feed rate at the center of the vortex, the stirring process is continued for certain time period after complete feeding of reinforcements particles. The

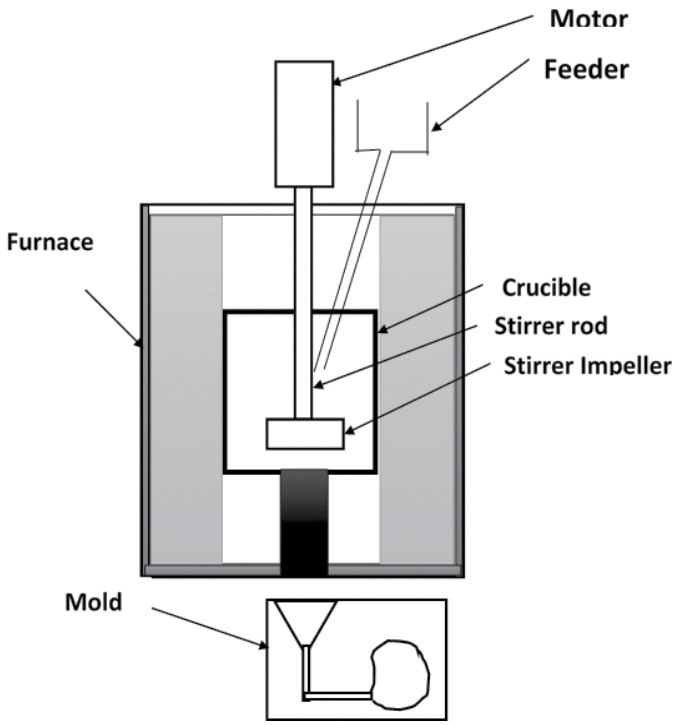

Figure 1. Schematic of stir casting setup.

molten mixture is then poured in preheated mold and kept for natural cooling and solidification. Further, post casting process such as heat treatment, machining, testing, inspection etc. has been done. There are various impeller blade geometry are available. Melting of the matrix material is very first step that has been done during this process.

2.1. Melting of matrix material

Out of various furnaces, bottom pouring furnace is suitable for fabrication of metal matrix composites in stir casting route, this type of furnace consist of automatic bottom pouring technique which provides instant pouring of the melt mix (matrix and reinforcement). Automatic bottom pouring is mainly used in investment casting industry. In this technique, a hole is created in the base of melting crucible to provide bottom pouring and was shielded by a cylinder-shaped shell of metals [15]. In stir casting process, the matrix material is melted and maintained a certain temperature for 2–3 h in this furnace. Simultaneously, reinforcements are preheated in a different furnace. After melting of the matrix material, the stirring process has been started to form the vortex.

2.2. Mechanical stirring

In stir casting process, the mechanical stirrer is coupled with the varying speed motor to control the speed of the stirrer. There are various stages of impeller stirrer i.e. single stage, double stage and multistage impeller. Double stage and multi stage stirrer are mainly used in

http://dx.doi.org/10.5772/intechopen.73485

chemical industries whereas single stage impeller stirrer is commonly used for fabrication of AMCs and HAMCs due flexibility and to avoid excessive vortex flow [12, 13]. **Figure 3** shows various stages of impeller stirrer.

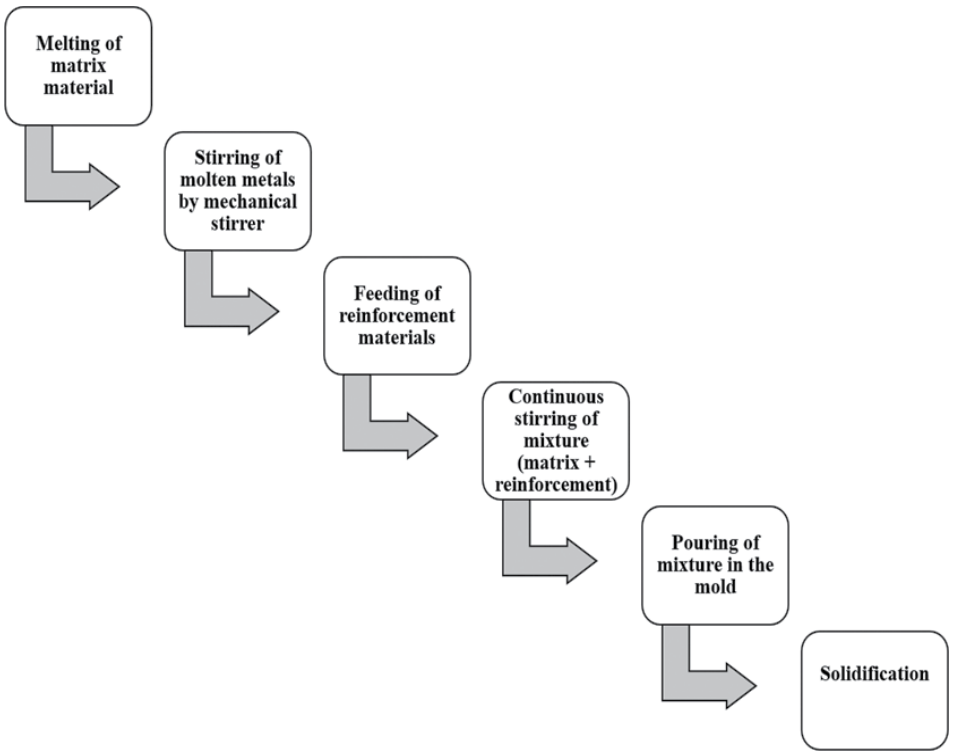

Figure 2. Process of stir casting.

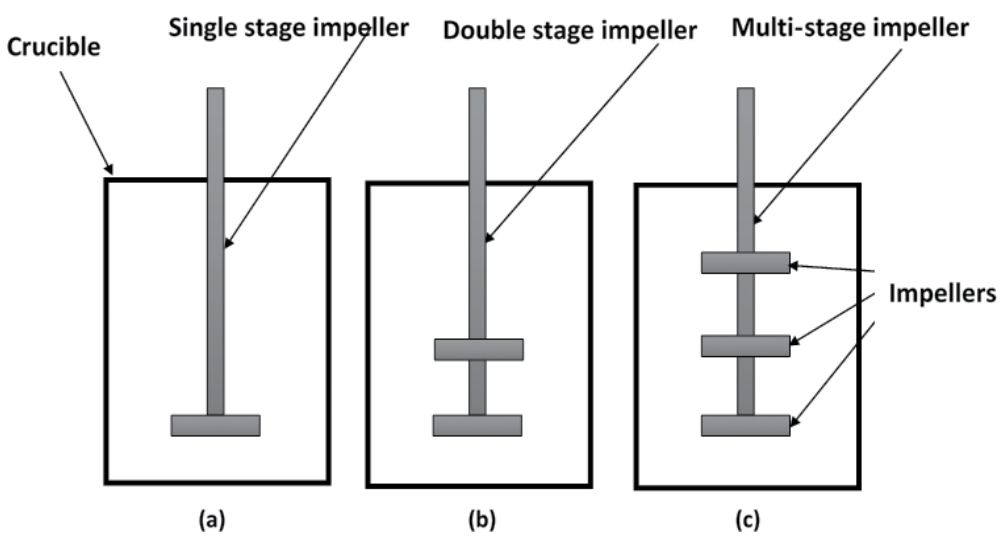

Figure 3. (a) Single stage impeller stirrer, (b) double stage impeller stirrer, (c) multistage impeller stirrer.

Stirring plays a vital role over the final microstructure and mechanical properties of the casted composites as it controls the distribution of reinforcements within the matrix. Optimum mechanical properties can be attained by the uniform distribution of reinforcement and this problem is a common to most of processing techniques, including stir casting [16]. This problem can be solved by optimal selection of stirring parameters.

Researcher has provided a range of stirring parameters based on the properties of the matrix, reinforcement, wettability and oxidation factors for various combination of material as listed in **Table 1**. This table shows the parameters selected by various authors for the fabrications of aluminum matrix composites and aluminum hybrid matrix composites. These parameters are type of matrix material, percentage of reinforcements, stirring speed, stirring time and feed rate. The range of certain stirring parameters has been used by the authors such as the stirring speed should be in the range of 450–700 rpm, stirring time in between 5 and 15 min federate in the range of 0.9–1.5 g/s for different percentage of reinforcements.

Mechanical properties of AMCs and HAMCs mainly depends on the dispersion of the reinforcements throughout the composite. The dispersion of reinforcements is governed by stirring parameters. Hence, performing experiment with selecting random stirring parameters may not provide homogeneous dispersion of reinforcement particle which leads to lower mechanical properties. Therefore, understanding of effect of stirring parameters and selection of optimal stirring process parameters is crucial. The effect of various stirring parameters with suggested optimal values of this parameters is discussed further.

2.3. Effect and optimization of stirring process parameters

There are some significant stirring process parameters which affect the distribution of reinforcement at most. These parameters are stirring speed, stirring time, blade angle, stirrer size, position of the stirrer and feed rate of reinforcements. The main purpose of introducing stirrer is to form vortex in melt which transfers the reinforcement particles in the matrix melt and maintain them in suspension. There are various types of stirrer are existing for this purpose but

S. N.	Matrix	Reinforcement	Reinforcement %	Stirring speed (rpm)	Stirring time (min)	Feed rate	Reference
1	A6061/1545K	B_4C	5 wt. %	450	–	–	[16]
2	A384	SiC	10 wt. %	500, 600, 700	5, 10, 15	–	[17]
3	LM25	B_4C/Al_2O_3	Wt. % (0, 2, 3)/ (0, 2, 3)	550	10	–	[14]
4	Al 6061/Al 7075	B_4C/graphite	Wt. % 10/5	500/700	5	0.9–1.5	[18]
5	Al 7075	B_4C	10 vol. %	500	–	–	[19]
6	Al 7075	Graphite	5, 10, 15, 20 wt. %	500	5	–	[20]
7	Al 6061	Nano Al_2O_3	0.5, 1, 1.5 wt. %	450	15	–	[21]

Table 1. Stirring parameters selected by the authors.

http://dx.doi.org/10.5772/intechopen.73485

for minimizing the power requirement stirrer are designed such that it provide high degree of axial flow [11].

2.3.1. Stirring speed

Stirring speed is a significant parameters which affect the distribution of the reinforcement particles within the matrix material. Prabu et al. investigated the effect of stirring speed and stirring time on the hardness of casted silicon carbide reinforced aluminum matrix composite, in which the stirring speed were selected 500, 600 and 700 rpm and the stirring time was taken as 5, 10 and 15 min. The experimental study concluded 600 rpm and 10 min is the best combination of stirring speed and stirring time for uniform hardness value through the composite which confirms the uniform distribution of SiC particles over the aluminum matrix. Further, Design of impeller i.e. impeller blade angle plays a vital role over the flow characteristic and power consumption by the stirring motors.

2.3.2. Impeller blade angle

The vortex formed by the stirring on solid-liquid mixing transfers reinforcements particles into the melt from the liquid surface whereas shearing action assist to break the accumulation formed by the reinforcement particles and lead to uniform distribution. Therefore, selection of a suitable blade angle is crucial to acquire good level of axial flow and shearing action.

To investigate the effect of impeller blade angle, researchers used water model and CFD model. They selected blade angle as 15, 30, 45, 60 and 90°. In a water model Ravi et al. investigated the effect of impeller blade angle over the distribution of solid particles in the liquid. They found at low angle ($\alpha = 15°$) particles are dispersed below the stirrer. Impeller with blade angle ($\alpha = 30°$) performed well and shows uniform dispersion without concentration of particles. Whereas, impeller with high blade angle ($\alpha > 30°$), most of the solid particles concentrate at just below the tip of the impeller blade which results more radial variation. Thus, 30° was concluded as optimal value of blade angle with respect to stirrer axis which is in good agreement with FEM Model by Sahu and Sahu and Lu and Lu. They attempted to reduce stagnant and dead zones in the flow pattern with blade angle 30, 45, 60 and 90° with respect to the impeller axis. Inactive zone in the cylindrical portion and bottom portion of the crucible are said stagnant zone and dead zone respectively. High blade angle ($\alpha > 90°$) lead to high level of shearing flow and consume high power as well. Shearing action ensure the solid particle suspension in the melt but without axial suction pressure it is difficult to suck solid particles into the melt. The axial flow can be increased by decreasing the blade angle and significant axial flow was seen close to the liquid surface when the blade angle decreased to 30° [2, 12, 13] (**Figure 4**). Moreover, stirring time plays an important role over the distribution of solid particles and power consumption by the stirring motor.

2.3.3. Stirring time

Stirring time is a significant process parameter in stir casting process. Lower stirring time may lead to clustering of particle reinforcements and results non-homogeneous distribution of reinforcement particles. Whereas, higher stirring time may lead to the deformation of the

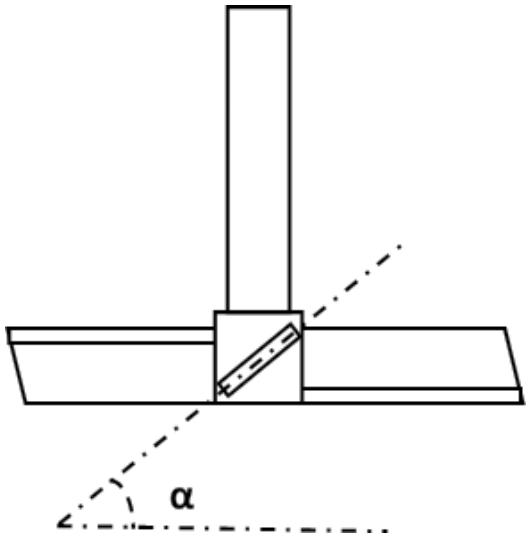

Figure 4. Impeller blade angle.

stainless steel stirrer impeller blade at very high working temperature. The working temperature of some reinforcement such as boron carbide with aluminum matrix are very high. This temperature range is 850–950°C, which may deform the stirrer impeller. Moreover, unwanted high stirring time also consumes more power which leads to rise in fabrication cost of composite. Therefore, optimal value of stirring time is essential. Prabu et al. studied effect of stirring time on microstructure and hardness of Al/SiC composite has been investigated and suggested 10 min as optimal value of stirring to achieve better distribution of reinforcements and uniform value of hardness throughout the composite [17]. Apart from stirring time, the position of stirrer is important and discussed further.

2.3.4. Impeller position

The position of the impeller should not be more than 30% of the height of the fluid from base of the crucible to avoid agglomeration of reinforcements particles at the bottom of the crucible. **Figure 5** shows the position of stirrer impeller. In which height of impeller (h) from the bottom of the crucible is given in Eq. (2) [11].

$$h \geq 0.3H_0 \tag{2}$$

Where h is the position of the impeller from the bottom of crucible and H_0 is the height of the fluid.

2.3.5. Impeller blade size

The impeller blade size is the diameter of the impeller blade which is given in term of the diameter of the crucible. The size of impeller plays a substantial role over the distribution of particles. If the size impeller is too small then the reinforcement particles persist suspended at

http://dx.doi.org/10.5772/intechopen.73485

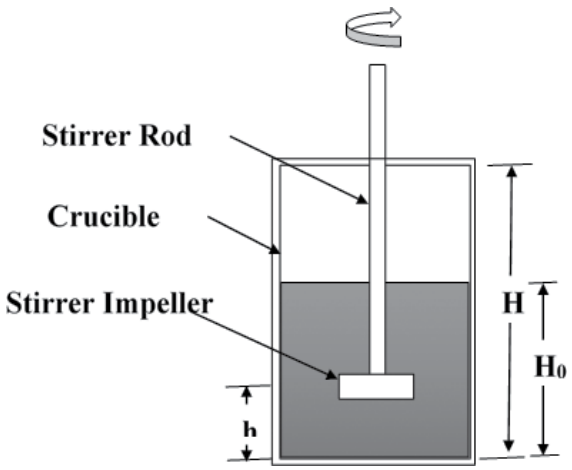

Figure 5. Position of stirrer in the crucible.

the periphery of the crucible which cause lack of suspension of particles at the center. Whereas if the impeller size is too large then the reinforcements particles concentrated at the center of the crucible bottom. Hence, optimal size of impeller is that size which provides distributed particle in both center as well as the periphery of the crucible at the similar speed. So the optimal diameter of the impeller d, is 0.5 times of D, the diameter of crucible for flat base crucible single stage stirring at 550 rpm [13], and 0.55 times of D, the diameter of crucible for semispherical base crucible and multistage stirring at 1000 rpm [12] (**Figure 6**). Whereas the blade width b is equal to 0.1–0.2 times of D, the crucible diameter [11].

At the initial stage of stirring process, Ekman boundary layer theory is well recognized. This theory is associated with particle lifting in rotating fluid phenomenon. Particle dispersion number (PDN) is a correlation between observed particle lifting in the Ekman layer and flow

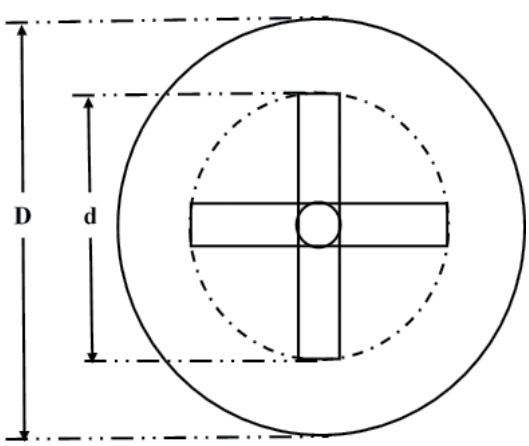

Figure 6. Impeller and crucible diameter.

parameters. A secondary flow in the axial direction is formed due to the momentum transfer from high momentum region to low momentum region through Ekman layer. For single-phase fluid, the spin-up time scale t and character velocity V_E in Ekman layer is given in Eqs. (3) and (4) respectively.

$$t = \left(E\Omega^2\right)^{-1/2} \tag{3}$$

$$V_E = \frac{H_0}{t} \tag{4}$$

Where E is the Ekman number, Ω is angular velocity of the container and H_0 is the height of the melt.

To correlate the observed particle lifting in the Ekman layer with the flow parameters, a particulate dispersion number PDN, defined as the ratio of the characteristic velocity in the Ekman boundary layer to the terminal falling velocity. When this number is much greater than unity, the settling velocity is smaller than the axial velocity of the secondary flow, and thus the particles will be convected to the top of the melt. On the contrary, the particles will remain at the bottom when PD is smaller than unity. For flow in a coaxial rotating cylinder, PD is given by Eq. (5) [11].

$$PDN = \left[\frac{H_0(\mu\omega)^{\frac{1}{2}}}{r_i^{\frac{1}{4}} d^{\frac{3}{4}} V_t}\right] \tag{5}$$

Where, H_0 is the height of the melt, μ the viscosity of the slurry, ω is the angular velocity of the container, r_i is the radius of the inner cylinder, d is the gap between the inner and outer cylinder, V_t is the particles settling velocity. Feeding of reinforcement particles is key parameters to avoid clustering of particles which is discussed further.

2.3.6. Feed rate

Mechanical stirrer forms vortex and reinforcements particles are feed in the center of the vortex. Feeder should be designed in such a manner that it allows continuous flow of particles. High feed rate results particles accumulation in the composite and low federate is difficult to achieve due to the formation of lumps of small solid particles. Thus, selection of optimal rate of feeding is crucial. Less than 0.8 g/s is very difficult to achieve and greater than 1.5 g/s results particle accumulation, hence the optimal rate of feeding is in the range of 0.8–1.5 g/s to avoid the accumulation of reinforcements in the composite and achieve homogeneous dispersion of reinforcement particles throughout the composite [11, 18, 22].

Fabrication of AMCs and HAMCs by stir casting method with optimal combination of above stated stirring process parameters govern the mechanical properties of the composites and discussed further.

2.3.7. Optimal values

Author were used different models for the optimization of stirring parameters. The models used by authors are water model, FEM model and experimental model. Authors were

attempted to find the optimal values of stirring parameters for single stage and multistage impeller stirrer, which is listed in **Table 2**.

Based on extensive review on stirring parameters the position of the stirrer is advised as 25–30% of the height of the melt height from the bottom of the crucible to avoid the dead zone, which is the reason of the agglomeration of reinforcements at the bottom of the crucible [12]. In case of water model, if the impeller blade angle was taken less than 30° then the solid particle dispersed below the stirrer. Impeller with 30° blade angle displays homogeneous distribution without concentration of particles. While, for impeller blade angle more than 30°, most of the solid particles concentrated at just below the tip of the impeller blade. In case of FEM Model, angle ($\alpha < 30°$) showed good axial flow but less shearing action, whereas ($\alpha > 30°$) showed good shearing action but less axial flow. Blade angle as 30° provides good level of axial flow and shearing action to such the solid particles into the melt from the melt surface and break the accumulation of mixing particles. Thus impeller blade angle 30° is suggested as optimal value to achieve homogeneous dispersion of reinforcements particles in the melt [2, 12, 13]. Stirrer size ($d < 0.5$ D) cause lack of suspension of particles at the center while stirrer size ($d > 0.55$ D) results particles concentrated at the center of the crucible base. Thus optimal diameter is 0.5 D at 550 rpm for single stage stirring and 0.55 at 1000 rpm for multistage stirring [12, 13]. The blade width b is in the range 0.1 D–0.2 D, where D is crucible diameter [11]. Hence, optimal size of impeller is proposed as in the range of 0.5D–0.55D to achieve particle distributed in both center as well as the periphery of the crucible at the similar speed. The stirring speed varies in the range of 200–1000 rpm, based on the reinforcement because of the wettability and oxidation factor. For multistage impeller stirring and CFD model, the optimal value of rpm is selected based on least value of stagnant zone and dead zone as better flow characteristic results good distribution of solid particles in the fluid. For multistage stirrer 1000 rpm has recommended as optimal value [12]. But in case of single stage impeller stirring 550 rpm as optimal value [13]. Stirring time less than 10 min ($t < 10$ min) lead to non-uniform distribution of reinforcements due to accumulation of reinforcement particles. Whereas stirring time more than 10 min ($t > 10$ min) cause deformation of stainless stirrer at high temperature which lead to non-homogeneous distribution of particles. Stirrer time of 10 min ($t = 10$ min) shows

Author	Stirring speed (N)	Blade angle (α)	Diameter of impeller (d)	Position of impeller (h)	Stirring time (t)
	rpm	°	mm	mm	min
Single stage impeller stirrer					
Sahu and Sahu [13]	550	30	0.5D	$0.25H_0$	10
Prabu et al. [17]	600	–	–	–	10
Ravi et al. [2]	250–270	30	–	$0.3H_0$	–
Hashim et al. [11]	–	–	–	$0.3H_0$	–
Multi-stage impeller stirrer					
Lu and Lu [12]	1000	30	0.55D	$0.25H_0$	–

Table 2. Optimal values of stirring parameters.

uniform distribution of reinforcement particles without deformation of stirrer, thus 10 min is suggested as optimal value of stirring time [13, 17]. Feed rate less than 0.8 g/s is very difficult to achieve and greater than 1.5 g/s results particle accumulation, hence the optimal rate suggested as 0.8–1.5 g/s to avoid the accumulation of reinforcements in the composite and achieve homogeneous dispersion of reinforcement particles throughout the composite [11, 18, 22].

3. Applications

AMCs and HAMCs are used in wide range applications such as automobile applications aerospace applications, electronics applications and sports applications due to its attractive properties. In automobiles applications, these are mainly used in engines, suspension system, driveline, housing and bakes. Whereas in aerospace applications jet engine blade, satellite solar reflector and missile fins are their main application. **Table 3** shows of applications of AMCs and HAMCs in various industries i.e. automobile, aerospace, military, electronics and sports applications. The applications of the Aluminum matrix composites and the hybrid aluminum matrix composites are in various types of industries such as automobile industries, aerospace industries, electronic industries, sports and aerospace and military industries. It is mainly used in the engines of the automobiles and aerospace. It is also used in the brakes, and driveline as in disk brake rotors and propeller shaft etc. The complete details of applications is in the below table.

Automobile applications	**Engine**	Valve train, piston rod, piston pin, covers, cylinder heads, crank shaft main bearing, cylinder blocks, engine cradle, connecting rod, Piston Crown, Piston Ring Groove, Rocker Arm, Valve, Wrist Pin, Cylinder Block (liner), Connecting Rod
	Suspension	Struts
	Driveline	Propeller shaft, drive shaft, Shift Forks, Drive Shaft, Gears, Wheels, sprocket, pulley
	Housing	Differential bearing, Gear box, pumps
	Brakes	Disk brake rotors, calipers brake disk, car brake disk, brake rotor, rear drum
Aerospace/military applications		Missile fins, aircraft electrical ac doors, metal mirror optics, satellite solar reflector, wing panel, precision components, space shuttle mid-fuselage tubular, struts, jet engine blade
Electronics applications		Current collectors, multichip electronic module, electronic packaging
Sports		Tennis racket skis, bicycle frame, wheel rims, golf club heads

Table 3. Applications of AMCs and HAMCs [23–25].

4. Conclusion

The present discussion discovers the importance of the selection of the stirring parameters over the properties of the stir casted composite desired for current demand of the industries. This review has investigated the effect and optimization of stirring parameters. The range of stirring speed may vary depending upon the properties of the reinforcements and matrix

material, wettability and chemical properties from 200 to 1000 rpm. For multistage impeller stirring 1000 rpm has suggested as optimal value. But in case of single stage impeller stirring 550 rpm gives an optimal speed of stirring, as higher speed causes excessive tabulation. Also it is concluded that Impeller Blade angle at 30° angle gives optimal value, which will provides suitable combination axial flow and shearing action with lower power consumption. Position of the impeller should be kept at more the 25–30% of the height of the liquid from bottom the crucible. Optimal stirring time of 10 min is suggested. Diameter of the impeller should in the range of 50–55% of the diameter of the crucible and reinforcement federate, as in the range of 0.8–1.5 g/s to avoid the accumulation of reinforcement particles. This study also reveals that the fabrication of HAMCs and AMCs by stir casting route by optimal selection of parameters provides high strength, low cost and light weight composites.

The present discussion discovers the importance of the selection of the stirring parameters over the properties of the stir casted composite desired for current demand of the industries. This review has investigated the effect and optimization of stirring parameters. Position of the impeller is suggested to kept at more than 25–30% of the height of the liquid from base the crucible to avoid particle clustering. Further, the optimal value of impeller Blade angle must be at 30° to achieve suitable combination axial flow and shearing action with lower power consumption. Diameter of the impeller should in the range of 50–55% of the diameter of the crucible to avoid particle concentration at the center of the base of crucible. Moreover, the range of stirring speed may vary depending upon the properties of the reinforcements and matrix material, wettability and chemical properties from 200 to 1000 rpm. For multistage impeller stirring 1000 rpm gives as optimal value whereas single stage impeller stirring 550 rpm gives as optimal speed of stirring respectively, as higher speed causes excessive tabulation. Furthermore, optimal value of stirring time is suggested as 10 min to achieve homogeneous distribution of particles without deforming the stirrer and low power consumption. Feed rate should be in the range of 0.8–1.5 g/s to avoid the accumulation of reinforcement particles. This study also reveals that the fabrication of HAMCs and AMCs by stir casting route by optimal selection of parameters provides high strength, low cost and light weight composites.

Abbreviations

D Crucible diameter

d Impeller blade diameter

H Height of crucible

h Height of impeller from the bottom of the crucible

H_0 Height of fluid in the crucible

N Stirring speed

t Stirring time

α Impeller blade angle

Author details

Mohit Kumar Sahu and Raj Kumar Sahu*

*Address all correspondence to: raj.mit.mech@gmail.com

National Institute of Technology, Raipur, Chhattisgarh, India

References

[1] Singh J, Chauhan A. Characterization of hybrid aluminum matrix composites for advanced applications – A review. Journal of Materials Research and Technology. 2016; **5**:159-169. DOI: 10.1016/j.jmrt.2015.05.004

[2] Ravi KR, Sreekumar VM, Pillai RM, et al. Optimization of mixing parameters through a water model for metal matrix composites synthesis. Materials and Design. 2007;**28**:871-881. DOI: 10.1016/j.matdes.2005.10.007

[3] Naher S, Brabazon D, Looney L. Simulation of the stir casting process. Journal of Materials Processing Technology. 2003;**144**:567-571. DOI: 10.1016/S0924-0136(03)00368-6

[4] Surappa MK. Aluminium matrix composites: Challenges and opportunities. Sadhana. 2003;**28**:319-334. DOI: 10.1007/BF02717141

[5] Suresha S, Sridhara BK. Wear characteristics of hybrid aluminium matrix composites reinforced with graphite and silicon carbide particulates. Composites Science and Technology. 2010;**70**:1652-1659. DOI: 10.1016/j.compscitech.2010.06.013

[6] Rajmohan T, Palanikumar K, Ranganathan S. Evaluation of mechanical and wear properties of hybrid aluminium matrix composites. Transactions of the Nonferrous Metals Society of China. 2013;**23**:2509-2517. DOI: 10.1016/S1003-6326(13)62762-4

[7] Sahu MK, Valarmathi A, Baskaran S, Anandakrishnan V, Pandey RK. Multi-objective optimization of upsetting parameters of Al-TiC metal matrix composites: A grey Taguchi approach. Proceedings of the Institution of Mechanical Engineers, Part B: Journal of Engineering Manufacture. 2014;**228**:1501-1507. DOI: 10.1177/0954405413519434

[8] Porter MM, McKittrick J, Meyers MA. Biomimetic materials by freeze casting. JOM. 2013;**65**:720-727. DOI: 10.1007/s11837-013-0606-3

[9] Pai BC, Ramani G, Pillai RM, Satyanarayana KG. Role of magnesium in cast aluminium alloy matrix composites. Journal of Materials Science. 1995;**30**:1903-1911. DOI: 10.1007/BF00353012

[10] Kalaiselvan K, Murugan N, Parameswaran S. Production and characterization of AA6061-B4C stir cast composite. Materials and Design. 2011;**32**:4004-4009. DOI: 10.1016/j.matdes.2011.03.018

[11] Hashim J, Looney L, Hashmi MSJ. Particle distribution in cast metal matrix composites—Part II. Journal of Materials Processing Technology. 2002;**123**:258-263. DOI: 10.1016/S0924-0136(02)00099-7

[12] Lu J, Lu Z. Optimization of stirring parameters through numerical simulation for the preparation of aluminum matrix composite by stir casting process. Journal of Manufacturing Science and Engineering. 2010;**132**:061007:1-7. DOI: 10.1115/1.4002851

[13] Sahu MK, Sahu RK. Optimization of stirring parameters using CFD simulations for HAMCs synthesis by stir casting process. Transactions of the Indian Institute of Metals. 2017;**70**:2563-2570. DOI: 10.1007/s12666-017-1119-5

[14] Vijaya Ramnath B, Elanchezhian C, Jaivignesh M, Rajesh S, Parswajinan C, Siddique Ahmed Ghias A. Evaluation of mechanical properties of aluminium alloy–alumina–boron carbide metal matrix composites. Materials and Design. 2014;**58**:332-338. DOI: 10.1016/j.matdes.2014.01.068

[15] Campbell J. Complete Casting Handbook. University of Birmingham, UK: Elsevier; 2015. DOI: 10.1016/B978-0-444-63509-9.00009-1

[16] Pozdniakov AV, Zolotorevskiy VS, Barkov RY, Lotfy A, Bazlov AI. Microstructure and material characterization of 6063/B4C and 1545K/B4C composites produced by two stir casting techniques for nuclear applications. Journal of Alloys and Compounds. 2016;**664**: 317-320. DOI: 10.1016/j.jallcom.2015.12.228

[17] Prabu SB, Karunamoorthy L, Kathiresan S, Mohan B. Influence of stirring speed and stirring time on distribution of particles in cast metal matrix composite. Journal of Materials Processing Technology. 2006;**171**:268-273. DOI: 10.1016/j.jmatprotec.2005.06.071.1016/j.matdes.2014.06.05

[18] Baradeswaran A, Vettivel SC, Elaya Perumal A, Selvakumar N, Franklin Issac R. Experimental investigation on mechanical behaviour, modelling and optimization of wear parameters of B4C and graphite reinforced aluminium hybrid composites. Materials and Design. 2014;**63**:620-632. DOI: 10.1016/j.matdes.2014.06.054

[19] Baradeswaran A, Elaya Perumal A. Influence of B4C on the tribological and mechanical properties of Al 7075-B4C composites. Composites. Part B, Engineering. 2013;**54**:146-152. DOI: 10.1016/j.compositesb.2013.05.012

[20] Baradeswaran A, Perumal AE. Wear and mechanical characteristics of Al 7075/graphite composites. Composites. Part B, Engineering. 2014;**56**:472-476. DOI: 10.1016/j.compositesb.2013.08.073

[21] Ezatpour HR, Sajjadi SA, Sabzevar MH, Huang Y. Investigation of microstructure and mechanical properties of Al6061-nanocomposite fabricated by stir casting. Materials and Design. 2014;**55**:921-928. DOI: 10.1016/j.matdes.2013.10.060

[22] Auradi V, Rajesh GL, Kori SA. Processing of B_4C particulate reinforced 6061Aluminum matrix composites by melt stirring involving two-step addition. Procedia Materials Science. 2014;**6**:1068-1076. DOI: 10.1016/j.mspro.2014.07.177

[23] Mavhungu ST, Akinlabi ET, Onitiri MA, Varachia FM. Aluminum matrix composites for industrial use: Advances and trends. Procedia Manufacturing. 2017;**7**:178-182. DOI: 10.1016/j.promfg.2016.12.045

[24] Eliasson J, Sandstrom R. Applications of aluminium matrix composites. Key Engineering Materials. 1995;**104**:3-36. DOI: 10.4028/www.scientific.net/KEM.104-107.3

[25] Rohatgi P. Cast aluminum-matrix composites for automotive applications. JOM. 1991;**43**: 10-15. DOI: 10.1007/BF03220538

Edited by T.R. Vijayaram

Major casting processing advancements have been made in experimental and simulation areas. Newly developed advanced casting technologies allow foundry researchers to explore detailed phenomena associated with new casting process parameters helping to produce defect-free castings with good quality. Moreover, increased computational power allows foundry technologists to simulate advanced casting processes to reduce casting defects. In view of rapid expansion of knowledge and capability in the exciting field of casting technology, it is possible to develop new casting techniques. This book is intended to discuss many casting processing technologies. It is devoted to advanced casting processing technologies like ductile casting production and thermal analysis, casting of metal matrix composites by vortex stir casting technique, aluminum DC casting, evaporative casting process, and so on. This book entitled *Advanced Casting Technologies* has been organized into seven chapters and categorized into four sections. Section 1 discusses the production of ductile iron casting and thermal analysis. Section 2 depicts aluminum casting. Section 3 describes the casting manufacturing aspects of functionally graded materials and evaporative casting process. Section 4 explains about the vortex stir casting technique to process metal matrix composite castings. All the chapters discussed in detail the processing steps, process parameters involved in the individual casting technique, and also its applications. The goal of the book is to provide details on the recent casting technologies.

Published in London, UK

IntechOpen

ISBN 978-1-83881-297-3